



universität  
wien

# Diplomarbeit

Titel der Diplomarbeit

Deletion of the tail fibre protein of  $\phi$ Ch1 and  
further characterization of the inversion within its gene locus

Verfasserin

Petra Till, BSc

angestrebter akademischer Grad

Magistra der Naturwissenschaften (Mag. rer. nat.)

Wien, 2011

Studienkennzahl (lt. Studienblatt): A 490

Studienrichtung (lt. Studienblatt): Diplomstudium Molekulare Biologie

Betreuerin: Ao. Univ.-Prof. Dipl.-Biol. Dr. Angela Witte







# Table of contents

---

<b>1. Introduction</b>	<b>11</b>
<b>1.1. Archaea</b>	<b>11</b>
1.1.1. Classification of the living world – a historical overview	11
1.1.2. Properties of the <i>Archaea</i>	12
1.1.2.1. <i>Archaea</i> vs. <i>Bacteria</i> – differences and common characteristics	13
1.1.2.2. <i>Archaea</i> vs. <i>Eucarya</i> – differences and common characteristics	14
1.1.2.3. Unique characteristics of <i>Archaea</i>	17
1.1.3. Evolution of the <i>Archaea</i>	18
1.1.4. Phylogeny and diversity	20
1.1.5. Halophilic and haloalkaliphilic <i>Archaea</i>	22
1.1.5.1. Adaptions to hypersaline conditions	23
1.1.5.2. Adaptations to high pH	25
1.1.6. <i>Natrialba magadii</i>	26
1.1.6.1. Characteristics of <i>Nab. magadii</i>	26
1.1.6.2. Two laboratory strains: L11 and L13	27
1.1.6.3. <i>Nab. magadii</i> in the lab – transformation, vectors, genetic markers	27
<b>1.2. Archaeal viruses</b>	<b>29</b>
1.2.1. Morphotypes – classification of archaeal viruses	30
1.2.2. Haloarchaeal viruses	32
1.2.3. $\phi$ Ch1 – a haloalkaliphilic virus	33
1.2.3.1. Morphology and structural proteins of $\phi$ Ch1	34
1.2.3.2. Life cycle of $\phi$ Ch1	36
1.2.3.3. Genomic organization of $\phi$ Ch1	37
1.2.3.4. The invertible region of $\phi$ Ch1	39
1.2.3.5. Gp34 <sub>52</sub> – the putative tail fibre protein	44
<b>2. Material and Methods</b>	<b>46</b>
<b>2.1. Material</b>	<b>46</b>
2.1.1. Strains	46
2.1.2. Growth media	46

2.1.3. Antibiotics and additives .....	47
2.1.4. Vectors.....	48
2.1.5. Primer .....	51
2.1.6. Marker.....	52
2.1.6.1. DNA ladders.....	52
2.1.6.2. Protein ladders .....	53
2.1.7. Enzymes.....	54
2.1.8. Antibodies.....	55
2.1.8.1. Primary antibodies .....	55
2.1.8.2. Secondary antibodies .....	55
2.1.9. KITS .....	55
2.1.10. Buffers and solutions.....	56
2.1.10.1. DNA Gel electrophoresis .....	56
2.1.10.2. Southern blot.....	57
2.1.10.3. SDS-PAGE and Western blot analysis .....	58
2.1.10.4. Protein purification (denaturing) .....	59
2.1.10.5. Transformation of <i>E. coli</i> and <i>Nab. magadii</i> .....	59
2.1.10.6. Buffers and solution for <i>Archaea</i> methods .....	60
2.1.10.7. Buffers and solution for phage methods.....	61
<b>2.2. Methods .....</b>	<b>61</b>
2.2.1. DNA cloning methods – cloning in <i>E. coli</i> .....	61
2.2.1.1. Gel electrophoresis.....	61
2.2.1.2. Polymerase chain reaction (PCR) .....	62
2.2.1.3. DNA purification .....	64
2.2.1.4. Restriction of DNA .....	65
2.2.1.5. Removal of 3' overhangs .....	65
2.2.1.6. Ligation .....	65
2.2.1.7. Transformation of <i>E. coli</i> .....	66
2.2.1.8. Quick Apply – screening for positive clones.....	67
2.2.1.9. Plasmid preparation from <i>E. coli</i> .....	67
2.2.1.10. Quantification of DNA and lyophilization.....	67
2.2.1.11. Alpha complementation.....	67
2.2.2. Cloning strategies of current projects .....	68
2.2.2.1. Strategies for the deletion of $\phi$ Ch1 ORF34 .....	68

2.2.2.2.	Complementation of $\phi$ Ch1- $\Delta$ ORF34.....	68
2.2.2.3.	Construction of eight <i>int1</i> clones comprising variations in single repeats .....	69
2.2.2.4.	Cloning of a putative activator of <i>int1</i> expression (ORF43/44).....	70
2.2.2.5.	Deletion of the start codon of <i>int1</i> ( $\Delta$ AUG- <i>int1</i> ) .....	70
2.2.3.	Methods for <i>Archaea</i> .....	71
2.2.3.1.	Transformation of <i>Nab. magadii</i> and screening for positive clones .....	71
2.2.3.2.	Generation and verification of a homozygous deletion mutant.....	72
2.2.3.3.	Isolation of <i>Nab. magadii</i> chromosomal DNA.....	73
2.2.3.4.	Time course experiments.....	74
2.2.3.5.	Extraction of (plasmid) DNA from <i>Nab. magadii</i> .....	74
2.2.4.	Phage methods.....	75
2.2.4.1.	Isolation of phage particles .....	75
2.2.4.2.	Isolation of phage DNA.....	76
2.2.4.3.	Precipitation of viral capsid proteins.....	77
2.2.4.4.	Phage titre analysis and some applications .....	77
2.2.5.	Protein methods.....	78
2.2.5.1.	Preparation of crude protein extracts.....	78
2.2.5.2.	Protein expression in <i>E. coli</i> .....	78
2.2.5.3.	Protein purification under denaturing conditions .....	79
2.2.5.4.	Dialysis of proteins .....	79
2.2.5.5.	SDS-PAGE.....	79
2.2.5.6.	Coomassie staining.....	80
2.2.5.7.	Western blot analysis .....	81
2.2.6.	Southern blot analysis .....	82
2.2.6.1.	Preparation of biotinylated DNA probes.....	82
2.2.6.2.	Separation and blotting of DNA samples to a membrane .....	83
2.2.6.3.	Blocking and hybridisation .....	83
2.2.6.4.	Developing of a southern blot.....	83
<b>3.</b>	<b>Results and Discussion .....</b>	<b>85</b>
<b>3.1.</b>	<b>Deletion of <math>\phi</math>Ch1 ORF34.....</b>	<b>85</b>
3.1.1.	Aim of the study and prognosis.....	86
3.1.2.	Production of a homozygous ORF34 deletion mutant.....	86
3.1.3.	Isolation and quantification of phage particles.....	89
3.1.4.	Characteristics of $\phi$ Ch1- $\Delta$ ORF34 particles and the lysogenic culture.....	90

3.1.4.1.	Growth and lysis behaviour of L11- $\Delta$ ORF34.....	90
3.1.4.2.	Expression of ORF34 in L11- $\Delta$ ORF34 – Western blot analysis.....	91
3.1.4.3.	Infectivity of $\phi$ Ch1- $\Delta$ ORF34 – phage titre analysis.....	92
3.1.4.4.	Visualization of $\phi$ Ch1- $\Delta$ ORF34 – electron microscopy.....	93
3.1.4.5.	Detection of flagella (protein FlaB1) in fractions of purified $\phi$ Ch1- $\Delta$ ORF34.....	96
3.1.5.	Complementation of $\phi$ Ch1- $\Delta$ ORF34 .....	98
3.1.5.1.	Retransformation with pRR007-ORF34 <sub>1/52</sub> and pNB102-ORF34 <sub>1/52</sub> .....	98
3.1.5.2.	Quick test – investigation of $\Delta$ ORF34 <sub>52</sub> complementation .....	98
3.1.6.	Discussion .....	101
<b>3.2.</b>	<b>Int1-mediated Inversion of <math>\phi</math>Ch1 ORF34 and ORF36 .....</b>	<b>103</b>
3.2.1.	Analysis of eight <i>int1</i> clones comprising variations in single repeats .....	103
3.2.1.1.	Aim of the study and prognosis.....	103
3.2.1.2.	Construction of the eight <i>int1</i> clones .....	104
3.2.1.3.	Inversion – time course experiment.....	106
3.2.1.4.	Discussion .....	109
3.2.2.	Investigation of a possible activator of <i>int1</i> expression.....	109
3.2.2.1.	Aim of the study and prognosis.....	109
3.2.2.2.	Cloning of the putative activator (ORF43/44) .....	110
3.2.2.3.	Inversion – time course experiment.....	110
3.2.2.4.	Discussion .....	113
3.2.3.	Deletion of the start codon of <i>int1</i> ( $\Delta$ AUG- <i>int1</i> ) .....	114
3.2.3.1.	Aim of the study and prognosis.....	114
3.2.3.2.	Cloning of <i>Nab. magadii</i> L13 $\Delta$ AUG- <i>int1</i> .....	114
3.2.3.3.	Inversion – time course experiment.....	114
3.2.3.4.	Discussion .....	116
<b>3.3.</b>	<b>Binding of gp34 to <i>Nab. magadii</i> P3.....</b>	<b>116</b>
3.3.1.	Aim of the study and prognosis.....	116
3.3.2.	Purification of gp34 <sub>52</sub> /gp36 <sub>52</sub> and quantification .....	117
3.3.3.	Phage titre analysis.....	117
3.3.4.	Discussion .....	120
<b>4.</b>	<b>References .....</b>	<b>123</b>
<b>5.</b>	<b>Appendix.....</b>	<b>131</b>
	Index of Figures and Tables.....	131



Acknowledgements.....	133
Abstract .....	135
Zusammenfassung.....	137
Curriculum Vitae.....	139



# 1. Introduction

---

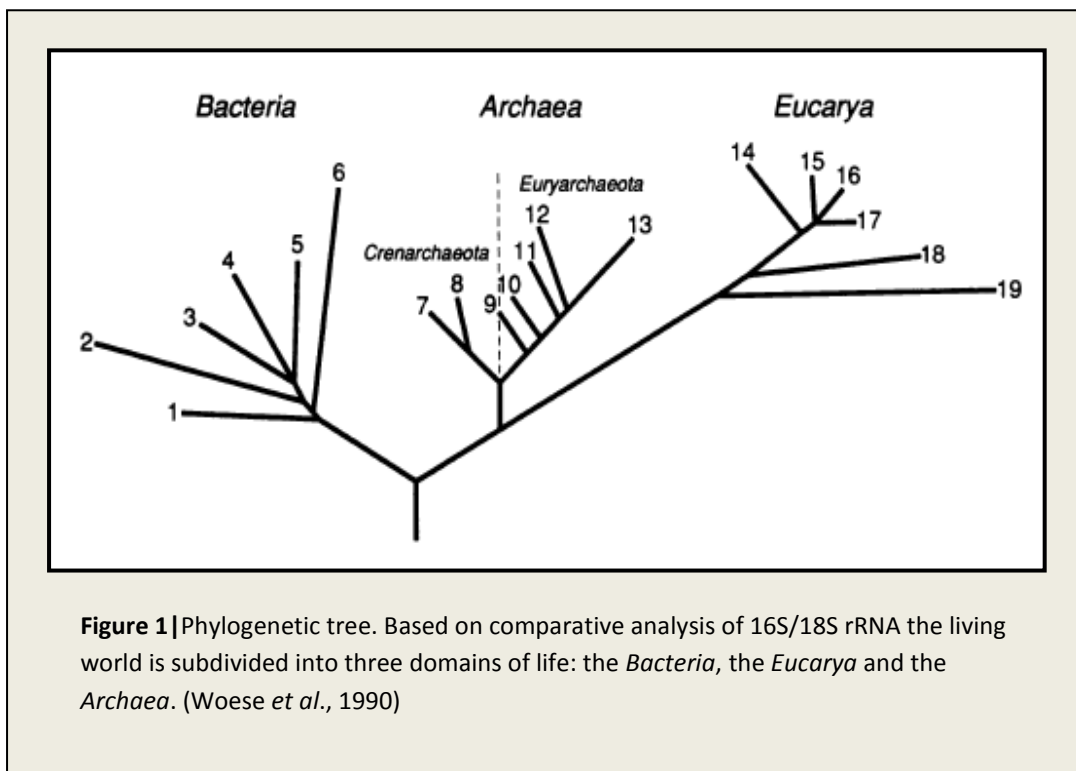
## 1.1. *Archaea*

### 1.1.1. Classification of the living world – a historical overview

Nowadays, phylogenetic distinction of the living world and the understanding of evolutionary relationships are mainly based on the comparative analysis of molecular sequences, rather than on phenotypic criteria. Especially the small subunit of ribosomal RNA is widely used for this approach as it is essential and therefore present in all self-replicating organisms while the sequence of this molecule is changed slowly during evolution (Woese and Fox, 1977; Fox *et al.*, 1977). Moreover, also unicellular species which cannot be cultivated in the laboratory so far can be categorized by detection of rRNA in samples from their natural habitats (Pace *et al.*, 1986; Allers and Mevarech, 2005). As a result characterization of molecular sequences leads to an expansion of the phylogenetic diversity (Barns *et al.*, 1996). On the other hand it enables comparison of even far distant relative organisms and reveals the true relationship of already classified living systems. Hence, the establishment of this approach also caused a dramatically reorganization of the basis of the conventional phylogenetic system (Woese and Fox., 1977).

Previously, it was only distinguished between plant and animal. This view first changed in 1866, when Ernst Haeckel defined the protists as a new category (Haeckel, 1866). Later two more kingdoms were recognized, the bacteria (Copeland, 1938) and the fungi (Whittaker, 1959), thereby dividing all organisms into Animalia, Plantae, Fungi, Protista and Monera (prokaryotes) according to their apparent phenotypic characteristics (Whittaker and Margulis, 1987). This concept, called the five-kingdom scheme, was then more and more replaced by the primary grouping of the living world into prokaryotes and eukaryotes, based on the level of their cellular organization (Chatton, 1938). In contrast to the former model, this dichotomy considers the differences within the four kingdoms Animalia, Plantae, Fungi and Protista (summarized as eukaryotes) as less significant than those to the Monera (prokaryotes) and therefore places them on the same taxonomic rank (Woese *et al.*, 1990). Further findings strongly supported this view. Yet analysis on a molecular level finally revealed that the primary categorization into eukaryotes and prokaryotes is not completely correct, as the latter do not form a monophyletic group (Woese *et al.*, 1990).

In 1977 Carl Woese published that the ribosomal RNA of a small group of methanogene microorganisms (assigned to the prokaryotes up to that point) is considerable different to the one of both categories, suggesting that these organisms form an additional, distinct domain: the *Archaeobacteria* (Woese and Fox, 1977). Subsequently, comparative genomics confirmed this theory and finally the division of the living world in three domains of life, the *Eucarya*, the *Bacteria* and the *Archaea*, was generally accepted (see figure 1). In course of time further species were assigned to the new domain (Barns *et al.*, 1996) and comparison of ribosomal RNA resulted in the subdivision of the *Archaea* into different kingdoms (Woese *et al.*, 1990; Allers and Mevarech, 2005), enclosing a diversity of these organisms that had never been expected.



### 1.1.2. Properties of the *Archaea*

Since *Archaea* were previously mixed with the *Bacteria*, it came as a surprise that they seem to be even closer related to the *Eucarya* than to the *Bacteria*, as the latter are splitting at an earlier time point in the evolutionary history. As illustrated in figure 1 they are on an intermediate position on the phylogenetic tree, though they must not be considered as a mosaic of *Bacteria* and *Eucarya* (Woese *et al.*, 1990). They share features with either domain, resembling the *Bacteria* mainly in their cellular and genomic organization and metabolic strategies. On the other hand, similarities to eukaryotes predominate on the level of information processing, e.g. proteins involved in DNA replication, transcription and translation (Allers and Mevarech, 2005). In addition to the common characteristics,

the *Archaea* are also represented by peculiar features which are found in neither organism of the two other domains.

#### **1.1.2.1. *Archaea* vs. *Bacteria* – differences and common characteristics**

The main reason for the initial misclassification of *Archaea* is buried in their cellular and genomic similarity to *Bacteria*. In contrast to eukaryotes, cells of these two domains are of a comparable size and lack a cellular nucleus as well as organelles (Brown and Doolittle, 1997). Nevertheless, they are significantly different as peptidoglycan is completely missing in the *Archaea*, a property which was originally attributed to *Eucarya* exclusively (Forterre *et al.*, 2002). Instead of the bacterial cell wall, a multitude of other, partly very unique cell-bordering structures are found in this domain (also including pseudopeptidoglycan). For that reason, in contrast to *Bacteria*, *Archaea* are not sensitive to most antibiotics like fosfomycin, vancomycin or the  $\beta$ -lactams (e.g. penicillin) which prevent synthesis of bacterial cell wall structures (Kandler and König, 1998). As a result, though the both domains share some basic features differing significantly to the eukaryotes, the *Archaea* can easily be distinguished from the *Bacteria* on a cellular level as well.

Another important common characteristic of the two prokaryotic groups is the structure of their genome. Both possess one large, circular chromosome comprising genes which are typically organized in an operon-like fashion. Beside, as many examples demonstrate, the genes of these clusters are often arranged in a similar order (Brown and Doolittle, 1997). In addition to the chromosome, prokaryotic cells frequently contain supplementary informations in the form of circular plasmids persisting in the cell (Brown and Doolittle, 1997). However, differences in the genomic context are rare. Though it may be mentioned that, in contrast to the bacterial genome, the chromosome of thermophilic *Archaea* is mainly present in a relaxed or positively supercoiled, rather than in a negatively supercoiled conformation due to the lack of a bacterial-like gyrase (Charbonnier and Forterre, 1994).

Despite most proteins involved in informational processes (DNA replication, transcription and translation) are generally closer related to the *Eucarya*, there are also some homologies to the *Bacteria*. Surprisingly taking into account that the archaeal and the bacterial genome are quite similar, the most unlike mechanism is the replication of the DNA. Initial studies suggested the presence of only one origin of replication in *Archaea*, resembling the situation in the *Bacteria* (Lopez *et al.*, 1999). But this assumption turned out to be wrong, as subsequently two or even more origins were localized in several archaeal species, e.g. *Halobacterium* spec. NRC-1 (Zhang and Zhang, 2003) and *Sulfolobus solfataticus* (Robinson *et al.*, 2004). However, more homologies between *Archaea*

and *Bacteria* are known in transcription and translation. Although the archaeal main proteins involved in this processes strongly resemble those of the eukaryotes, some transcription regulators showed to have bacterial homologues (Aravind and Koonin, 1999). One example is the similarity of archaeal elongation factors to the bacterial NusA and NusG working on elongation control and anti-termination (Bell and Jackson, 1998; 1996; Klenk *et al.*, 1997). Moreover, both, *Archaea* and *Bacteria*, use polycistronic mRNAs lacking 5'-end caps which are characteristic elements of eukaryotic mRNAs. Like in *Bacteria*, purine-rich Shine Dalgarno sequences are present upstream of the start codon on archaeal mRNAs, mediating recognition of the translation start site (Dennis, 1997; Allers and Mevarech, 2005).

In contrast to the informational proteins described above, probably due to extensive horizontal gene transfer operational proteins seem to share a high level of identity in *Archaea* and *Bacteria*. Mainly enzymes involved in central metabolic processes and maintenance of energy are well conserved, resulting in high similarity of the corresponding pathways (Rivera *et al.*, 1998; Jain *et al.*, 1999). *Archaea*, as well as *Bacteria* comprise both, heterotrophic and autotrophic species using either light or organic compounds as energy source (Huber *et al.*, 2000). Thus, they possess a variety of different metabolic and energetic pathways, most of them existing in both domains. One exception is the generation of methane which is restricted to the archaeal domain (Forterre *et al.*, 2002; Allers and Mevarech, 2005). Other operational proteins conserved among the *Archaea* and the *Bacteria* are cellular transporter, receptors and proteins involved in cell division. An example for the latter is an archaeal cell division protein homolog to the bacterial FtsZ. Later studies indicate that this protein also shows similarities to the eukaryotic tubulins, but yet is closer related to the bacterial version (Baumann and Jackson, 1996).

#### **1.1.2.2. *Archaea* vs. *Eucarya* – differences and common characteristics**

As discussed above the cellular and genomic features of *Archaea* are rather similar to *Bacteria* than to *Eucarya*. Nevertheless some characteristics generally assigned to the eukaryotes are also present in the third domain of life. First of all, in comparison to *Bacteria*, *Archaea* completely lack peptidoglycan, the main component of the bacterial cell wall. However, this structure is not found in any eukaryote either (Forterre *et al.*, 2002). For that reason *Archaea*, like members of the *Eucarya*, are not sensible to antibiotics directed against the synthesis of bacterial cell walls. In addition, also antibiotics inhibiting the large subunit of the ribosomes do not work in either of the two domains (Brown and Doolittle, 1997).

On the genomic level, many *Archaea* strongly resemble *Eucarya* both in the sequence and the structure of proteins mediating genome compaction. In both domains four types of such proteins, designated as histones, are present: H2A, H2B, H3 and H4 (White and Bell, 2002; Allers and Mevarech, 2005). In eukaryotes two copies of each of these chromatic proteins are combined, assembling to an octameric nucleosome wrapped by the DNA. Archaeal histones in contrast can also form homotetramers composed of two H3-H4 dimers, rather than only heteropolymeric structures (Brown and Doolittle, 1997; White and Bell, 2002). Moreover they lack C-terminal and N-terminal tails, the targets of posttranslational modification in eukaryotic histones, suggesting that they may not be involved in the regulation of gene expression. Anyway, although homologues of eukaryotic histones are widespread among the phylum *Euryarchaeota*, none have been discovered in members of the *Crenarchaeota* so far. Yet, other nucleic acid binding proteins like Alba are present at a wide range of both archaeal groups (White and Bell, 2002).

However, although it is not clear whether modulation of gene expression can be performed on the level of genome compaction like in the eukaryotes, most features of transcription, translation and DNA replication seem to be well conserved between *Archaea* and *Eucarya*. The most similar process is the genome replication, as nearly all archaeal proteins involved in this procedure have a eukaryotic homologue. Though, it has to be noted that in many cases several eukaryotic proteins working on the same mechanism are represented by only one equivalent in the *Archaea*. Thus, the latter seem to possess a more simplified version of the replication machinery (Edgell and Doolittle, 1997; Barry and Bell, 2006). One well described example is the archaeal homologue to the eukaryotic origin recognition complex (ORC). In *Eucarya* the ORC comprises six proteins, Orc1-6, binding to the origin and, as a result, recruiting many proteins which are needed for the initiation of replication like for example Cdc6 (Machida *et al.*, 2005). On the archaeal genome one to nine genes with significant similarities to both, *orc1* and *cdc6* are present. The numerous proteins in some species are suspected to fulfill different functions in replication; however, each Orc1/Cdc6 protein performs the work of both eukaryal proteins, Orc1 and Cdc6. Orc1/Cdc6 is highly conserved across the archaeal domain and only resembles the eukaryal version, in the sequence as well as on the structural level. To date, no homologies to the bacterial origin binding protein DnaA are known (Barry and Bell, 2006). Other proteins involved in DNA replication, which are supposed to be closer related to eukaryotic rather than to bacterial equivalents are e.g. replicative helicases, single strand binding proteins and primases (Edgell & Doolittle, 1997; Barry and Bell, 2006). For example eukaryotic primases are composed of a large (PriL) and a small (PriS) subunit forming a dimer in contrast to the monomeric DnaG of *Bacteria*. In *Archaea* homologues to both subunits are present resembling the eukaryotic protein in its structure including the existence of a Zn-binding site on the PriS-subunit (Barry and Bell,

2006). Moreover, both, *Archaea* and *Eucarya* possess a family B polymerase responsible for elongation of replicating nucleic acid strands. *Bacteria* in contrast, apart from *Escherichia coli*, completely lack this type of DNA replicating enzyme (Brown and Doolittle, 1997). In addition another sort of DNA polymerase which is supposed to be involved in discrimination between leading- and lagging-strand has been discovered in *Archaea* (Brown and Doolittle, 1997; Barry and Bell, 2006).

Just like the DNA replicating polymerase, the archaeal RNA polymerase (RNAP) working on transcription of DNA into RNA was shown to be homolog to the RNA polymerase II of eukaryotes (Huet *et al.*, 1983). In comparison to the much simpler bacterial enzyme, the RNAPs of both other domains are assembled of at least seven subunits (Brown and Doolittle, 1997). Yet, the archaeal protein does not only resemble the eukaryotic one in its complexity, but also in the sequence of most subunits (Bell and Jackson, 1998). Nevertheless there are significant differences to the eukaryotes, as only one RNAP is present in the *Archaea* while *Eucarya* possess three different polymerases, RNAP I-III (Brown and Doolittle, 1997).

However, in both, *Archaea* and *Eucarya*, the recruitment of the RNA polymerase to the transcription start site requires a subset of components and transcription factors (TF) (Allers and Mevarech, 2005). The first step in transcription initiation is the binding of TBP (TATA-box-binding protein) to a sequence element near the transcription start site on the DNA, namely the TATA-box. Both features are found in *Archaea*, as well as in eukaryotes. The archaeal TATA-box-binding protein resembles the eukaryotic one in both, its sequence and in its structure, albeit the variable amino-terminal domain of the latter is missing (Bell and Jackson, 1998). In the *Eucarya* TBP is part of a large complex, TFIID, which is attached to the promoter region and leads to the recruitment of further transcription factors involved in transcription initiation, e.g. TFIIB (Brown and Doolittle, 1997). A protein showing structural homologies to TFIIB, termed TFB, is also present in *Archaea*. Crystallization of the archaeal transcription factor B in complex with TBP and the TATA-element revealed that the proteins are bound to the DNA in inverse orientation compared to the eukaryotic TFIIB. This raises the question whether and how the archaeal initiator proteins are able to determine the polarity of transcription (Bell and Jackson, 1998). Anyway, in *Archaea* TBP and TFB seem to be sufficient for the initiation of transcription, while the eukaryotic system is apparently much more complex including a multitude of transcription factors (Allers and Mevarech, 2005). However, less is known about the similarities to eukaryotes concerning regulation and transcription elongation. Initially a homologue to the eukaryotic elongation factor TFIIS was discovered in *Archaea*, but further studies indicated that this element may only be a subunit of the RNA polymerase (Bell and Jackson, 1998). As mentioned above several archaeal elongation factors are supposed to be closer related to the *Bacteria*, rather than to the *Eucarya*.



Also proteins mediating archaeal translation share high similarity with their eukaryal counterparts. Compared to the simplified system in the *Bacteria* composed of only three translation initiation factors, more than ten proteins fulfilling different roles exist in *Archaea* and eukaryotes (Allers and Mevarech, 2005). For example an archaeal homologue to the eukaryotic initiation factor eIF-1A avoids assembling of the two ribosomal subunits previously to association of the small subunit with the aminoacyl-tRNA, GTP and the mRNA (Brown and Doolittle, 1997; Bell and Jackson, 1998). Moreover counterparts to the eukaryotic eIF-4A helicase and the eIF-2 complex mediating recruitment of the tRNA and GTP to the small ribosomal subunit are found in *Archaea*. In contrast, no archaeal equivalent to eIF-4 exists, as archaeal mRNAs lack the 5'-cap which is normally recognized by this protein (Bell and Jackson, 1998). Beside, also factors mediating elongation and termination of translation like eEF-1 $\alpha$ , eEF-2 or eRF are found in both domains. They are involved in charging aminoacyl tRNAs to the A-site of the ribosome, translocation of the ribosome during growing of the polypeptide strand and finally recognition of the stop codon (Bell and Jackson, 1998). In addition it has to be noted that in *Archaea* as well as in *Eucarya* the first amino acid recruited to the ribosome is a methionine, rather than N-formylmethionine like in *Bacteria* (Keeling and Doolittle, 1995). However, aminoacyl-tRNA synthetases as well as the ribosomes seem to be equally related to both other domains. Detailed studies indicate, that some ribosomal proteins are closer related to the *Bacteria* (RP L11) while others resemble eukaryotic counterparts (RP L10) (Brown and Doolittle, 1997). So it can be concluded that similarities concerning archaeal and eukaryal translation are reflected by many features, but mainly by the translational factors.

Mentionable homologies between *Archaea* and *Eucarya* are also found in systems responsible for DNA recombination and repair. In *Archaea* this processes are essential as many of these organisms are exposed to a harsh environment frequently causing genomic damage. For example the archaeal enzyme RadA mediating repair of damaged DNA by performing strand exchange strongly resembles the eukaryotic equivalent, a protein of the RecA family. Moreover counterparts to enzymes involved in excision repair exchanging bases in pyrimidine dimers are also found in some archaeal species (Allers and Mevarech, 2005).

### **1.1.2.3. Unique characteristics of *Archaea***

As already described in detail *Archaea* share properties with both, *Eucarya* and *Bacteria*, but they are also represented by features exclusively found in this domain. The most striking characteristic is the certain composition of the phospholipids within the archaeal cell membrane. In bacterial, as well as in eukaryotic lipids, fatty acids are connected with a glycerolphosphat backbone via ester linkages (Forterre *et al.*, 2002). Archaeal phospholipids in contrast comprise methyl

branched ether linked isoprene side chains. Moreover the hydrocarbon chains replace different phosphate groups of the glycerol, generating glycerol-1-phosphate (G1P) in *Archaea* and glycerol-3-phosphate (G3P) in the other domains, respectively. Besides, the archaeal lipid (L-glycerol) is reverse in its enantiomeric conformation compared to bacterial and eukaryal glycerol phosphates (D-glycerol) (Brown and Doolittle, 1997; Kandler and König, 1998). The unique composition of the lipids (especially the ether-linkages) as well as the presence of tetraether lipids in the cytoplasmic membrane, are supposed to be involved in maintaining stability and impermeability of the membrane even at high temperatures and under rough conditions, reflecting the hyperthermophilic nature of the archaeal ancestor (Forterre *et al.*, 2002). However, not only the membrane but the cell bordering structure of the *Archaea* as a whole is significantly different to the other domains. As mentioned above, *Archaea* completely lack peptidoglycan, the main compound of bacterial cell walls. Instead some species have cell walls composed of other elements like heteropolysaccharides or pseudopeptidoglycan. Members of the *Thermoplasmatales* in contrast do not possess any additional structures and are only bordered by the cell membrane containing glycoproteins. The majority of *Archaea* however is surrounded by a glycoproteinaceous envelope, termed the S-layer (Kandler and König, 1998; Forterre *et al.*, 2002). As both, the cell wall and the RNA polymerase are completely different among *Bacteria* and *Archaea*, another specific set of antibiotics is active in the latter (Brown and Doolittle, 1997). Anyway, in addition to the unique structural features, one metabolic capability is found in *Archaea* exclusively: methanogenesis (Forterre *et al.*, 2002).

### **1.1.3. Evolution of the *Archaea***

The discovery of the *Archaea* as the third domain of life changed the view on phylogenetic relationships and considerably supported reconstruction of the evolutionary history. The first classical phylogenetic tree comprising all three domains was created by Woese and colleagues based on the comparative analysis of small subunit ribosomal RNA (ss rRNA). It shows all life emerging from one common ancestor early splitting into the bacterial domain and the eukaryal-archaeal lineage which subsequently gave rise to the *Archaea* and the *Eucarya* by branching into two domains. This concept considers the latter two as sister groups, while the *Bacteria* are supposed to be the eldest domain, closest related to the common ancestor of all life (Woese *et al.*, 1990). However, this scheme can neither give a deeper insight in phylogenetic development of the *Archaea* since the groups within this domain are poorly resolute by rRNA analysis, nor does it describe the nature and origin of the common ancestor. Today the identity and characteristics of this progenitor, designated as last common ancestor (LCA) or last universal common ancestor (LUCA), are still unclear and a

controversial issue (Glansdorff *et al.*, 2008). In 1998 Carl Woese described the origin of extant life as a community of primitive cell, evolving as a diverse unit, in course of time becoming more complex until exchange between the different groups was not possible any more, thereby giving rise to the individual ancestors of the three certain domains (Woese, 1998). To a large extent this concept was based on the idea of high mutation rates and frequently occurring lateral gene transfer (LGT) within the simple ancestor cells. In contrast to this, these events were supposed to happen only rarely when cellular functions become more specific and, as a result, certain proteins cannot simply be replaced any more. Hence, both, the development of the common ancestor from progenotes (rudimentary self replicating units) as well as the similarities between *Archaea* and *Bacteria* in operational proteins can be explained by LGT in early stages of development (Woese, 1998). Further publications supported this view and highlighted the importance of LGT on evolutionary processes (Wolf *et al.*, 2001; Forterre *et al.*, 2002; Gribaldo and Brochier-Armanet, 2006). For example homologies between archaeal and eukaryal enzymes involved in informational processes were also traced back to early transferring events (Gribaldo and Brochier-Armanet, 2006). Yet, neither of these concepts of evolutionary processes clearly defines which domain is the closest related to the last common ancestor, only speculating about the chronologic order and relationships of *Archaea*, *Eucarya* and *Bacteria* in the phylogenetic tree. The most traditional model however is the classical rooting in the bacterial branch, implying that eukaryotes arose from the combination of early bacterial cells by endosymbiosis developing to a more complex system (Woese, 1998; Rivera and Lake, 2004). Moreover also the possibility that none of the three domains could be traced back to LUCA was not excluded and even a eukaryal basis was discussed (Gribaldo and Brochier-Armanet, 2006). Anyway, Woese clearly pointed out that the common ancestor of all life has had to be a quite primitive cell with limited functions, giving rise to more complex mechanisms, indicating a more prokaryote-like nature of LUCA (Woese and Fox, 1977; Woese, 1998). Recent studies in contrast define the common ancestor as a more complex system with eukaryal features but, so far, lacking cellular organelles (Glansdorff *et al.*, 2008). In this model the evolutionary development of the three domains of life is traced back to reductive evolution of LUCA giving rise to the *Bacteria* and the *Archaea*, whereas the *Eucarya* are supposed to be emerged from reception of primitive bacteria by the protoeukaryotic LUCA. Hence, similarities among two domains can be explained by the complex and diverse characteristics of the common ancestor, rather than by lateral gene transfer. Beside LUCA is described in more details as “*a complex community of protoeukaryotes with a RNA genome, adapted to a broad range of moderate temperatures, genetically redundant, morphologically and metabolically diverse*”, also mentioning certain features like e.g. the presence of *sn1,2* fatty acid lipids (Glansdorff *et al.*, 2008).

Despite this view is inconsistent with previous models in most aspects, it conforms to a hyperthermophilic origin of the archaeal domain (Glansdorff *et al.*, 2008). This assumption is also reflected by the adaptation to high temperatures found in all lineages primary branching from the archaeal ancestor (Gribaldo and Brochier-Armanet, 2006). Though methanogenesis also occurred early in the evolution of *Archaea*, it is probably not characteristic of the individual ancestor as initially assumed (Forterre *et al.*, 2002; Gribaldo and Brochier-Armanet, 2006). Yet, all present-day *Archaea* are supposed to originate in an anaerobic but maybe oxygen tolerant, chemolithotrophic or possibly heterotrophic precursor cell (Forterre *et al.*, 2002). However, the probably most striking feature of the archaeal ancestor is the presence of *sn2,3* isoprenyl ether lipids, a characteristic which enabled the establishment at high temperatures and had apparently been remained in all archaeal groups (Glansdorff *et al.*, 2008).

#### **1.1.4. Phylogeny and diversity**

According to comparative analysis of small subunit rRNA as well as Bergey's manual definition, the *Archaea* are subdivided into two main phyla: the *Crenarchaeota* and the *Euryarchaeota* (Woese *et al.*, 1990; Boone and Castenholz, 2001). In addition the *Nanoarchaeota* and the *Korarchaeota*, two smaller, probably very deeply branching lineages, were assigned to this domain later on, splitting the *Archaea* into four distinct phyla. The latter comprise a couple of uncultivated species which have only been postulated by the detection of DNA sequences in environmental samples (Barns *et al.*, 1996). The *Nanoarchaeota* however are represented by only few members, e.g. *Nanoarchaeum equitans*, small cocci colonizing rocks in hot submarine vents. They grow attached to large spherical *Crenarchaeota* of the genus *Ignococcus*, completely depending on these symbiotic associations. This certain life style can be traced back to their strongly reduced genome (less than 500 kilobases) lacking many important genes which are conserved among other archaeal groups (Huber *et al.*, 2002; Huber *et al.*, 2003). Thus, the *Nanoarchaeota* have to be clearly differentiated from the other archaeal phyla such as the *Crenarchaeota*, another more basal lineage. Based on ss rRNA analysis the latter is subdivided into three orders, the *Desulfurococcales*, the *Sulfolobales* and the *Thermoproteales*, all of them inhabiting mainly hot environments (Forterre *et al.*, 2002). Nevertheless, also uncultivated crenarchaeal species living at moderate or even low temperatures have been detected in marine water samples (Forterre *et al.*, 2002; Barns *et al.*, 1996). The *Euryarchaeota* however also contain hyperthermophiles, but are much more phenotypic diverse, including also methanogens, psychrophilic, halophilic, alkaliphilic, thermoacidophilic and other multiple extremophilic species. It can be distinguished between nine euryarchaeal orders: *Archaeoglobales*, *Halobacteriales*, *Methanobacteriales*, *Methanococcales*, *Methanomicrobiales*, *Methanosarcinales*, *Methanopyrales*, *Thermococcales* and *Thermoplasmatales* (Forterre *et al.*, 2002).

Despite their poor phylogenetic presence compared to other domains (only 4 phyla compared to p.e. 23 within the *Bacteria*, Boone and Castenholz, 2001), the *Archaea* are a group of “metabolically diverse organisms coexisting with *Bacteria* and *Eucarya* in the majority of Earth environments, both terrestrial and aquatic, including also extreme ones, such as high or low pH, low temperature, high salinity or pressure” (Gribaldo and Brochier-Armanet, 2006). The initial view that this domain is composed of only a few methanogene members was quickly replaced as further species were discovered, but though the idea that *Archaea* are original organisms inhabiting hostile environments exclusively persisted for a very long time (Olsen, 1994). Yet, nowadays it is known that the *Archaea* are not limited to extreme habitats, as well as conversely not all extremophiles necessarily have to be members of the archaeal branch. In fact, all three domains are found side by side, colonizing the same environments all over the world (Rothschild and Mancinelli, 2001). So the *Archaea* are widely distributed, especially in the oceans as they constitute up to 30 % of the entire picoplanktonic cell population (DeLong, 2001). Hence, they have to be considered as significant components of the global ecological system, both, because of their substantial contribution to total biomass, but also due to their presence at a variety of hostile environments. Adaption to high temperatures for example is common within the *Archaea*, since all archaeal phyla include hyperthermophilic species (Gribaldo and Brochier-Armanet, 2006). However, though they are also found within the bacterial branch, hyperthermophiles are clearly dominated by the *Archaea*. Exposed to temperatures above 80°C these organisms are mainly challenged to prevent denaturation of their proteins and nucleic acids as well as maintaining stability of their cytoplasmic membrane. Psychrophilic *Archaea* in contrast, living at low temperatures, run the risk of getting damaged due to the formation of ice crystals (Rothschild and Mancinelli, 2001). However, *Archaea* can also be adapted to other tasking conditions such as radiation, high pressure e.g. at deep aquatic environments (barophily) or extensive desiccation (xerophily) (Marteinsson *et al.*, 1999; Rothschild and Mancinelli, 2001; Zivanovic *et al.*, 2009). Cellular desiccation can be achieved simply by reduced availability of water, but also by the presence of high salt concentrations in the external environment (Rothschild and Mancinelli, 2001). Organisms living under such conditions, the so called halophiles, have to cope with osmotic stress due to a continuous efflux of water from the cytoplasm to the surrounding medium, resulting in cellular dehydration. Thus, they have to make use of certain strategies to keep their osmotic balance (Oren, 1999). Moreover in many cases adaption to high salinity implies the absolute requirement of extracellular ions in order to maintain cellular stability. Yet, there are also halotolerant microbes which are able to live under high salt concentrations for a certain period of time, but are not addicted to it (Rothschild and Mancinelli, 2001). Within the archaeal lineage halotolerant and halophilic species are members of the euryarchaeal order *Halobacteriales* and the class *Methanotherma*, respectively (Oren, 2008a). The former order also includes a certain group of

organisms adapted to both, high salinity and high pH values: the haloalkaliphiles (Kamekura *et al.*, 1997). In addition to osmotic demands, these *Archaea* are energetically challenged due to the limitation of H<sup>+</sup>-ions in the surrounding medium. As well as acidophilic organisms living at low pH, alkaliphiles are capable of extruding the external milieu by active and passive mechanisms, maintaining a neutral cytoplasmic pH, thereby preventing denaturation of internal biological structures. Anyway, strategies enhancing stability of the genome, proteins and membranes as well as efficient repair mechanisms reducing cellular damage are essential in microbes exposed to rough environmental conditions in general (Rothschild and Mancinelli, 2001). Those approaches enabling life at high salt concentrations and elevated pH values will be discussed in the next chapter in detail.

### 1.1.5. Halophilic and haloalkaliphilic *Archaea*

Halotolerant and halophilic representatives are found in all three domains: the *Eucarya*, the *Bacteria* and the *Archaea* (Oren 2002). Usually they are phylogenetically mixed with non-halophilic relatives, forming inhomogeneous taxonomic lineages. Yet, there are three groups comprising halophilic organisms almost exclusively. Two of them belong to the bacterial lineage: the aerobic, heterotrophic *Bacteria* of the family *Halomonadaceae* (*Gammaproteobacteria*) and anaerobic, fermentative *Bacteria* of the order *Halanaerobiales* (*Firmicutes*). The third group however is an archaeal family branching from the euryarchaeal order *Halobacteriales*: the *Halobacteriaceae* (Oren, 2008a). Beside, a methanogene class of the *Euryarchaeota*, the *Methanotherma*, also contains species living at hypersaline environments, yet this group mainly consists of moderate halophiles. Anyway, no halotolerant or halophilic members are known within the other three archaeal phyla (Oren 2002; Oren, 2008a).

However, in the course of this work only halophilic *Archaea* assigned to the *Halobacteriaceae* are on the focus of closer consideration. This family is composed of 26 genera known to date: *Halobacterium*, *Haloadaptus*, *Halalkalicoccus*, *Haloarcula*, *Halobaculum*, *Halobiforma*, *Halococcus*, *Haloferax*, *Halogeometricum*, *Halomicrobium*, *Halopiger*, *Haloplanus*, *Haloquadratum*, *Halorhabdus*, *Halorubrum*, *Halosimplex*, *Halostagnicola*, *Haloterrigena*, *Halovivax*, *Natrialba*, *Natrinema*, *Natronobacterium*, *Natronococcus*, *Natronolimnobius*, *Natronomonas*, and *Natronorubrum* (Oren, 2008b). All of them are strictly aerobic organisms, mainly extreme halophiles which totally require salt concentrations of more than 20 % for optimal growth (Lanyi, 1974). They are widespread over a broad range of hypersaline habitats, including marine water (e.g. the Dead Sea), soda lakes and saltern crystallizer ponds as well as environments resulting from evaporation of seawater (Oren 2002). In addition to the high concentrations of NaCl, some hypersaline lakes like Lake Magadi

(Kenya) or Wadi Natrun (Egypt) exhibit especially high pH values ranging from 10.5 to 12. The haloalkaliphilic *Archaea* populating these habitats, e.g. members of the genera *Natrialba*, *Natronobacterium* or *Natronomonas*, are well established at the predominating conditions, reaching titres up to  $10^8$  cells per ml of water (Horikoshi, 1999). Hence, they have to be highly adapted to both, high salt concentrations and high pH values.

#### **1.1.5.1. Adaptions to hypersaline conditions**

As already mentioned above, the main challenge for organisms living in hypersaline habitats is the regulation of their osmotic state since high concentrations of salt in the external medium usually result in rapid loss of water to the environment (Oren, 1999). In the microbial world two fundamentally different tactics have evolved to overcome this problem. The so called “high-salt-in strategy” implies the compensation of the high external NaCl concentrations by the accumulation of salt (usually KCl) inside the cell. As a result both, intracellular and extracellular proteins are exposed to high salinity; hence specific adaptations are required to maintain their function (Oren, 1999; Oren, 2008a). The strategy used by most halophilic organisms in contrast, the “compatible solute strategy”, does neither include a change in intracellular salt concentrations nor general proteomic adaptations. Instead of this it is based on the biosynthesis and/or uptake of low-molecular-weight compounds working as organic osmotic solutes such as polyols (e.g. glycerol), sugars, amino acids and derivatives as well as glycine betaine (Oren, 1999; Oren, 2008a). These organic compatible solutes are known to interact with cellular enzymes, protecting them from harmful effects, thereby supporting their functionality at stressful conditions. However, the production of these molecules requires high energetical investment, hence this mechanism is much more expensive than the “high-salt-in strategy” (Oren, 1999). So it can be concluded that both strategies involve advantages for halophilic cells: while using organic compatible solutes for osmoregulation does not require adaptations of the entire proteomic machinery, intercellular accumulation of potassium chloride is less costly. Nevertheless, the “high-salt-in strategy” is much less widespread in nature than the “compatible solute strategy” as it is not applied by halophilic *Eucarya* at all and limited to one bacterial order, the *Haloanaerobiales*. Within the archaeal domain however, this approach is of central importance as it is commonly used by the extreme halophilic members of the family *Halobacteriaceae* (Oren, 1999; Oren, 2008a). On one hand haloarchaea, like halophiles in general, have to be able to totally exclude sodium chloride from the interior of the cells which is mainly achieved by  $\text{Na}^+/\text{H}^+$ -antiporters (Oren 2002). Yet, in addition they have to show significant alterations in their cellular membranes, as well as in both, intracellular and extracellular proteins in order to enable stability in contact with external and internal hypersaline conditions.

Cellular membranes: As already discussed in detail archaeal membranes are highly stable in general as they possess *sn2,3* isoprenyl ether lipids (Glansdorff *et al.*, 2008). In addition the membranes of extreme halophilic *Archaea* like the *Halobacteriaceae* share some unique structural and compositional characteristics which are found within these group of organisms exclusively. For example the lipids completely lack inositol, serin and ethanolamine head groups (Technov *et al.*, 2006). The most striking feature however is the common presence of archaetidylglycerol methylphosphate (PGP-Me), an archaeal analogue of phosphatidylglycerol methylphosphate. This certain phospholipid is limited to haloadapted membranes where it amounts to 50-80 % of the polar membrane lipids, suggesting a function in enhancing membrane stability at high salt concentrations. Indeed the relevance of PGP-Me to prevent aggregation of membranes under these conditions could be demonstrated (Technov *et al.*, 2006).

Proteomic adaptations: Most importantly, the proteins adapted to high salt concentrations are characterized by a large proportion of acidic amino acids like glutamic and aspartic acid. For example in *Halobacterium* species these residues were determined to contribute more than 10 mole percent of the total content, resulting in very low isoelectric points around 4.2. In cell envelope proteins they were even stated to account for about 20 mole- % (Reistadt, 1970; Fendrihan, 2006). Yet, this high excess of negative charges within haloadapted proteins leads to repulsive electrostatic forces which can be compensated by additional linkages preventing protein unfolding, e.g. residue interactions or disulfide bridges (Lanyi, 1974). Further effects crucial for the stability of the proteins are hydrophobic interactions. Exposed to high salt concentrations proteins get tightly packaged. Hence, some residues which use to get in contact with the aqueous phase at low salinity may preferentially be buried in the interior of the protein at hypersaline conditions, resulting in the formation of new hydrophobic bonds (Lanyi, 1974). Although they are reduced in their number, these interactions are highly important since hydrophobic amino acids were found to be rare in haloadapted proteins (Lanyi, 1974; Fendrihan, 2006). Yet, other studies indicated that only the content of aliphatic amino acids with longer side chains is low, while the number of small residues such as glycine, alanine or valine is increased (Madern *et al.*, 1995). However, to maintain the hydrophobic interactions stabilizing halophilic proteins, high amounts of salt in the surrounding solutes are absolutely necessary (Fendrihan, 2006). Moreover especially cations were shown to be of crucial importance for the stability, as they interact with the highly negatively charged haloadapted biological structures (Lanyi, 1974). Yet, due to these proteomic adaptations, members of the *Halobacteriaceae* totally depend on the presence of high salt concentrations. Thus, compared to some organisms applying the “compatible solute”, they are not able to tolerate a low salt content in the external environment and hence are limited to hypersaline habitats exclusively (Oren, 1999; Oren, 2008a).



### 1.1.5.2. Adaptations to high pH

Although alkaliphilic organisms are exposed to high pH values in their natural habitats (above pH 9), estimation of the internal pH revealed that their cytoplasm is in a neutral rather than in an alkaline range. For example the internal pH of one alkaliphilic bacterial member, the *Micrococcus* sp. strain 31-2, was determined to be around pH 7.5 based on the catalytic pH optimum of the intracellular enzyme  $\beta$ -galactosidase. Furthermore also approaches implying the detection of weak bases distributed inside and outside of the cells supported the assumption of an almost neutral intracellular pH (Horikoshi, 1999). As a result, in contrast to cell walls and membranes, intracellular proteins do not have to be adapted to alkaline conditions. Nevertheless, concerning proteins which are segregated to the extracellular medium, specific alterations are absolutely required in order to enable stability at high pH. However, all approaches enhancing these adaptations imply a modulation of the amino acid composition. One strategy is based on the variation of amino acids which are involved in the formation of hydrogen bonds, resulting in a shift of the pKa towards higher values. Another possibility, like in haloadapted proteins, is an increased content of acidic amino acids (aspartic and glutamic acid) resulting in highly negative net charge of the proteins (Shirai *et al.*, 2008). The latter phenomenon however is also found in alkaline cell bordering structures like cell walls and membranes which are often characterized by a large excess of acidic polymers. Studies on *Bacillus* species for example indicate that polymers such as gluconic, galacturonic, glutamic and aspartic acid are common in cell walls of alkaliphilic members, while they are absent in those of the neutrophilic *Bacillus subtilis*. The function of these additional negative charges is supposed to be the adsorption of the positively charged  $\text{Na}^+$  and  $\text{H}_3\text{O}^+$  ions while hydroxide ions (dominating at high pH) are repulsed, hence reducing the pH at the immediate cell surface (Horikoshi, 1999).

However, in addition to its adaptations to alkaline conditions, the certain role of the cellular membrane in extruding the basic milieu from the interior of the cell has to be highlighted (Horikoshi, 1999). On one hand of course the membrane has to be completely impermeable for certain ions in order to separate the external and internal conditions. On the other hand active transporters are needed to maintain the optimal intracellular milieu and generate electrochemical gradients (Horikoshi, 1999; (van de Vossenberg *et al.*, 1999). The major transport systems used by haloalkaliphilic *Archaea* are  $\text{Na}^+/\text{H}^+$ -antiporters combined with  $\text{H}^+$ -coupled respiration in order to regulate the pH within the cell. These  $\text{Na}^+/\text{H}^+$ -antiporters drive both, the uptake of  $\text{H}^+$  and the extrusion of  $\text{Na}^+$  at the same time, establishing an optimal system under haloalkaline conditions as sodium ions are abundant in hypersaline environments while protons are rare at high pH (van de Vossenberg *et al.*, 1999). However, the formation of an electrochemical gradient due to  $\text{H}^+$  transport results in the generation a proton motive force (pmf) composed of two factors: the transmembrane

electric potential ( $\Delta\Psi$ ) and the transmembrane pH gradient ( $\Delta\text{pH}$ ) (van de Vossenberg *et al.*, 1999). This energetic storage is finally able to drive endogenous processes in haloalkaliphilic cells.

### **1.1.6. *Natrialba magadii***

A typical representative of haloalkaliphilic *Archaea* belonging to the euryarchaeal family *Halobacteriaceae* is *Natrialba magadii*. Together with other prokaryotes this rod shaped archaeon populates one of the highly alkaline soda lakes of the east African Rift valley, the Lake Magadi in Kenya (Jones *et al.*, 1998). When *Nab. magadii* was first isolated from its natural habitat in 1984, it was assigned to the genus *Natronobacterium* according to its morphology. By that time the discovered microorganisms were divided into two groups: rods forming the genus *Natronobacterium* and cocci, combined to the genus *Natronococcus* (Tindall *et al.*, 1984). In 1997 however comparative analysis of 16S rRNA highlighted the close phylogenetic relationship of the former *Natronobacterium magadii* to two *Natrialba asiatica* strains (93.3 and 93.7 % sequence similarity, respectively), resulting in the transfer of *Natronobacterium magadii* to the genus *Natrialba* (Kamekura *et al.*, 1997). Although this classification is not supported by analysis of membrane lipids, it is still accepted today.

#### **1.1.6.1. Characteristics of *Nab. magadii***

The cells of *Nab. magadii* are motile rods with a length of 0.5 – 0.7 $\mu\text{m}$  (Tindall *et al.*, 1984). Like other members of the *Halobacteriaceae* they have an orange to red color due to the presence of carotenoids (e.g.  $\alpha$ -bacterioruberin) stored in their membrane, leading to reddish coloration of the water they inhabit (Oren, 2002). Cultivated in the laboratory, optimal growth of *Nab. magadii* was observed at 4M sodium chloride and pH values of 8.5 – 10.5. However, to avoid lysis of the cells concentrations of at least 2M NaCl are absolutely required. In addition, reflecting the lack of these ions in its natural environment, low concentrations of  $\text{Mg}^{2+}$  (below 10mM) are needed. Moreover *Nab. magadii* is sensible to low temperatures while optimal growth is achieved at 37 – 42°C (Tindall *et al.*, 1984). However, even at ideal conditions one generation cycle takes about nine hours in the logarithmic growth phase; hence *Nab. magadii* grows very slowly compared to other, more popular microorganisms, e.g. *E. coli* (generation time: 20 minutes).

### 1.1.6.2. Two laboratory strains: L11 and L13

In 1997, spontaneous lysis of the *Nab. magadii* wild type strain isolated from its natural habitat gave rise to the discovery of a temperate virus persisting in this archaeon during its lysogenic cycle: the halophage  $\phi$ Ch1 (Witte *et al.*, 1997). However, repeated subculturing and testing of single colonies of the original organism revealed a non-lysogenic *Nab. magadii* strain, termed L13. In contrast to the wild type strain carrying  $\phi$ Ch1 as a prophage, this cured strain can be re-infected with the virus, hence serving as an indicator strain. In addition, for laboratory work a *Nab. magadii* strain resembling the wild type was isolated from plaques resulting from re-infection of L13. This strain, named L11, of course contains the virus  $\phi$ Ch1 which is integrated into the host chromosome until it enters the lytic cycle during stationary growth of the *Nab. magadii* culture (Witte *et al.*, 1997). Both strains, L11 and L13 (see figure 2), are currently used in our laboratory for detailed studies of  $\phi$ Ch1 and its host *Natrialba magadii*, respectively.

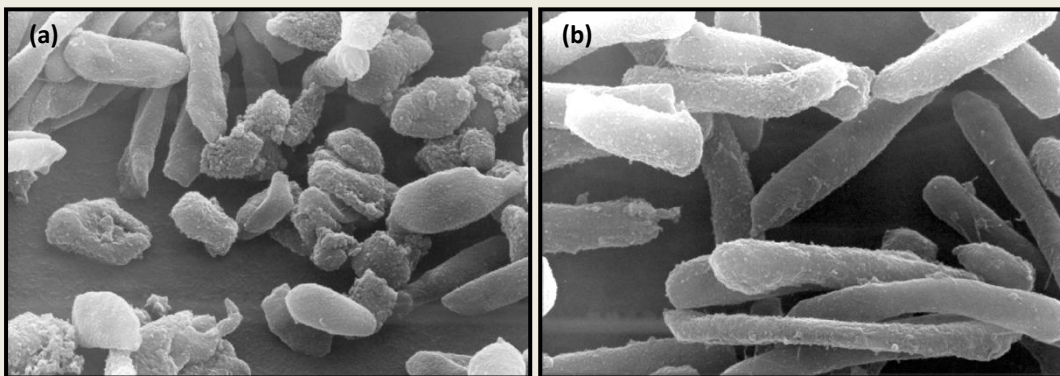


**Figure 2** | *Natrialba magadii*. Electron micrographs of the haloalkaliphilic archaeon *Nab. magadii*, initially isolated from Lake Magadi (Kenya). **(a)** Wild type strain L11 carrying  $\phi$ Ch1 as a prophage. **(b)** Strain L13, cured from the virus.

### 1.1.6.3. *Nab. magadii* in the lab – transformation, vectors, genetic markers

In the very beginning of working with *Nab. magadii* in the laboratory, neither selection markers and vectors, nor an efficient transformation method for haloalkaliphilic *Archaea* was available. However, the transformation strategy applied today is derived from an approach evolved in 1987 by Cline and Doolittle for the transfection of the halophilic archaeon *Halobacterium salinarum* (initially termed *Halobacterium halobium*) with the DNA from the phage  $\phi$ H. This method is based on the generation of spheroblasts by treatment with EDTA. This chelating agent withdraws

Mg<sup>2+</sup> ions stabilizing the S-layer, thereby resulting in the removal of this glycoproteinaceous envelope and, thus, enables transfection of the competent cells. The uptake of foreign DNA however was mediated by coupling to polyethylene glycol 600 (PEG 600) (Cline and Doolittle, 1987). Later on, based on this principle, methods for the transformation of several archaeal species were developed and summarized in a manuscript termed “The Halohandbook” (Dyall-Smith, 2008). In alkaliphilic *Archaea* like *Nab. magadii* however the S-layer is not stabilized by divalent cations, thus it cannot be affected by the addition of EDTA. Instead of this, spheroblast cells of *Nab. magadii* can be generated by primary treatment with bacitracin, an agent interfering with the glycosylation of the S-layer proteins, followed by partially enzymatic digestion performed by proteinase K. Immediately afterwards, introduction of foreign DNA by PEG mediated transformation is possible (Iro *et al.*, in prep). This method evolved in the laboratory of Angela Witte is still successfully used today.

Anyway, for the transformation of *Natrialba magadii* shuttle vectors for *E. coli* and *Nab. magadii* had to be constructed. The first vector working efficiently in both organisms was developed by Iro and co-workers (Iro *et al.*, in prep). This plasmid is based on the construct of a pKS<sub>II</sub><sup>+</sup> vector, hence possessing an origin of replication active in *E.coli* as well as an ampicillin resistance (*bla*) for cloning in the bacterium. This system was supplemented with the *gyrB* gene of *Haloferax alicantei*, providing a novobiocin resistance for selection in *Nab. magadii*, yielding the vector pNov-1. Moreover, to enable amplification in the archaeon, different constructs of the region comprising the putative origin of replication of the *Nab. magadii* specific phage  $\phi$ Ch1 were cloned onto this vector. This region, ranging from ORF53 to ORF54, shows remarkable sequence homologies to the *repH* gene of pNRC100, a plasmid found in *Haloarcula marismortui* (Iro *et al.*, in prep). In general, RepH is known to be a part of the replicons of plasmids persisting in halophilic *Archaea* (Ng and DasSarma, 1993; Klein *et al.*, 2002). Hence, this region of  $\phi$ Ch1 was supposed to enable the replication of the new shuttle vector in *Nab. magadii* too. Indeed, incorporation of three different fragments into pNov-1 yielded high transformation efficiencies of the corresponding plasmids, termed pRo-3, pRo-5 and pRo-6. The best results however were achieved with the vector pRo-5, which has successfully been employed for transformation of *Nab. magadii* up to date (Iro *et al.*, in prep).

Only few other plasmids of haloarchaea, e.g. pNB102, can be used in *Nab. magadii*. However, the production of different shuttle systems is constricted by the poor presence of genetic markers, as most antibiotics working in *Bacteria* are not active in *Archaea*. However, two selectable markers are commonly used in *Nab. magadii*: resistances against novobiocin (*nov*) and mevinolin (*mev*), respectively. In *Bacteria* the antibiotic novobiocin is known to prevent the binding of ATP to the B subunit of the DNA gyrase, an enzyme working on the introduction of negative supercoils into the bacterial genome. As a result the function of this enzyme is blocked, causing inhibition of bacterial

growth (Holmes and Dyall-Smith, 1991). The same effect was observed in *Archaea*, suggesting a similar mechanism in targeting the DNA gyrase of this domain. The resistance to novobiocin however was discovered in a spontaneous mutated strain of the genus *Haloferax*. Comparative analysis of this mutant and the wild type genome revealed the presence of three base exchanges in the ATP binding region of the DNA gyrase, probably resulting in a reduced affinity of the archaeal enzyme to the drug in the resistant cells (Holmes and Dyall-Smith, 1991).

Just like novobiocin, the mevinolin resistance determinant was initially isolated from a *Haloferax* strain (Lam and Doolittle, 1992). Investigation of further mutants revealed that tolerance to mevinolin can be achieved by two different kinds of alterations: the introduction of a point mutation in the promoter region and a variation in the number of tandem repeat elements. Both events however result in an overexpression of the gene coding for the 3-hydroxy-3-methylglutaryl-coenzyme A (HMG-CoA) reductase, which is usually inhibited by mevinolin. In *Archaea* this enzyme is of crucial importance as it catalyses synthesis of mevalonate, which is urgently needed for the production of isoprenoid side chains, components of the peculiar archaeal lipids (Lam and Doolittle, 1992).

## 1.2. Archaeal viruses

The first archaeal virus ever discovered (later termed Hs1) was isolated in 1974 by Torsvik and Dundas from its host *Halobacterium salinarum* (former *H. halobium*), immediately followed by Ja1, another halovirus infecting a broader range of halophilic *Archaea*. Both viruses possess icosahedral heads surrounding dsDNA genomes as well as contractile tails, thereby resembling bacteriophages of the family *Myoviridae*, e.g. phage T4 (Torsvik and Dundas, 1974; Wais *et al.*, 1975; Torsvik and Dundas, 1980). The description of further viruses found in members of the archaeal domain in the following years strengthened the idea that this head-tail composition was the predominating morphotype in archaeal viruses (Prangishvili *et al.*, 2006a). However, this assumption turned out to be not correct since, on the contrary, a high variety of particle forms was found in samples derived from natural archaeal habitats (Prangishvili 2003; Prangishvili *et al.*, 2006a). Most of these morphotypes are very unique, limited to the archaeal domain, exclusively. Compared to bacterial viruses which mainly comprise non-enveloped head-tail particles (96 % of all dsDNA phages), only few archaeal viruses known today exhibit the typical head-tail morphology (Prangishvili *et al.*, 2006a). All of them infect members of the phylum *Euryarchaeota*, whereas the more peculiar morphotypes are mainly associated with the *Crenarchaeota*. In addition, the viruses of both phyla are highly

different in terms of their life styles. While euryarchaeal viruses grow lytically or lysogenic, often integrating into the host-chromosome, crenarchaeal viruses are characterized by stable relationships to their mainly hyperthermophilic hosts without bursting the cells, thereby avoiding contact with the almost harsh environments (Prangishvili *et al.*, 2006b). Anyway, despite these differences, in fact all of them possess either a linear or a circular double stranded DNA genome (Prangishvili *et al.*, 2006a).

Surprisingly however, primary categorization of archaeal viruses is neither based on the nature of their hosts nor on genomic features, but rather on morphological criteria. As a result the archaeal head-tail viruses are assigned to two families predominated by bacterial head-tail phages: the *Myoviridae* and the *Siphonoviridae* (Prangishvili *et al.*, 2006). In contrast many new families arise from the highly variable morphotypes found in the crenarchaeal lineage, including fusiform, bottle and droplet shaped, linear as well as spherical virions (Prangishvili *et al.*, 2006a).

### 1.2.1. Morphotypes – classification of archaeal viruses

Fusiform viruses are common in both, euryarchaeal and crenarchaeal hosts, including extreme halophilic, methanogene as well as hyperthermophilic species. Most of them are characterized by a temperate lifestyle and a circular organization of their genome. The nearly lemon-shaped virions of this morphotype are unique to the archaeal viruses and can be complemented by either one or two tails. These structural features, as well as genomic characteristics result in the division into two families, the *Fuselloviridae* (e.g. SSV1) and the *Bicaudaviridae* as well as one additional genus, the *Salterprovirus* (Prangishvili *et al.*, 2006a). One certain representative of the fusiform viruses is the *Acidianus* two-tailed virus (ATV), the sole member of the *Bicaudaviridae* family (see figure 3). This virus infects species of the genus *Acidianus*, which occur at acidic, hot springs; hence at an extracellular state it is usually exposed to high temperatures (Häring *et al.*, 2005b). Temperatures above 75°C induce the emerging of the typical two tails at both ends on the initially tail-less particles, probably mediating the adsorption to host cells. This mechanism of tail development however is absolutely unique in the viral world, limited to a few members of fusiform archaeal viruses (Prangishvili *et al.*, 2006a).

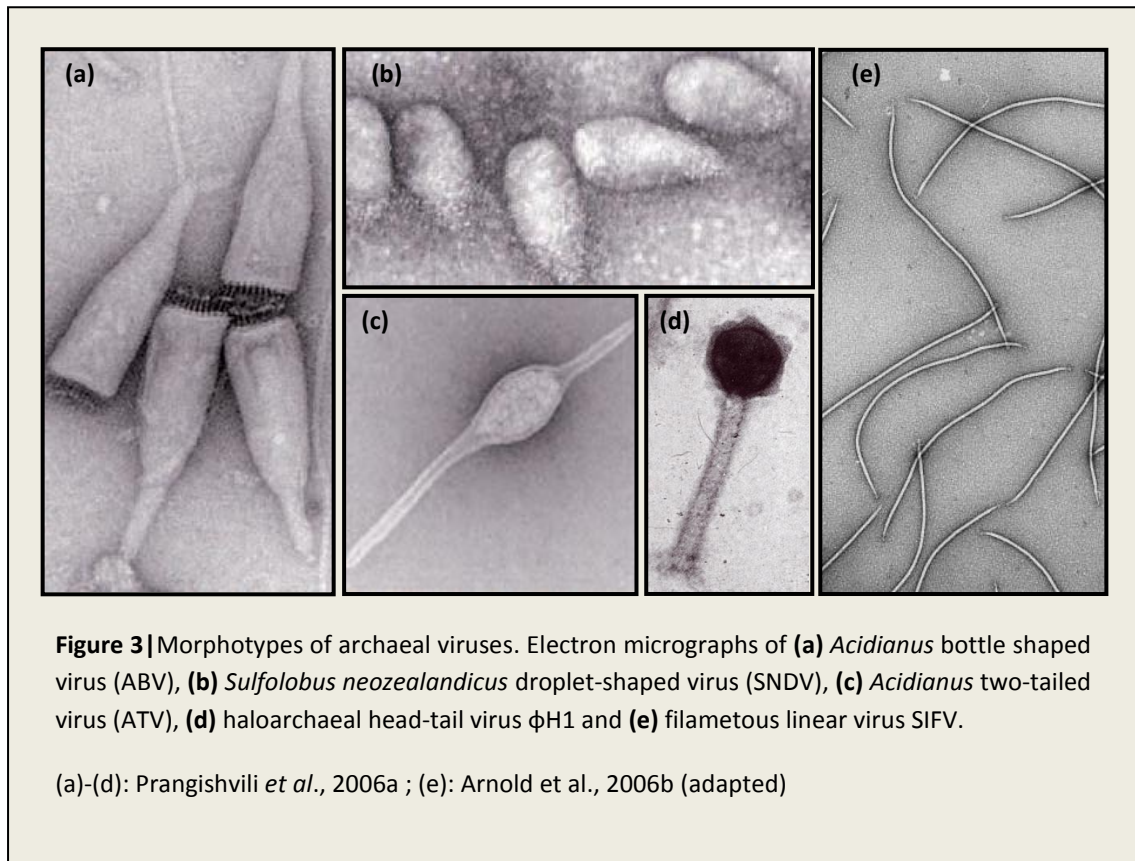
Another two, probably even more peculiar morphotypes give rise to the distinction of two further families: the *Ampullaviridae* (bottle-shaped virions) and the *Guttaviridae* (droplet-shaped virions). Each of them includes only one member, the *Acidianus* bottle-shaped virus (ABV) and the *Sulfolobus neozealandicus* droplet-shaped virus (SNDV), respectively (see figure 3). Nevertheless they

represent own families due to the inimitability of their particle forms (Häring *et al.*, 2005a; Arnold *et al.*, 2000a).

The linear viruses are also subdivided into two groups causing classification of two new families, the ***Rudiviridae*** (e.g. SIRV1) and the ***Lipothrixiviridae*** (e.g. SIFV, see figure 3), respectively. Both possess tube-shaped particles, but the *Rudiviridae* are stiff and straight including short polar tail fibre structures, while the *Lipothrixiviridae* are flexible and usually enveloped (Prangishvili *et al.*, 1999; Arnold *et al.*, 2000b; Prangishvili *et al.*, 2006a). They are highly dispersed at hot, terrestrial environments, infecting members of the crenarchaeal phylum such as *Acidianus*, *Sulfolobus* and *Thermoproteus* species (Prangishvili *et al.*, 2006a).

Compared to other morphotypes, the number of spherical viruses is generally low. Like linear viruses however some of them are associated with the *Crenarchaeota*, infecting hyperthermophilic species of the genera *Thermoproteus* and *Pyrobaculum*. These viruses, such as *Pyrobaculum* spherical virus (PSV) are taxonomically pooled together due to their genomic properties, forming the family ***Globuloviridae*** (Häring *et al.*, 2004). The other sort of spherical viruses found in both, *Crenarchaeota* and *Euryarchaeota*, is assigned to the bacterial family ***Tectiviridae*** (Prangishvili *et al.*, 2006a).

However, apart from a few spherical and fusiform members, most viruses infecting *Euryarchaeota* are head-tail viruses (see figure 3). Their host range comprises mesophilic and moderately thermophilic methane producing *Archaea* as well as extreme halophiles. As already mentioned they resemble bacterial head-tail phages in their composition, hence they are assigned to two families of bacteriophages: the ***Myoviridae***, including particles with contractile tail and the ***Siphonoviridae***, implying non-contractile tails. Though they are highly different concerning the size of their head and tails, all of them contain genomes consisting of linear dsDNA (Prangishvili *et al.*, 2006a; Prangishvili *et al.*, 2006b). Anyway, as this morphotype is most common in halophages, it is in the centre of focus in further discussions.



### 1.2.2. Haloarchaeal viruses

As described above, the first archaeal viruses were discovered in halophilic hosts including *Halobacterium salinarum* and hence happened to be the first haloviruses as well (Torsvik and Dundas, 1974; Wais *et al.*, 1975). During the following 15 years, the number of haloviruses increased to a total of nine members, all of them infecting *H. salinarum* (Dyall-Smith *et al.*, 2003). Later on, also other archaeal genera of the family *Halobacteriaceae*, e.g. *Haloarcula* and *Natrialba*, were found to carry virus-like particles (Prangishvili *et al.*, 2006a). Anyway, considering their high presence in hypersaline waters like the Dead Sea (titres around  $10^7$  pfu/ml), the number of described haloarchaeal viruses is surprisingly low (Dyall-Smith *et al.*, 2003). As mentioned above, the majority of known haloviruses exhibit a head-tail composition, yet the dominating morphotype found in samples from natural aquatic environments is the fusiform (Oren *et al.*, 1997; Dyall-Smith *et al.*, 2003). Well described examples for the latter morphotype are His1 and His2, two members of the genus *Salterprovirus*, both infecting *Haloarcula hispanica*. Though they are quite distant relatives they share a lytic life style as well as a linear dsDNA chromosome. However, only His1, but not His2 resembles the *Sulfolobus* spindle shaped virus (SSV1) on a morphological level (Bath and Dyall-Smith, 1998; Dyall-Smith *et al.*, 2003; Bath *et al.*, 2006). In contrast, two important representatives demonstrating the nature of head-tail phages are HF1 and HF2. Both viruses grow lytically and are



not integrating into the host genome. They were isolated from the same lake and are highly identical in terms of their virion shape and genome (80 % sequence identity), yet they infect a completely different range of hosts, including *Haloarcula*, *Halobacterium*, *Haloferax* and *Natrialba* (Nuttall and Dyall-Smith, 1993). However, there are numerous viruses showing this morphotype, e.g.  $\Psi$ M2 (Pfister *et al.*, 1998) and  $\Psi$ M199 (Luo *et al.*, 2001), yet only few of them are well described. Anyway, the best studied haloarchaeal head-tail virus is  $\phi$ H. Like other phages possessing icosahedral heads and contractile tails, it is assigned to the family *Myoviridae*, resembling bacteriophage P1 in terms of morphology as well as replication strategies and control of lysogeny (Dyall-Smith *et al.*, 2003). To maintain structural stability it requires concentrations of at least 3M sodium or potassium chloride, reflecting the halophilic nature of its host, *Halobacterium salinarum*. The 59 kb genome of  $\phi$ H consists of linear dsDNA and is characterized by an excess of guanine and cytosine (65 %). Moreover, it is terminally redundant and partially circularly permuted, mediating a headful packaging mechanism. Like one close relative, the halophage  $\phi$ Ch1 infecting *Nab. magadii*,  $\phi$ H is a temperate virus, switching between a stable lysogenic and a lytic cycle. Yet, in contrast to the  $\phi$ Ch1-DNA which integrates into the host genome,  $\phi$ H exists as circular prophage DNA in the host cell during its lysogenic state (Schnabel *et al.*, 1982). In addition, due to insertion elements flanking a certain part of the  $\phi$ H genome, the so called L-segment, an inversion event can lead to the exclusion of this region as a circular plasmid. This plasmid, termed p $\phi$ HL, can persist stably in the host cells, resulting in resistance to further  $\phi$ H infections, independently from the presence of the virus itself (Schnabel *et al.*, 1984). Interestingly the L-segment strongly resembles the central part of the genome of its relative  $\phi$ Ch1 (50 – 97 % sequence identity). Nevertheless, due to the lack of insertion elements in  $\phi$ Ch1, this special mechanism is unique to  $\phi$ H (Gropp *et al.*, 1992; Klein *et al.*, 2002).

### **1.2.3. $\phi$ Ch1 – a haloalkaliphilic virus**

As already mentioned above,  $\phi$ Ch1 was discovered in 1997 as a consequence of spontaneous lysis of the haloalkaliphilic archaeon *Nab. magadii*. Up to date, no other host of this virus has been found. Like *Nab. magadii*,  $\phi$ Ch1 is adapted to high salt concentrations as well as elevated pH values and, thus, has to be considered as the first (and so far only) haloalkaliphilic virus ever described infecting a member of the archaeal branch (Witte *et al.*, 1997). Yet, even though it is used to another pH range,  $\phi$ Ch1 is very similar to the halophilic virus  $\phi$ H with respect to several genomic and structural features. Like the latter, it belongs to the family of *Myoviridae*, hence possessing contractile tails and icosahedral heads (Schnabel *et al.*, 1982; Witte *et al.*, 1997). Both particles contain a linear dsDNA genome of almost equal size, which is terminally redundant. As a result, a similar packaging

mechanism based on circular permutation can be suggested (Schnabel *et al.*, 1982; Klein *et al.*, 2002). Moreover the two viruses share a temperate life style, albeit  $\phi$ Ch1 integrates into the host chromosome, whereas  $\phi$ H persists in the cell in an episomal state (Schnabel *et al.*, 1984; Witte *et al.*, 1997). However, already in 2002 when the complete DNA sequence of  $\phi$ Ch1 was established, it was stated that the genome sequences of these two viruses are highly similar. Especially the central part of the  $\phi$ Ch1 genome was found to resemble the L-segment of  $\phi$ H since comparative analysis revealed a nucleotide identity of 50-97 % (Klein *et al.*, 2002). Yet, by that time only about 60 % of the  $\phi$ H genome were sequenced (Dyall-Smith *et al.*, 2003). Recently, however, the complete sequence of the  $\phi$ H DNA has been determined too (Dyall-Smith, personal communication), hence enabling the observation of further crucial similarities between  $\phi$ H and  $\phi$ Ch1 in prospective studies.

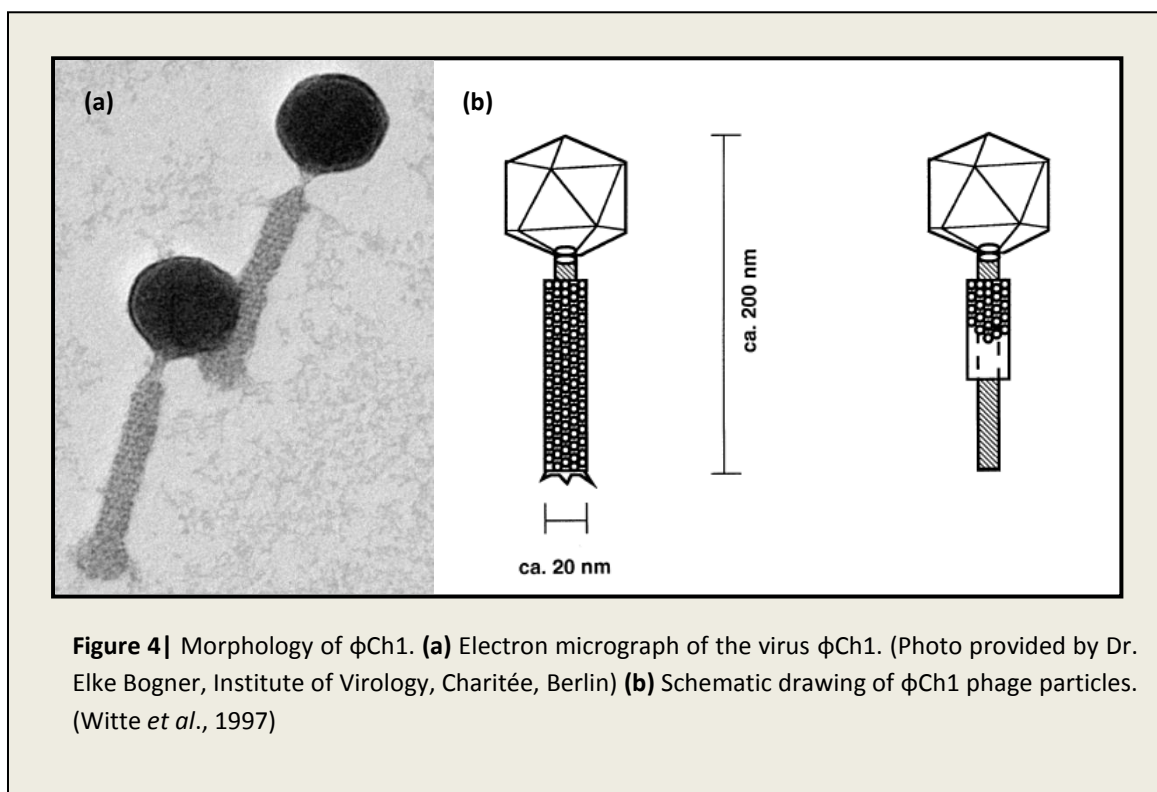
All this correlations of  $\phi$ Ch1 and  $\phi$ H suggest a close relationship of these two viruses, though their hosts are phylogenetically distant, inhabiting different environments with varying conditions. Nevertheless, the presence of pH gradients in saline lakes may have enabled a quite near localization of *Nab. magadii* and *H. salinarum* and, thus, the exchange of certain genetic modules between  $\phi$ Ch1 and  $\phi$ H in course of evolution (Klein *et al.*, 2002; Dyall-Smith *et al.*, 2003).

Anyway, today, both viruses belong to the best studied viruses infecting haloarchaeal hosts. Though  $\phi$ H was the first of them to be discovered and in the centre of extensive research from 1982 to 1994 (Dyall-Smith *et al.*, 2003),  $\phi$ Ch1 established a certain role as the only known virus of haloalkaliphilic *Archaea*. Due to detailed investigations of  $\phi$ Ch1 highlighting general properties of this virus and the function of several gene products involved in certain mechanisms, the knowledge about  $\phi$ Ch1 can not be considered as minor important compared to  $\phi$ H. Moreover past projects yielded several methods and supporting tools (e.g. shuttle vectors) enabling work with this virus and its haloalkaliphilic host *Nab. magadii*, respectively (Witte *et al.*, 1997; Baranyi *et al.*, 2000; Klein *et al.*, 2000; Klein *et al.*, 2002; Rössler *et al.*, 2004; Iro *et al.*, 2007).

### **1.2.3.1. Morphology and structural proteins of $\phi$ Ch1**

As a member of the family *Myoviridae*,  $\phi$ Ch1 is characterized by a typical head-tail morphology (illustrated in figure 4). The particles are composed of icosahedral heads which are 70nm in diameter and contractile tails 130nm in length, assembling to virions with a total length of 200nm. The contractile tails cover an internal shaft, yielding structures with a width of approx. 20nm. Moreover, on electron micrographs certain structural elements are visible at the ends of the tails: the tail fibres (Witte *et al.*, 1997). Like most haloadapted proteins, the tail fibre protein of  $\phi$ Ch1 has a low isoelectric point (pI = 3.7) due to an excess of acidic amino acids. This however results in a mobility

shift of the 41-54 kDa protein during separation of phage protein extracts via SDS-PAGE, hence yielding a signal at 66 kDa. The expression of the protein can be detected at the beginning of the stationary growth phase (98h after inoculation), as it is usually the case for structural proteins (Rössler *et al.*, 2004). In many tailed bacteriophages tail fibre proteins are known to be involved in interaction with receptors on the surface of bacterial host cells, hence initiating the process of infection. A similar function however is supposed in the archaeal virus  $\phi$ Ch1, yet it has not been proven so far (Rössler *et al.*, 2004). In course of this work the relevance of the tail fibre protein for infection of the archaeal cells was observed by deletion of the putative corresponding gene region, the open reading frame 34 (ORF34).



Anyway, also other structural proteins of  $\phi$ Ch1 particles are well described and in the centre of scientific interest. The most important one is protein E, the main capsid protein of this virus, encoded by ORF11 of the  $\phi$ Ch1 genome. It is expressed in high amounts during the late phase of the viral life cycle and gets associated with the membrane of the host cell after translation. For the release of the progeny virus particles, proteolytic cleavage of protein E is necessary, yielding the mature 35.8 kDa protein (Klein *et al.*, 2000).

Apart from protein E, separation of complete mature phage particles on denaturing polyacrylamide gels enables discrimination of three further major proteins (A, H and I) as well as five minor proteins of  $\phi$ Ch1 (B, C, D, F and G) (Witte *et al.*, 1997). Interestingly, the major protein A

(80 kDa) shows the same N-terminal amino acid composition as the 14.4 kDa protein H, which is encoded by ORF19. Hence it is supposed that protein A is either a homo- or a heteromultimer of the gene product of ORF19 as well. Compared to the major structural proteins, minor proteins such as protein B, C and D (encoded by ORFs 9, 7 and 8, respectively) are present in much lower quantities in mature viral particles (Klein *et al.*, 2002). Though they are visible on protein gels as separate bands and can be detected by an antibody raised against the surface of  $\phi$ Ch1.

Furthermore all structural proteins of this halovirus in general are characterized by low isoelectric points, thus enabling exposure to high salinity and pH. As a result of these adaptations of viral proteins,  $\phi$ Ch1 particles are highly sensitive to low salt concentrations. Experiments based on dialysis of virions revealed that concentrations below 2M NaCl cause a loss of infectivity of  $\phi$ Ch1, either because of complete dissociation of the proteins, or due to dramatic changes in their conformation (Witte *et al.*, 1997).

### **1.2.3.2. Life cycle of $\phi$ Ch1**

Spontaneous lysis of the wild type strain L11 occurs at the beginning of the stationary growth phase, releasing mature particles of  $\phi$ Ch1. The delay in the onset of lysis suggests a lysogenic phase in addition to the lytic phase in the life cycle of the virus; hence  $\phi$ Ch1 is considered as a temperate phage. This means that previously to the formation of the phage particles, the virus exists in a prophage state, either by persisting in the host cell in an episomal state, or by integration into the host chromosome. The latter strategy was confirmed by hybridisation of the *Nab. magadii* chromosome with a  $\phi$ Ch1-specific DNA probe. This method also enabled mapping of the concrete position on the host-DNA where the phage is integrated (Witte *et al.*, 1997).

This temperate lifestyle however requires precise regulation. Past studies show the presence of two putative repressor genes probably involved in preventing early onset of the lytic cycle during the lysogenic state: ORF48 and ORF49 (Klein *et al.*, 2002). ORF48 resembles the sequence of the  $\phi$ H repressor, but yet is expressed constitutively during the whole life cycle of  $\phi$ Ch1. Thus it cannot be the control element defining the time point of lysis, albeit a function of ORF49 is assumed (Iro *et al.*, 2007). ORF49 in contrast is upregulated in the logarithmic and/or stationary growth phase and the corresponding gene product is supposed to inhibit another repressor which avoids the onset of lysis. This protein had already been suspected to be involved in regulation of the  $\phi$ Ch1 status since a spontaneous duplication of the gene region resulted in an earlier onset of lysis (Iro *et al.*, 2007). However in recent studies its function as a repressor of the lytic phase was investigated in detail and further confirmed.

### 1.2.3.3. Genomic organization of $\phi$ Ch1

The halovirus  $\phi$ Ch1 comprises a linear dsDNA genome with a size of 58 498 base pairs (Klein *et al.*, 2002). In addition mature particles contain several RNA species, yet they were confirmed to be completely host derived (Witte *et al.*, 1997). The DNA genome is terminally redundant and circularly permuted, indicating a “headful” mechanism of DNA-packaging similar to that observed in  $\phi$ H (Klein *et al.*, 2002). Its total nucleotide sequence was determined in 2002 by Klein *et al.*, thus enabling prediction of 98 open reading frames (ORFs) and their organization into functional genetic modules. All ORFs of the  $\phi$ Ch1 genome, except for four starting with GTG (ORFs 3, 41, 79 and 83, respectively), have an ATG as a start codon. They are arranged as transcriptional units as they are tightly packaged, predominately facing the same reading directions (Klein *et al.*, 2002). Moreover, the entire nucleotide sequence is characterized by an overproportional content of the bases guanine and cytosine (61.9 %), reflecting the constitution of the host genome (Witte *et al.*, 1997; Klein *et al.*, 2002). This feature is typical for members of the initially defined haloarchaeal group *Natronobacteria* in general (Tindall *et al.*, 1984).

Surprisingly however, in contrast to the genome of *Nab. magadii*, the DNA of  $\phi$ Ch1 was found to be partially methylated (Witte *et al.*, 1997). Restriction analysis revealed a Dam-like methylation of adenine residues within certain recognition sites (5'-GATC-3'), while modifications were not observed at any cytosine residues. Furthermore it was confirmed that methylation is restricted to some parts of the viral genome population and occurs on both DNA strands, whereas the rest of the genome completely lacks these modifications (Witte *et al.*, 1997). The reason for this phenomenon was found when the virus encoded enzyme performing these modifications, the methyltransferase M. $\phi$ Ch1-I, was identified. This enzyme is not expressed until far advanced  $\phi$ Ch1 development; hence not the whole viral DNA can be methylated before packaging of the DNA is finished (Baranyi *et al.*, 2000). Anyway, the purpose of these modifications on the  $\phi$ Ch1 genome is not clear, since the genome of the only known host, *Natrialba magadii*, lacks adenine methylation. Hence, an adaption to this host in order to avoid cellular defense mechanisms can be excluded (Baranyi *et al.*, 2000).

However, later on M. $\phi$ Ch1-I was shown to be encoded by ORF94 of the  $\phi$ Ch1 genome. Moreover two additional methyltransferases were discovered: M.*Nma* $\phi$ Ch1-II and M.*Nma* $\phi$ Ch1-III. The genes coding for all these enzymes involved in DNA modification were shown to be clustered on the virus chromosome (Klein *et al.*, 2002). Their organization can be seen in figure 5.

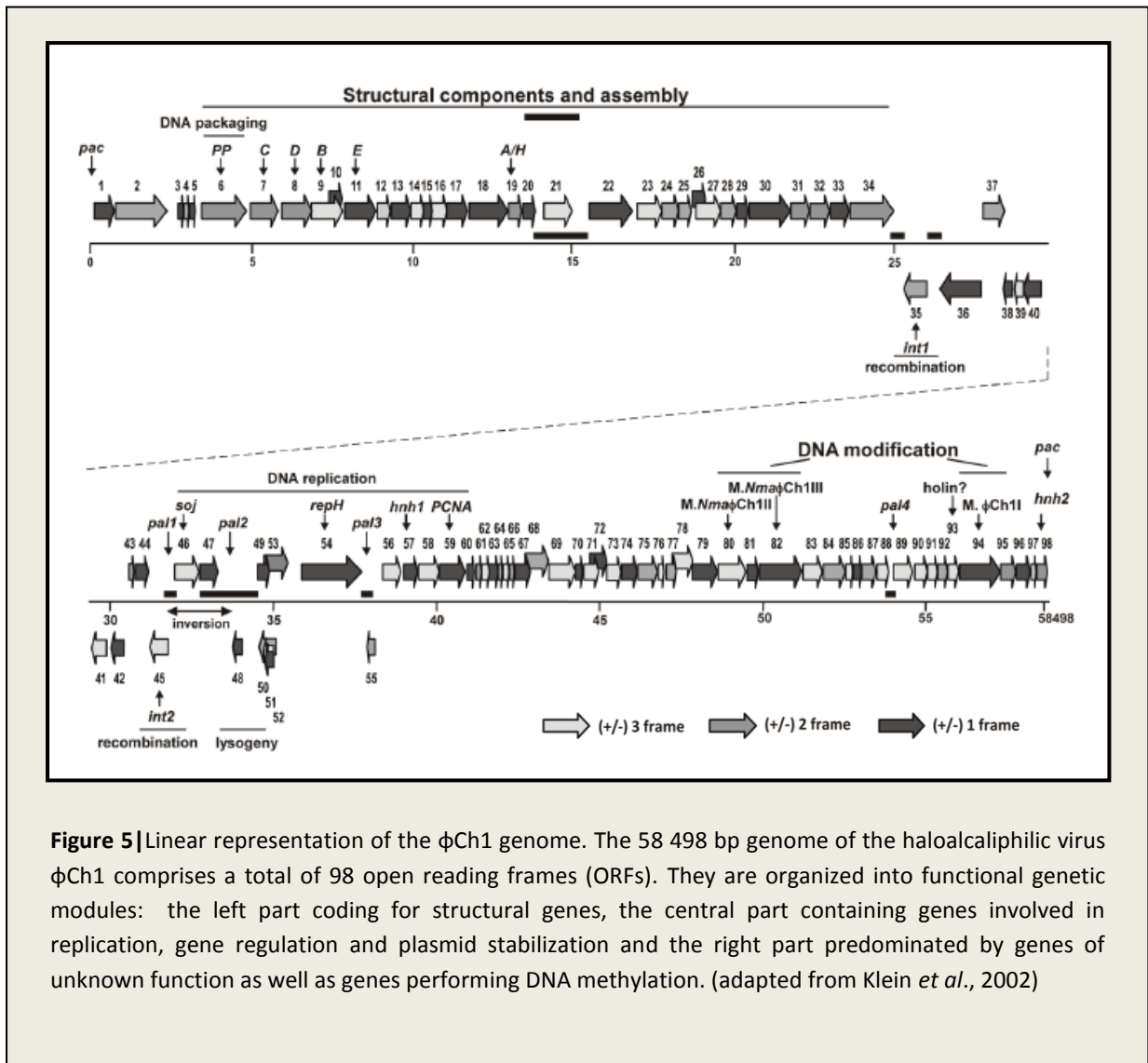


**Figure 5** | Linear representation of the  $\phi$ Ch1 genome. The 58 498 bp genome of the haloalcaliphilic virus  $\phi$ Ch1 comprises a total of 98 open reading frames (ORFs). They are organized into functional genetic modules: the left part coding for structural genes, the central part containing genes involved in replication, gene regulation and plasmid stabilization and the right part predominated by genes of unknown function as well as genes performing DNA methylation. (adapted from Klein *et al.*, 2002)

In general, the sequenced genome of  $\phi$ Ch1 can be separated into three parts mirroring the proposed functions of the encoded proteins (see figure 5). While the left part of the genome comprises structural compounds, the right part is predominated by proteins with unknown functions as well as the enzymes performing DNA modification. All the ORFs of these two regions are arranged in the same direction. The ORFs located to the central part in contrast include both, leftward- and rightward transcribed genes. They encode for proteins involved in replication, gene regulation and plasmid stabilization (Klein *et al.*, 2002). Initially the putative functions of the 98  $\phi$ Ch1 ORFs were determined as a consequence of comparison to other known sequences stated in databases. This analysis revealed a total of 48 matches, but only 17 ORFs showed similarities to proteins with known functions (Klein *et al.*, 2002). Later on, however, further studies were performed in order to confirm the proposed functions of the proteins encoded by these open reading frames.

In this way also the origin of replication of  $\phi$ Ch1 could be identified. It is located to the central part of the genome, at the region ranging from ORF53 to ORF54. Both ORFs share significant sequence similarities with *repH* of the *Haloarcula marismortui* plasmid pNRC100, encoding for the replication protein RepH. While the most striking homologies of ORF54 are present at the C-terminal part of the corresponding protein, similarities of ORF53 are less significant and restricted to the N-terminal end (Klein *et al.*, 2002; Iro *et al.*, in prep). Moreover ORF54 resembles other sequences required for plasmids replication in different archaeal representatives, e.g. *Halobacterium salinarum* and *Haloferax volcanii* (Ng and DasSarma, 1993; Klein *et al.*, 2002). In addition AT-rich promotor regions (typical for replication starts) were identified upstream of ORF53 and downstream of ORF54, respectively. All these facts indicate that the whole region comprising both ORFs and their surrounding sequences represent the origin of replication in  $\phi$ Ch1 (Klein *et al.*, 2002; Iro *et al.*, in prep). As discussed above this DNA sector was successfully used for the construction of a shuttle vector working in *E. coli* and *Nab. magadii* (Iro *et al.*, in prep).

Another crucial region of the  $\phi$ Ch1 DNA comprises ORF34 located to the left part, as well as ORF35 and ORF36 assigned to the central part of the genome (Klein *et al.*, 2002). ORF35 encodes for the site-specific recombinase Int1 which is known to perform inversion reactions resulting in an exchange of the 3'-ends of the neighboring ORF34 and ORF36, respectively. This event however gives rise to the production of the protein gp34<sub>52</sub> carrying the C-terminus of gp36, which is supposed to be the tail-fibre protein of the virus  $\phi$ Ch1 enabling interaction with its host *Nab. magadii* (Rössler *et al.*, 2004). The function of this protein as well as the mechanism of the inversion within its gene locus will be discussed in the next chapter.

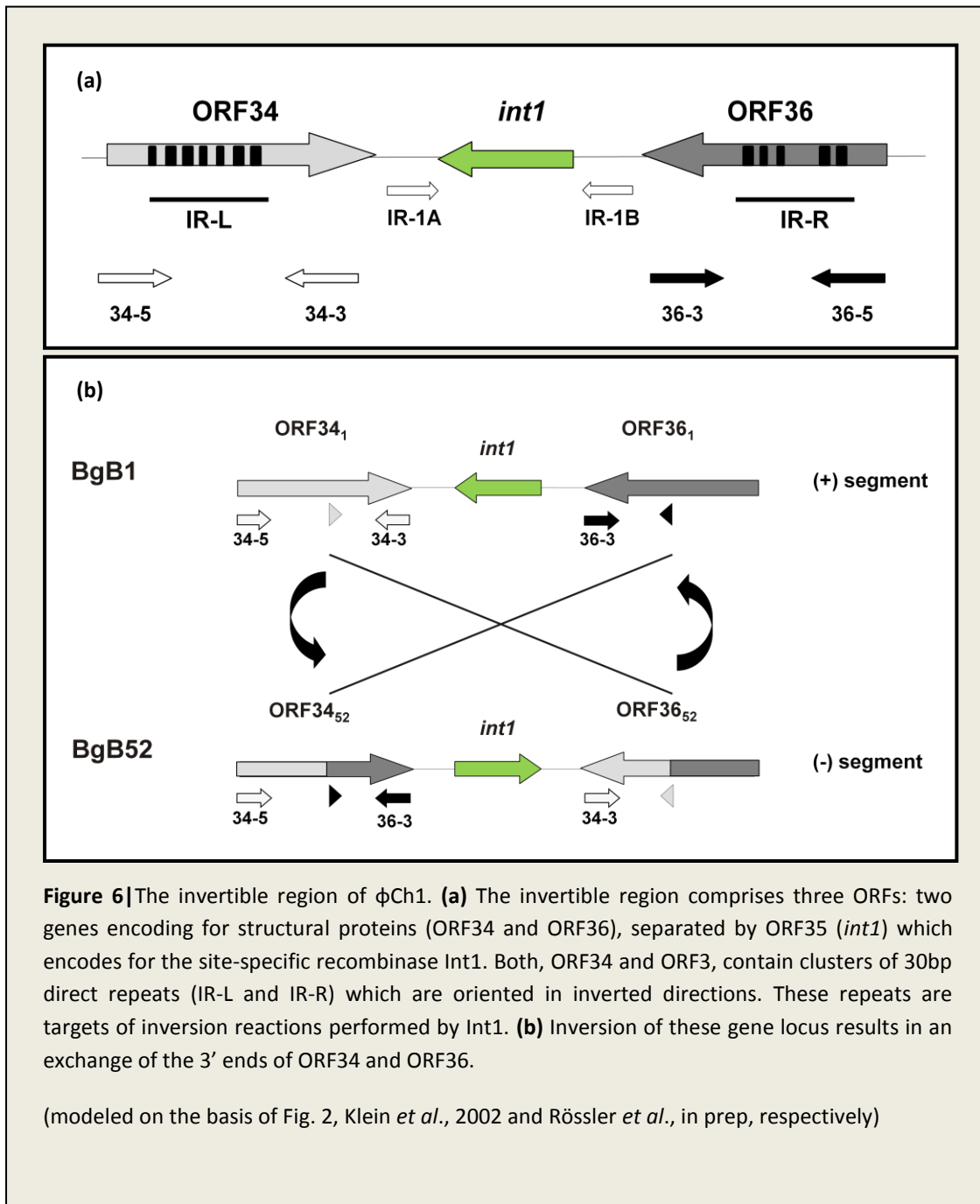
#### **1.2.3.4. The invertible region of $\phi$ Ch1**

The invertible region on the  $\phi$ Ch1 genome consists of three open reading frames: ORF34, ORF35 and ORF36, respectively. Based on comparative analysis of its sequence, ORF35, also designated as *int1*, was shown to code for a site-specific recombinase of the  $\lambda$  integrase family, the Integrase 1 (Int1). Another site-specific recombinase of the same integrase type is present in the halophage  $\phi$ Ch1: Int2, encoded by ORF45 (Klein *et al.*, 2002). In general it can be distinguished between two families of site-specific recombinases: the resolvase/invertase family and the  $\lambda$  integrase family. In comparison to the former, the  $\lambda$  integrase family represents a highly divergent group, involved in numerous processes such as transposition, integration of viral or plasmid DNA into the cellular genome, resolution of circular DNA forms as well as DNA excision or inversion, thereby effecting gene expression (Hallet and Sherratt, 1997). The only striking common characteristic of these enzymes is the presence four conserved amino acid residues, Arg-His-Arg-Tyr (RHRY) forming a

tetrad at the C-terminal region (Argos *et al.*, 1986; Abremski and Hoess, 1992; Blakely and Sherrat, 1996). This motive is also found in Int1 of the halophage  $\phi$ Ch1. It is composed of three separate regions on the polypeptide strand, BoxA, BoxB and BoxC which come close together during folding of the protein, providing the four certain amino acids RHRY (Rössler *et al.*, 2004). The catalytic tyrosine of this recombinase is supposed to mediate strand cleavage and delocalization, thus resulting in the formation of an intermediate holliday junction which then is resolved by rejoining of the DNA strands (Hallet and Sherrate, 1997; Rössler *et al.*, 2004).

Initially, the exact effect of this process on the life cycle of  $\phi$ Ch1 was not clear. A possible influence of either Int1 or Int2 on the integration of the viral DNA into the chromosome of its host was suggested, but also other functions were discussed (Klein *et al.*, 2002). Later on however it was confirmed, that Int1 is required and sufficient in order to perform inversion reactions within the neighboring ORFs flanking its gene locus: ORF34 and ORF36 (Rössler *et al.*, 2004; Ladurner, 2008). These two ORFs both encode for structural proteins and are oriented in opposite directions; so in contrast to ORF34, which is rightward transcribed, ORF36, just like *int1*, points leftwards (Klein *et al.*, 2002). Yet, only ORF34 possesses a functional promoter (Rössler *et al.*, in prep). However, both, ORF34 and ORF36, contain clusters composed of numerous 30bp direct repeats and one final inverted repeat: IR-L (within ORF34) and IR-R (within ORF36) (Klein *et al.*, 2002). These two repeat clusters are oriented in an inverted direction with respect to each other (Klein *et al.*, 2002). Hence, recombination events within these two ORFs performed by Int1, result in inversion of this gene region, thus leading to an exchange of the 3' ends of ORF34 and ORF36. For that reason  $\phi$ Ch1 DNA isolated from mature phage particles includes two kinds of this gene region differing in their orientation: the non-inverted segment (+ orientation) and the inverted segment (- orientation) (Rössler *et al.*, 2004).





Moreover, as IR-L and IR-R comprise a high number of repeats which can serve as recombination sites, inversion events usually yield products of different length, varying in the number of repeats. In addition site-specific recombination is not necessarily restricted to one single event, but instead of this can happen several times within one DNA strand, resulting in a multitude of possible different variants of this gene region. Yet, the most striking characteristic of these variants is the orientation of *int1* and the rest of the invertible region (Rössler *et al.*, 2004). In 2004 the variability of the invertible region was studied by analysis of different versions resulting from cloning

of the *Bgl*II-B fragments in *E. coli*. The *Bgl*II-B fragment comprises 5995bp of the  $\phi$ Ch1 genome, ranging from ORF31 to ORF36, including the invertible region. Out of the 60 different clones found in *E. coli*, five were analyzed in detail. Three of them, BgB1, BgB5 and BgB51 were shown to share an (+) orientation of *int1*, resembling the non-inverted fragment. In contrast BgB43 and BgB52 are the products of an inversion resulting in the exchange of the 3' ends of ORF34 and ORF36 (- orientation). Yet, all five clones differ significantly in the constitution of their clusters IR-L and IR-R and in the numbers of repeats (Rössler *et al.*, 2004). Also on the protein level a variation in the number of the corresponding amino acid repeats, MADV, was confirmed (see table 1). However, for further experiments, the fragments of the two clones BgB1 and BgB52 were chosen as representatives of the (+) and (-) orientated variant of the invertible region, respectively.

Clone	ORF34			ORF36			Orientation
	No. of repeats	pI	MW (kDa)	No. of repeats	pI	MW (kDa)	
pBGB1	14	3.67	47.94	6	3.69	44.95	+
pBGB5	13	3.7	52.99	8	3.65	39.89	+
pBGB43	4	3.82	51.09	14	3.63	41.26	-
pBGB51	13	3.69	54.00	7	3.66	38.89	+
pBGB52	9	3.69	54.66	14	3.63	41.26	-

**Table 1** | Repeat clusters within gp34 and gp36. Observation of five different variants of gp34 and gp36, respectively. Variations in the number of MDAV repeats, differences in properties (pI and MW) and orientation of the invertible fragment are shown. (Rössler *et al.*, 2004)

In 2008 when the shuttle vector pRo-5 was established, the influence of Int1 on the inversion reaction could be observed in its natural environment (Ladurner, 2008). For that purpose, two constructs based on the (-) orientated fragment of clone BgB52 were produced: one plasmid carrying the whole invertible region (pRo-5 52-2) and the other plasmid comprising ORF34 and ORF36, but lacking *int1* (pRo-5 52-3). Both constructs, pRo-5 52-2 and pRo-5 52-3, were transformed into the cured strain of *Nab. magadii*, L13. The two resulting cultures then were used to perform time course experiments in order to detect changes in the orientation of the invertible region with the time and with respect to the absence and presence of Int1. Hence, samples were taken from the growing cultures at different time points and the orientation of the sequence of interest was confirmed by PCR analysis. For that purpose, two different sets of primers were used: 34-5 / 36-3, detecting the (-) orientated fragment resembling BgB52 and 34-5 / 34-3, amplifying (+) orientated, in this case inverted variants (Ladurner, 2008). However, as illustrated in figure 7 inversion products could only be detected in the clone expressing *int1* (pRo-5 52-2), but not in the culture lacking the corresponding enzyme (pRo-5 52-3). Yet, the non-inverted fragment yielded a product in both clones at all time points. These results clearly demonstrate that the ability to perform an inversion reaction within ORF34 and ORF36 totally depends on the presence of the site-specific recombinase Int1

(Ladurner, 2008). Moreover, a PCR product resulting from inversion specific primers was first detected after a growth time of 78 hours; hence the inversion was supposed to happen in the stationary growth phase of *Nab. magadii* L13 (Ladurner, 2008). This finding however does not correlate to observations in the wild type strain L11 showing the expression of *int1* in the early logarithmic growth phase (Rössler *et al.*, in prep). A possible reason for early expression of *int1* could be the presence of another protein working as an activator in the lysogenic strain L11. Yet, this assumption has not been confirmed so far.

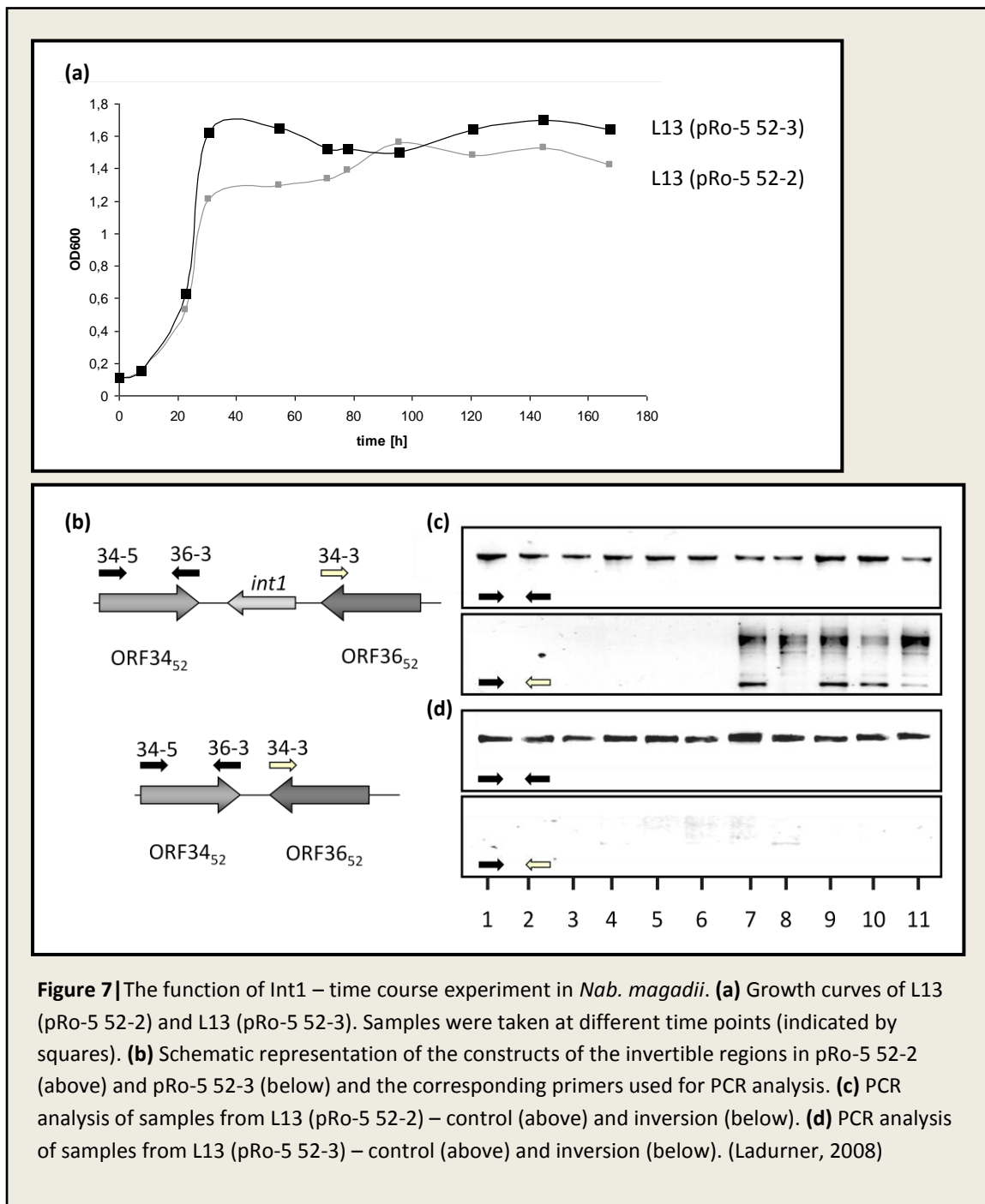


**Figure 7** | The function of Int1 – time course experiment in *Nab. magadii*. **(a)** Growth curves of L13 (pRo-5 52-2) and L13 (pRo-5 52-3). Samples were taken at different time points (indicated by squares). **(b)** Schematic representation of the constructs of the invertible regions in pRo-5 52-2 (above) and pRo-5 52-3 (below) and the corresponding primers used for PCR analysis. **(c)** PCR analysis of samples from L13 (pRo-5 52-2) – control (above) and inversion (below). **(d)** PCR analysis of samples from L13 (pRo-5 52-3) – control (above) and inversion (below). (Ladurner, 2008)

### 1.2.3.5. Gp34<sub>52</sub> – the putative tail fibre protein

The expression of ORF34 starts 98h after inoculation, at the beginning of the stationary growth phase, so after inversion within its gene region (Rössler *et al.*, 2004). The resulting product can be detected by western blot analysis using an antiserum directed against structural components of the mature  $\phi$ Ch1 particles ( $\alpha$ - $\phi$ Ch1) and an antibody specifically raised against gp36 ( $\alpha$ -gp36), respectively. The latter was shown to give signals at 66 kDa with the gene product of both, ORF34 and ORF36 due to the high number of repetitive elements found in both proteins, resulting in sequence similarities of 33 % (Rössler *et al.*, 2004). Hence based on this method it can neither be distinguished between gp34 and gp36, nor between non-inverted and inverted gene products.

However, the variability of gp34 and gp36 on the protein level has already been demonstrated by investigation of some gene products resulting from cloning of the *Bgl*II-B fragment in *E. coli* (see table 1) (Rössler *et al.*, 2004). As inversion of the invertible region leads to an exchange of the 3' ends of ORF34 and ORF36, it also gives rise to the production of two different variants of gp34: the unmodified gp34<sub>1</sub> and one version carrying the C-terminus of gp36, namely gp34<sub>52</sub>. Both, gp34<sub>1</sub> and gp34<sub>52</sub> represent different versions of the putative tail-fibre protein of  $\phi$ Ch1 (Rössler *et al.*, in prep). In bacteriophages structural components such as tail fibres are widely used targets for interaction with the host cell receptors in order to initiate the process of infection (Rössler *et al.*, 2004). Hence, alterations of these proteins can result in an increase of the host range, as varying tail fibre proteins enable attachment to different hosts. Such effects are well described in phages P1 and Mu (Sandmeier, 1994). In both cases the production of tail-fibre proteins with alternative C-terminal ends is caused by inversion events within the corresponding gene regions (Glasgow *et al.*, 1989).

The components of the invertible region as well as the encoded proteins are supposed to be quite similar to those found in  $\phi$ Ch1 (Rössler *et al.*, 2004). Yet, in  $\phi$ Ch1 the function of expression of alternative tail fibre proteins is not clear, since *Nab. magadii* represents the only known host infected by this virus (Witte *et al.*, 1997). However, recently the ability of both gp34<sub>1</sub> and gp34<sub>52</sub> to bind to the surface of *Natrialba magadii* was observed (Rössler *et al.*, in prep). For that purpose, in a first experiment both proteins were produced in *Haloflexax volcanii*. After incubation of the resulting cell extract with *Nab. magadii*, the components bound to the cell surface and the unattached proteins were separated by centrifugation. Finally the presence of gp34<sub>1</sub> and gp34<sub>52</sub> in the supernatants and cell fractions was detected by western blot analysis using the antibody  $\alpha$ -gp36 (Rössler *et al.*, in prep). The results clearly indicate that only gp34<sub>52</sub>, but not gp34<sub>1</sub> is attached to the cell surface of *Nab. magadii*. Binding assays of the same proteins produced in and purified from *E. coli* cells further supported this finding. Moreover further experiments indicated that the C-terminal part of the

protein is involved in interaction with the host cell, while the N-terminal part is supposed to be associated with the viral capsid and the shaft of the tail, an arrangement which is common in other head-tail phages, e.g. T4 (Markhof *et al.*, 1993; Rössler *et al.*, in prep). This view also correlates with the fact that the C-terminus of gp34 comprises a galactose-binding site, which is suspected to interact with glycosylated structures on the archaeal host cell, e.g. flagella or S-layer proteins (Rössler *et al.*, in prep).

Finally it can be concluded, that gp34<sub>52</sub>, the gene product of ORF34 carrying the C-terminus of gp36 is supposed to be the tail fibre protein of  $\phi$ Ch1, probably involved in binding to the cells of its host *Natrialba magadii* via interaction of its C-terminal part. Thus, a crucial role of this viral protein in infection of the archaeal cell is very likely, but yet has to be confirmed. For that purpose a  $\phi$ Ch1 mutant lacking this protein was constructed in the course of this diploma work.

## 2. Material and Methods

---

### 2.1. Material

#### 2.1.1. Strains

<i>Domain</i>	<i>Strain</i>	<i>Genotype</i>	<i>Source</i>
<i>Bacteria</i>	<i>E. coli</i> XL-1 Blue	<i>endA1, gyrA96, hsdR17 (r<sub>k</sub>-m<sub>k+</sub>), lac, recA1, relA1, supE44, thi, (F', lac<sup>f</sup>, lacZΔM15, proAB<sup>+</sup>, tet)</i>	Stratgene
	<i>E. coli</i> Rosetta	F <sup>-</sup> , <i>ompT, hsdS<sub>B</sub> (r<sub>B</sub><sup>-</sup>m<sub>B</sub><sup>-</sup>), gal, dcm, lacY1, (DE3), pRARE<sub>6</sub>, (Cm<sup>R</sup>)</i>	Novagen
<i>Archaea</i>	<i>Nab. magadii</i> L11	wild type, φCh1 integrated	Witte <i>et al.</i> , 1997
	<i>Nab. magadii</i> L13	cured from φCh1	Witte <i>et al.</i> , 1997
	<i>Nab. magadii</i> L11Δ34	ORF34 deficient φCh1 integrated	this thesis
	<i>Nab. magadii</i> P3	NEP deficient L13	Derntl, 2009

#### 2.1.2. Growth media

LB (rich medium for *E. coli*):

Peptone            10 g  
NaCl                5 g  
Yeast Extract     5 g

pH 7.0

add dH<sub>2</sub>O to a final volume of 1 liter, autoclave it

for agar plates add 15 g/l Agar

NVM (rich medium for *Nab. magadii*):

Casaminoacids	8.8 g
Yeast Extract	11.7 g
Tri-Na citrate	0.8 g
KCl	2.35 g
NaCl	235 g

pH 9.0

add dH<sub>2</sub>O to a final volume of 934 ml, autoclave it

for agar plates add 8 g/l Agar

for soft agar add 4 g/l Agar

After autoclaving, the medium has to be complemented to 1 l by addition of:

0.57 M Na <sub>2</sub> CO <sub>3</sub> (dissolved in sterile ddH <sub>2</sub> O)	65 ml
1M MgSO <sub>4</sub> (autoclaved)	1 ml
20mM FeSO <sub>4</sub> (dissolved in sterile ddH <sub>2</sub> O)	1 ml

### 2.1.3. Antibiotics and additives

<i>Domain</i>	<i>Additive</i>	<i>Stock conc.</i>	<i>Final conc.</i>	<i>Remarks</i>
<i>Bacteria</i>	Ampicillin	20 mg/ml	100 µg/ml	dissolved in ddH <sub>2</sub> O, sterile filtered, stored at 4°C
	Tetracycline	10 mg/ml	10 µg/ml	dissolved in ½ Vol. ddH <sub>2</sub> O, completed by ½ Vol. 96 % EtOH, stored at -20°C (light protected)
	Chloramphenicol	40 mg/ml	20 µg/ml	dissolved in 96 % EtOH, stored at -20°C
	IPTG	1 M	0.5 – 1 mM	dissolved in ddH <sub>2</sub> O, stored at -20°C
	X-Gal	100 mg/ml	40 µg/ml	dissolved in DMF, stored at -20°C
<i>Archaea</i>	Novobiocin	3 mg/ml	3 µg/ml	dissolved in ddH <sub>2</sub> O, sterile filtered, stored at -20°C (light protected)
	Mevinolin	10 mg/ml	7.5 µg/ml	isolated from pulverized tablets, dissolved in 96 % EtOH, stored at -20°C
	Bacitracin	7 mg/ml	70 µg/ml	dissolved in ddH <sub>2</sub> O, sterile filtered, stored at 4°C

## 2.1.4. Vectors

<i>Plasmid</i>	<i>Features</i>	<i>Source</i>
pUC19	<i>bla</i> , pMB1ori, lacZa, mcs	Yanisch-Perron <i>et al.</i> , 1985
pKS <sub>II</sub> <sup>+</sup>	mcs, <i>bla</i> , ColE1 ori, lacZa	Stratagene
pRSET-A	mcs, <i>bla</i> , EK, PT7, RBS, His-tag, pUC ori, f1 ori	Invitrogen
pQE30	<i>bla</i> , ColE1, N-terminal Poly(His)6-tag	Quiagen
pBAD24	<i>bla</i> , <i>araC</i> , <i>rrnB</i> , mcs, PBAD promoter, pBR322 ori	Guzman <i>et al.</i> , 1995
pRo-5	<i>bla</i> , ColE1 ori, <i>gyrB</i> (Nov <sup>R</sup> ), ϕCh1 derived ori	Iro <i>et al.</i> , in prep
pNB102	<i>bla</i> , ColE1 ori, <i>hmg</i> (Mev <sup>R</sup> ), pNB101 ori	Zhou <i>et al.</i> , 2004
pRR007	modified pKS <sub>II</sub> <sup>+</sup> , <i>hmg</i> (Mev <sup>R</sup> ) under 16S promoter control, ϕCh1 derived ori, MCS	Selb, 2009
pMDS11	<i>bla</i> , f1 ori, ColE1 ori, <i>gyrB</i> (Nov <sup>R</sup> ), pHK2 ori	Holmes <i>et al.</i> , 1991
pJAS35	<i>bla</i> , ColE1 origin, pHK2 origin, <i>gyrB</i> (Nov <sup>R</sup> ), P <sub>fdx</sub>	Pfeifer <i>et al.</i> , 1994
pBGB1	pKS <sub>II</sub> <sup>+</sup> (mcs, <i>bla</i> , ColE1 ori, lacZa) with ϕCh1 <i>BgIII</i> -B fragment (ORF31-ORF36) in (+) orientation	Rössler <i>et al.</i> , 2004
pBGB52	pKS <sub>II</sub> <sup>+</sup> (mcs, <i>bla</i> , ColE1 ori, lacZa) with ϕCh1 <i>BgIII</i> -B fragment (ORF31-ORF36) in (-) orientation	Rössler <i>et al.</i> , 2004
pKS <sub>II</sub> <sup>+</sup> ΔORF34-fragment 1	pKS <sub>II</sub> <sup>+</sup> (mcs, <i>bla</i> , ColE1 ori, lacZa) with upstream region of ϕCh1 ORF34	this thesis
pKS <sub>II</sub> <sup>+</sup> ΔORF34-fragment 1+2	pKS <sub>II</sub> <sup>+</sup> (mcs, <i>bla</i> , ColE1 ori, lacZa) with upstream and downstream regions of ϕCh1 ORF34	this thesis
pKS <sub>II</sub> <sup>+</sup> ΔORF34-deletion cassette	pKS <sub>II</sub> <sup>+</sup> (mcs, <i>bla</i> , ColE1 ori, lacZa) with upstream and downstream regions of ϕCh1 ORF34, disrupted by <i>gyrB</i> (Nov <sup>R</sup> , derived from pMDS11)	this thesis
pRR007-ORF34 <sub>1</sub>	pRR007 (mcs, <i>bla</i> , ColE1 ori, lacZa, <i>hmg</i> (Mev <sup>R</sup> ) under 16S promoter control, ϕCh1 derived ori) with ϕCh1 ORF34 <sub>1</sub>	this thesis
pRR007-ORF34 <sub>52</sub>	pRR007 (mcs, <i>bla</i> , ColE1 ori, lacZa, <i>hmg</i> (Mev <sup>R</sup> ) under 16S promoter control, ϕCh1 derived ori) with ϕCh1 ORF34 <sub>52</sub>	this thesis
pNB102-ORF34 <sub>1</sub>	pNB102 ( <i>bla</i> , ColE1 ori, <i>hmg</i> (Mev <sup>R</sup> ), pNB101 ori) with	this thesis



	φCh1 ORF34 <sub>1</sub>	
pNB102-ORF34 <sub>52</sub>	pNB102 ( <i>bla</i> , ColE1 ori, <i>hmg</i> (Mev <sup>R</sup> ), pNB101 ori) with φCh1 ORF34 <sub>52</sub>	this thesis
pQE30-flaB1	pQE30 ( <i>bla</i> , ColE1, N-terminal poly(His)6-tag ) with <i>Nab. magadii</i> flaB1	Lab Angela Witte, 2006
pBAD24-584	pBAD24 ( <i>bla</i> , <i>araC</i> , <i>rrnB</i> , mcs, PBAD promoter, pBR322 ori) with φCh1 Int1- IRLHind IRRXba	Lab Angela Witte, 2007
pBAD24-586	pBAD24 ( <i>bla</i> , <i>araC</i> , <i>rrnB</i> , mcs, PBAD promoter, pBR322 ori) with φCh1 Int1- IRLHind DRRXba	Lab Angela Witte, 2007
pBAD24-608	pBAD24 ( <i>bla</i> , <i>araC</i> , <i>rrnB</i> , mcs, PBAD promoter, pBR322 ori) with φCh1 IDR IRL int1 (int1 IRRDIRL)	Lab Angela Witte, 2007
pBAD24-615	pBAD24 ( <i>bla</i> , <i>araC</i> , <i>rrnB</i> , mcs, PBAD promoter, pBR322 ori) with φCh1 ΔIRR IRL	Lab Angela Witte, 2007
pBAD24-661	pBAD24 ( <i>bla</i> , <i>araC</i> , <i>rrnB</i> , mcs, PBAD promoter, pBR322 ori) with φCh1 IRL-IRM1 int1	Lab Angela Witte, 2007
pBAD24-662	pBAD24 ( <i>bla</i> , <i>araC</i> , <i>rrnB</i> , mcs, PBAD promoter, pBR322 ori) with φCh1 IRL-IRM4 int1	Lab Angela Witte, 2007
pBAD24-663	pBAD24 ( <i>bla</i> , <i>araC</i> , <i>rrnB</i> , mcs, PBAD promoter, pBR322 ori) with φCh1 IRL-IRM7 int1	Lab Angela Witte, 2007
pBAD24-664	pBAD24 ( <i>bla</i> , <i>araC</i> , <i>rrnB</i> , mcs, PBAD promoter, pBR322 ori) with φCh1 IRL-IRM11 int1	Lab Angela Witte, 2007
pUC19-fdx	pUC19 ( <i>bla</i> , pMB1ori, lacZa, mcs) with fdx-promoter (from <i>Hbt. salinarum</i> )	this thesis
pUC19-fdx-584	pUC19 ( <i>bla</i> , pMB1ori, lacZa, mcs) with fdx-promoter and φCh1 Int1- IRLHind IRRXba	this thesis
pUC19-fdx-586	pUC19 ( <i>bla</i> , pMB1ori, lacZa, mcs) with fdx-promoter and φCh1 Int1- IRLHind DRRXba	this thesis
pUC19-fdx-608	pUC19 ( <i>bla</i> , pMB1ori, lacZa, mcs) with fdx-promoter and φCh1 IDR IRL int1 (int1 IRRDIRL)	this thesis
pUC19-fdx-615	pUC19 ( <i>bla</i> , pMB1ori, lacZa, mcs) with fdx-promoter and φCh1 ΔIRR IRL	this thesis
pUC19-fdx-661	pUC19 ( <i>bla</i> , pMB1ori, lacZa, mcs) with fdx-promoter and φCh1 IRL-IRM1 int1	this thesis
pUC19-fdx-662	pUC19 ( <i>bla</i> , pMB1ori, lacZa, mcs) with fdx-promoter	this thesis

	and $\phi$ Ch1 IRL-IRM4 int1	
pUC19-fdx-663	pUC19 ( <i>bla</i> , pMB1ori, lacZa, mcs) with fdx-promoter and $\phi$ Ch1 IRL-IRM7 int1	this thesis
pUC19-fdx-664	pUC19 ( <i>bla</i> , pMB1ori, lacZa, mcs) with fdx-promoter and $\phi$ Ch1 IRL-IRM11 int1	this thesis
pRo-5-fdx-584	pRo-5 ( <i>bla</i> , ColE1 ori, <i>gyrB</i> , $\phi$ Ch1 derived ori) with fdx-promoter and $\phi$ Ch1 Int1- IRLHind IRRXba	this thesis
pRo-5-fdx-586	pRo-5 ( <i>bla</i> , ColE1 ori, <i>gyrB</i> , $\phi$ Ch1 derived ori) with fdx-promoter and $\phi$ Ch1 Int1- IRLHind DRRXba	this thesis
pRo-5-fdx-608	pRo-5 ( <i>bla</i> , ColE1 ori, <i>gyrB</i> , $\phi$ Ch1 derived ori) with fdx-promoter and $\phi$ Ch1 IDR IRL int1 (int1 IRRDIRL)	this thesis
pRo-5-fdx-615	pRo-5 ( <i>bla</i> , ColE1 ori, <i>gyrB</i> , $\phi$ Ch1 derived ori) with fdx-promoter and $\phi$ Ch1 $\Delta$ IRR IRL	this thesis
pRo-5-fdx-661	pRo-5 ( <i>bla</i> , ColE1 ori, <i>gyrB</i> , $\phi$ Ch1 derived ori) with fdx-promoter and $\phi$ Ch1 IRL-IRM1 int1	this thesis
pRo-5-fdx-662	pRo-5 ( <i>bla</i> , ColE1 ori, <i>gyrB</i> , $\phi$ Ch1 derived ori) with fdx-promoter and $\phi$ Ch1 IRL-IRM4 int1	this thesis
pRo-5-fdx-663	pRo-5 ( <i>bla</i> , ColE1 ori, <i>gyrB</i> , $\phi$ Ch1 derived ori) with fdx-promoter and $\phi$ Ch1 IRL-IRM7 int1	this thesis
pRo-5-fdx-664	pRo-5 ( <i>bla</i> , ColE1 ori, <i>gyrB</i> , $\phi$ Ch1 derived ori) with fdx-promoter and $\phi$ Ch1 IRL-IRM11 int1	this thesis
pNB102/43-44	pNB102 ( <i>bla</i> , ColE1 ori, <i>hmg</i> (Mev <sup>R</sup> ), pNB101 ori) with possible activator of <i>int1</i> expression in $\phi$ Ch1 (ORF43+44)	this thesis
pUC19- $\Delta$ AUG-int1-fragment1	pUC19 ( <i>bla</i> , pMB1ori, lacZa, mcs) with $\phi$ Ch1 ORF34 (upstream of ORF35 ( <i>int1</i> ) AUG)	this thesis
pUC19- $\Delta$ AUG-int1-fragment1+2	pUC19 ( <i>bla</i> , pMB1ori, lacZa, mcs) with $\phi$ Ch1 ORF34-ORF36, lacking ORF35 ( <i>int1</i> ) AUG	this thesis
pRo-5- $\Delta$ AUG-int1	pRo-5 ( <i>bla</i> , ColE1 ori, <i>gyrB</i> , $\phi$ Ch1 derived ori) with $\phi$ Ch1 ORF34-ORF36, lacking ORF35 ( <i>int1</i> ) AUG	this thesis

---

### 2.1.5. Primer

<i>Primer</i>	<i>Sequence (*)</i>	<i>Restriction site</i>
Int His3	5' – GTT ACT CAC GCT AGC AAA ACG AAG GAT GAA – 3'	n/a
Jas Int5	5' – ACG <b>TCC ATG GCG</b> CAT CAC CAT CAC CAT CAC ATG TCC AAA GAG AGA CAT GC – 3'	<i>NcoI</i>
34-5	5' – CAG CAG <b>AGA TCT</b> ATG AGT AAA ATC TGG GAA CCG AG – 3'	<i>BglII</i>
34-3	5' – CAG CAG <b>AAG CTT</b> CAG ATC AGG TTT ATA TTG CTG AAG T – 3'	<i>HindIII</i>
36-3	5' – CAG CAG <b>AAG CTT</b> ATT CAG GTT TCA TGT CGC TG – 3'	<i>HindIII</i>
p28-	5' – GAG CCG TGT TCG TTC TG – 3'	n/a
p28+	5' – TCT GGC CTG AAT GAC GA – 3'	n/a
34-3-X	5' – CAG CAG <b>TCT AGA</b> GGT TCG TGC CGG AGT C – 3'	<i>XbaI</i>
44-3	5' – CAG CAG <b>TCT AGA</b> CAA ACC ACA GAA CGG ACG – 3'	<i>XbaI</i>
Nov-6	5' – GGG ATC GCA GAG GAG C – 3'	n/a
TR-1	5' – AAT TGC GGC CGC CGC GTT GAA GGC A – 3'	<i>NotI</i>
TR-2	5' – AAT <b>TTC TAG ATC</b> CTG GGC CTC TTT GAA – 3'	<i>XbaI</i>
Int13-Xba	5' – CAG CAT <b>CTA GAA</b> GGA TGA AGT GGC GCG – 3'	<i>XbaI</i>
flaB2-1	5' – GAC <b>CGG ATC CAT</b> GTT CAC TAA CGA CAC CGA – 3'	<i>BamHI</i>
flaB2-2	5' – CAG <b>GAA GCT TAG</b> AGT CGG ACC GCT TC – 3'	<i>HindIII</i>
CH3-8	5' – CTG AGA AGT ACA TCC GGA TTT – 3'	n/a
34-Kpn	5' – CAG CAG <b>GGT ACC</b> CGG CGT TCG AGG TCA – 3'	<i>KpnI</i>
36-5-HindIII	5' – GAC GAC <b>AAG CTT</b> ATG GAT CCG ATC AGC G – 3'	<i>HindIII</i>
43-Kpn-5	5' – CAG CAG <b>GTA CCG</b> TTG TGC CAG CCG T – 3'	<i>KpnI</i>
34-3-Xba	5' – CAG <b>CTC TAG AGT</b> ATA TCC CTC GTC GAA G – 3'	<i>XbaI</i>
D54-2	5' – GAC <b>CGA ATT CGC</b> GAG ATC TTC ACC GTT GAA GC – 3'	<i>EcoRI</i>
79-Pst	5' – GAT <b>ACT GCA GCT</b> CTT TGT ACC GAT GCG TC – 3'	<i>PstI</i>
79-Nae	5' – GAT <b>AGC CGG CGA</b> CTC TCA CAA GAT CTC – 3'	<i>NaeI</i>
Nov-9	5' – GAT GTC GGT CAT CGC GG – 3'	n/a

3602-Xba	5' – GGC <b>CTC TAG</b> ATC CAA AGA GAG ACA TGC CC – 3'	<i>XbaI</i>
3601-Xba	5' – GGC <b>CTC TAG</b> AAC AAC ACG CCG GTC A – 3'	<i>XbaI</i>
34-XbaI-a	5' – GAC <b>GTC TAG</b> ACT CCG ATG AAC ACG ACA CTC – 3'	<i>XbaI</i>
fdx-1	5' – GAA <b>TGG TAC</b> CCT GAC GCC GCG GGC AGC – 3'	<i>KpnI</i>
fdx-2	5' – GAA <b>TTC TAG</b> ACC ATG GGC ATC ACC AGA GTT – 3'	<i>XbaI</i>
D34-1	5' – GAC <b>CTC TAG</b> AGT ACC GAA CGC ATC TCG – 3'	<i>XbaI</i>
D34-2	5' – GCA ACC CGG <b>GAA GCT</b> TCT CGT AGC TCT GGT TTT CCT – 3'	<i>HindIII</i>
D34-3	5' – GAC <b>CAA GCT</b> TAA CTG ATC TTC ACA CCG GAT – 3'	<i>HindIII</i>
D34-4	5' – GAA <b>AGG TAC</b> CGA GAG ACA TGC CCA CGA – 3'	<i>KpnI</i>
D34-3-Sma	5' – GAC <b>CAA GCT TCC CGG</b> GAA CTG ATC TTC ACA CCG GAT – 3'	<i>HindIII, SmaI</i>
34-inv1	5' – GAG CGG TGG CGT CGA C – 3'	n/a
34-inv2	5' – GTC ATC CAG TCG CCG C – 3'	n/a
36-inv1	5' – GTT GTA CCG GTC CGA GAT ATA GTC A – 3'	n/a
NB-1	5' – TCT ACC GGG TGC TGA ACG – 3'	n/a
NB-2	5' – CGC TGA TGT ACG AAC CGA G – 3'	n/a

\* bold sequences represent recognition sites for restriction endonucleases

## 2.1.6. Marker

### 2.1.6.1. DNA ladders

<i>Application</i>	<i>Marker</i>	<i>Fragments</i>	<i>Source/Manufacture</i>
Agarose gel	$\lambda$ - <i>BstEII</i>	8453, 7242, 6369, 5687, 4822, 4324, 3675, 2323, 1929, 1371, 1264, 702 [bp]	$\lambda$ -DNA (Fermentas), digested with restriction endonuclease <i>Eco91I</i> ( <i>BstEII</i> ) in Buffer O (Fermentas)
	$\lambda$ - <i>PstI</i>	11501, 5077, 4749, 2838, 2556, 2443, 2140, 1986, 1700, 1159, 1093, 805, 514, 468, 448, 339, 264, 247, 216, 211, 200, 164, 150, 94, 87, 72, 15 [bp]	$\lambda$ -DNA (Fermentas), digested with restriction endonuclease <i>PstI</i> in Buffer O (Fermentas)

Material and Methods

6 % PAA gel	pUC19 <i>HaeIII</i>	587, 458, 434, 298, 257, 174, 102, 80, 18, 11 [bp]	pUC19 plasmid DNA, digested with restriction endonucleases <i>BsuR1</i> ( <i>HaeIII</i> ) in Buffer R (Fermentas)
	pUC19 <i>Sau3AI</i>	955, 585, 341, 258, 141, 105, 78/75, 46, 36, 18/17, 12/11.8 [bp]	pUC19 plasmid DNA, digested with restriction endonucleases <i>Sau3AI</i> in NEBuffer 1 (New England BioLabs)
	100 bp DNA Ladder	1517, 1200, 1000, 900, 800, 700, 600, 500/517, 400, 300, 200, 100 [bp]	New England BioLabs #N3231L
Southern blot	Biotinylated 2-Log DNA Ladder	10, 8, 6, 5, 4, <b>3</b> , 2, 1.5, 1.2, <b>1</b> , 0.9, 0.8, 0.7, 0.6, <b>0.5</b> , 0.4, 0.3, 0.2, 0.1 [kbp]	New England BioLabs #N7554S

### 2.1.6.2. Protein ladders

<b>Marker</b>	<b>Fragments</b>	<b>Source</b>
PageRuler™ Unstained Protein Ladder	200, 150, 120, 100, 85, 70, 60, 50, 40, 30, 25, 20, 15, 10 [kDa]	Fermentas; #SM0661
Unstained Protein Molecular Weight Marker	116, 66.2, 45, 35, 25, 18.4, 14.4 [kDa]	Fermentas #SM0431
PageRuler™ Plus Prestained Protein Ladder - 1	250, 130, 100, 70, 55, 35, 25, 15, 10 [kDa]	Fermentas #SM1811
PageRuler™ Plus Prestained Protein Ladder - 2	170, 130, 100, 70, 55, 40, 35, 25, 15, 10 [kDa]	Fermentas #SM0671
PageRuler™ Plus Prestained Protein Ladder - 3	250, 130, 100, 70, 55, 35, 25, 15, 10 [kDa]	Fermentas #SM1819

### 2.1.7. Enzymes

<i>Category</i>	<i>Enzyme</i>	<i>Source</i>	<i>Application/Remarks</i>
Restriction enzymes	diverse	Fermentas	applied with appropriate buffers according to the manufacturer's instructions; double digests were performed as suggested on the Fermentas webpage: <a href="http://www.fermentas.com/en/tools/doubledigest">http://www.fermentas.com/en/tools/doubledigest</a>
	<i>Sau3AI</i>	New England BioLabs #R0169S	applied with NEBuffer 1 according to the manufacturer's instructions
Polymerases	<i>Pwo</i>	PeqLab Cat. 01-5020	polymerase from <i>Pyrococcus woessii</i> with 3' – 5' exonuclease activity (proofreading function); preferentially used for cloning approaches; applied with corresponding buffer
	<i>Pfu</i>	Promega Cat. M776A	polymerase from <i>Pyrococcus furiosus</i> with 3' – 5' exonuclease activity (proofreading function); used for cloning approaches; applied with corresponding buffer
	GoTaq®	Promega #M31745	no proofreading activity; used for analytical PCRs; applied with corresponding buffer
	Dream Taq®	Fermentas Cat. EP0702	no proofreading activity; alternatively used for analytical PCRs; applied with corresponding buffer
	T4 DNA Polymerase	Fermentas #EP0061	used for blunting of restriction sites by removal of 3' overhangs (enhanced 3' – 5' exonuclease activity); applied with adequate Fermentas buffers according to the manufacturer's instructions
Other enzymes	T4 DNA Ligase	Fermentas #EL0011	used for the generation of phosphodiester bonds between 5' phosphate- and 3' hydroxyl groups; applied with the corresponding buffer according to the manufacturer's instructions
	Proteinase K	Rocher Cat. 19133	used for generation of spheroblast cells at a final concentration of 20µg/ml (optimal concentration experimentally determined)

## 2.1.8. Antibodies

### 2.1.8.1. Primary antibodies

<i>Antibody</i>	<i>Application</i>	<i>Source</i>	<i>Remarks</i>
$\alpha$ -gp34 (rabbit)	antiserum rabbit 17 diluted 1:2000 in TBS, 0.3 % BSA	Moravian-Biotechnology	purification of $\phi$ Ch1 gp34 and immunization of rabbits in course of this thesis
$\alpha$ -FlaB1 (rabbit)	antiserum rabbit 23 diluted 1:1000 in TBS, 0.3 % BSA	Moravian-Biotechnology	purification of <i>Nab. magadii</i> FlaB1 and immunization of rabbits in course of this thesis

### 2.1.8.2. Secondary antibodies

<i>Antibody</i>	<i>Application</i>	<i>Source</i>	<i>Remarks</i>
$\alpha$ -rabbit	antibody diluted 1:5000 in TBS	GE Healthcare Cat. NA934V	conjugated with horseradish peroxidase (HRP)

## 2.1.9. KITS

All KITS were used with supplied buffers and solutions according to manufacturer's instructions

<i>Purpose</i>	<i>Product</i>	<i>Source</i>
DNA purification	QIA® Gel Extraction Kit: Buffers PB and PE	Quiagen, Cat. 28706
DNA purification – elution from gel	QIA® Gel Extraction Kit: QG, PE and Elution Buffer	Quiagen, Cat. 28706
Mini prep	Gene JET™ Plasmid Miniprep Kit: Resuspension Solution, Lysis Solution, Neutralisation Solution, Wash Solution	Fermentas, #K0503
Southern blot – labeling of the probe	NEBlot® Phototope® Kit	New England Biolabs, #N7550S
Southern blot – development of the blot	Phototope™-Star Detection Kit for Nucleic Acids	New England Biolabs, #N7020S
Western blot – development of the blot	Super Signal® West Pico Chemiluminescent Substrate	Thermo Scientific, # 34080

## 2.1.10. Buffers and solutions

### 2.1.10.1. DNA Gel electrophoresis

#### Agarose gels:

50x TAE:		x % Agarose gel:
Tris base	2 M	solid agarose
Acetic acid	1 M	1x TAE
EDTA	0.1 M	
adjust pH 8.2 with HCl		

#### 6 % PAA gels:

10x TBE:		30% AA solution:		6 % PAA gel:	
Tris base	108 g	Acrylamide	29 %	30 % AA solution	1.2 ml
Boric acid	60 g	N,N'-Bisacrylamide	1 %	1x TBE	4.8 ml
EDTA	7.4 g			10 % APS	60 $\mu$ l
				TEMED	6 $\mu$ l
adjust pH 8.0 with Boric acid					
add ddH <sub>2</sub> O to a final volume of 1 l					

#### Loading dye:

5x DNA loading dye:	
Tris-HCl, pH 8.0	50 mM
SDS	0.1 %
Bromphenol blue	0.05 %
Xylene blue	0.05 %
Sucrose/Saccharose (after autoclaving)	25 %



### 2.1.10.2. Southern blot

#### 20x SSC:

NaCl	3 M
Na-citrate	0.3 M

pH 7.2

#### 50 x Denhardt's solution:

Ficoll 400	1 g
Polyvinylpyrrolidone	1 g
BSA	1 g

add ddH<sub>2</sub>O to a final volume of 100 ml  
store at -20°C

#### Hybridisation Buffer :

ddH <sub>2</sub> O	55 ml
20x SSC	25 ml
50x Denhardt's solution	10 ml
10 % BSA	5 ml
1 M NaH <sub>2</sub> PO <sub>4</sub>	5 ml
20 % SDS	500 µl
0.5 M EDTA	200 µl

store at -20°C

#### Blocking solution:

NaCl	7.3 g
Na <sub>2</sub> HPO <sub>4</sub>	2.41 g
NaH <sub>2</sub> PO <sub>4</sub>	0.96 g
SDS	50 g

adjust pH 7.2  
add ddH<sub>2</sub>O to a final volume of 1 l

#### 10x Wash solution II:

Tris base	12.1 g
NaCl	5.85 g
MgCl <sub>2</sub>	2.03 g

adjust pH 9.5  
add ddH<sub>2</sub>O to a final volume of 100 ml

#### 1x Wash solution I:

1:10 dilution of Blocking solution

#### Other solutions:

0.25 M HCl  
0.4 M NaOH / 0.6 M NaCl  
1.5 M NaCl / 0.5 M Tris-HCl (pH 7.5)  
0.4 M NaOH  
0.2 M Tris / HCl  
hering sperm 100 µg/ml  
2x SSC / 0.1 % SDS  
4x SSC / 0.1 % SDS  
0.1x SSC / 0.1 % SDS

### 2.1.10.3. SDS-PAGE and Western blot analysis

2x Protein sample buffer (Laemmli):

Tris-HCl, pH 6.8	0.12 mM
SDS	4 %
glycerol	17.4 %
$\beta$ -mercaptoethanol	2 %
bromphenol blue	0.02 %

5 mM Sodium phosphate buffer (pH 6.8):

A) Na H <sub>2</sub> PO <sub>4</sub>	0.2 M
B) Na <sub>2</sub> HPO <sub>4</sub>	0.2 M

combination of 2.55 ml solution A and 2.45 ml solution B, filled up to a final volume of 200 ml

4x Separation gel buffer:

Tris-HCl, pH 8.8	1.5 M
SDS	0.4 %

4x Stacking gel buffer:

Tris-HCl, pH 6.8	0.5 M
SDS	0.4 %

30% AA solution:

Acrylamide	29 %
N,N'-Bisacrylamide	1 %

10x SDS-PAGE running buffer:

Tris base	0.25 M
Glycine	1.92 M
SDS	1 %

Coomassie staining solution:

Methanol	40 %
Acetic acid	10 %
Coomassie Brilliant Blue R-250	0.25 %

Destaining solution:

Acetic acid	10 %
(Methanol	10 %)

resolving of Coomassie Brilliant Blue R-250 in methanol before addition of acedic acid and ddH<sub>2</sub>O

Transblot buffer:

Tris base	48 mM
Glycine	39 mM
SDS	0.037 % (v/v)
Methanol	20%

10x TBS/TBS-T:

Tris base	30.29 g
NaCl	80.06 g
KCl	2.01 g
(Tween 20	5ml)

adjust pH 8.0 with HCl  
add ddH<sub>2</sub>O to a final volume of 1 l

Ponceau S solution:

Ponceau S	0.5 %
TCA	3 %

#### 2.1.10.4. Protein purification (denaturing)

##### Buffer B (Lysis buffer):

NaH <sub>2</sub> PO <sub>4</sub>	100 mM
Tris-HCL	10 mM
Urea	8 M

adjust pH 8.0 with NaOH  
(immediately before use)

##### Buffer C (Wash buffer):

NaH <sub>2</sub> PO <sub>4</sub>	100 mM
Tris-HCL	10 mM
Urea	8 M

adjust pH 6.3 with HCl  
(immediately before use)

##### Buffer E (Elution buffer):

NaH <sub>2</sub> PO <sub>4</sub>	100 mM
Tris-HCL	10 mM
Urea	8 M

adjust pH 4.5 with HCl  
(immediately before use)

##### 10x PBS:

NaCl	8 % (w/v)
KCl	0.2 % (w/v)
NaH <sub>2</sub> PO <sub>4</sub>	1.44 % (w/v)
NaH <sub>2</sub> PO <sub>4</sub>	0.24 % (w/v)

adjust pH 7.4

##### Dialysis buffer 1:

Urea	4 M
NaCl	2 M
Tris base	50 mM

adjust pH 9.5 with HCl

##### Dialysis buffer 2:

NaCl	4 M
Tris base	50 mM

adjust pH 9.5 with HCl

#### 2.1.10.5. Transformation of *E. coli* and *Nab. magadii*

##### Transformation of *E. coli* – generation of competent cells:

##### MOPS I:

MOPS	100 mM
CaCl <sub>2</sub>	10 mM
RbCl <sub>2</sub>	10 mM

adjust pH 7.0 with KOH

##### MOPS II:

MOPS	100 mM
CaCl <sub>2</sub>	70 mM
RbCl <sub>2</sub>	10 mM

adjust pH 6.5 with KOH

##### MOPS IIa:

MOPS	100 mM
CaCl <sub>2</sub>	70 mM
RbCl <sub>2</sub>	10 mM
Glycerol	15 %

adjust pH 6.5 with KOH

Transformation of *Nab. magadii*:

Buffered high salt spheroblasting solution:

Tris-HCl, pH 8.0	50 mM
NaCl	2 M
KCl	27 mM
Sucrose	15 %

Buffered high salt spheroblasting solution with glycerol:

Tris-HCl, pH 8.0	50 mM
NaCl	2 M
KCl	27 mM
Sucrose	15 %
Glycerol	15 %

Unbuffered high salt spheroblasting solution:

NaCl	2 M
KCl	27 mM
Sucrose	15 %

60 % PEG 600:

thawed PEG 600 (stored at -80°C)	600 µl
Unbuffered spheroblasting solution	400 µl

**2.1.10.6. Buffers and solution for *Archaea* methods**

Isolation of chromosomal DNA from *Nab. magadii*:

diverse material:

Desoxycholat	14 mM
Phenol/Chloroform	1:1
Isopropanol	
EDTA	solid
CsCl	solid
Ethidium bromide solution	10 mg/ml
Butanol	

High alkaline salt solution:

NaCl	4 M
Tris base	50 mM

Extraction of plasmid DNA from *Nab. magadii*:

Solution I (Resuspension sol.):

NaCl	2 M
------	-----

Solution II (SDS/OH sol.):

SDS	1 %
NaOH	0.2 M

Solution III (K-Acetate sol.):

K-Acetate	5 M
-----------	-----

diverse material:

Isopropanol	
EtOH	70 %

### 2.1.10.7. Buffers and solution for phage methods

#### Isolation of phage particles:

High alkaline salt solution:	Buffer Solution 1.1, 1.3, 1.5:	PEG 6000
NaCl        4 M	NaCl        2 M	
Tris base   50 mM	Tris base   50 mM	
	adjust pH 8.5 – 9	
Solution 1.1:	Solution 1.3:	Solution 1.5:
CsCl        20 g	CsCl        90 g	CsCl        135 g
Buffer      200 ml	Buffer      200 ml	Buffer      200 ml

#### Precipitation of phage proteins:

diverse material:

TCA	50 %
Ammoniac	

## 2.2. Methods

### 2.2.1. DNA cloning methods – cloning in *E. coli*

#### 2.2.1.1. Gel electrophoresis

In general for observation of DNA probes, small aliquots were mixed with 5 µl 5x DNA loading dye, loaded onto DNA gels and separated in electric fields according to their size. Afterwards the DNA was stained by incubation of the gel in an ethidium bromide bath (10 µg/ml) and visualized under a UV-transilluminator.

The nature of the gels used for this purpose was depending on the size of the DNA-fragment: small fragments (> 1000 bp) were usually separated on a 6 % PAA gel, whereas DNA fragments larger than 1000 bp were observed on a 0.8% agarose gel. In some cases however, e.g. for southern blots, agarose gels with a higher percentage of agarose were used for analysis of small DNA fragments.

- **Agarose gels:**

For preparation of an agarose gel the required amount of agarose was filled up with 1x TAE buffer and completely melted by heating in the microwave. After cooling down, the clear solution was poured in the provided gel tray of the desired size (large gel tray: 300 ml; medium gel tray: 100 ml; small gel tray: 50 ml gel). For final use, the solidified gel was put into an electrophoresis apparatus and covered with 1x TAE buffer. The prepared DNA samples were loaded onto the gel and separated by setting an electric potential of usually about 10 V/cm. The duration of the run was adapted to the fragment size and the purposes of electrophoresis, respectively.

- **6% PAA gel:**

For casting of a 6 % PAA gel the components were mixed as described in section 2.1.10.1. Immediately after adding APS and TEMED the gel was poured between two glass plates fixed in a casting system provided by Biorad (Mini – Protean® 3 system). The completely polymerized gel was set into the corresponding running apparatus and covered with 1x TBE buffer. After carefully removing the comb, the gel was ready for loading and separation of DNA samples. The electrophoretic separation within a 6 % PAA gel was performed for 26 minutes, applying a power of 20 mA/gel.

### **2.2.1.2. Polymerase chain reaction (PCR)**

Polymerase chain reaction (PCR) was performed in order to amplify DNA, either for increasing the material used for cloning strategies (preparative PCR), or for detection of certain DNA fragments in probes isolated from living cells (analytical PCR). Depending on the purpose, different templates and polymerases were used. Anyway, the primers applied for all PCR approaches were obtained from VBC genomics. Delivered in a lyophilized form they were solved in ddH<sub>2</sub>O, yielding 1 µg/µl stocks, which were diluted 1:10 for final use. Based on the G-C content of the primers the melting temperatures ( $T_M$ ) were calculated using the program Gene Runner from Hastings Software (Version 3.01). The primer annealing temperature applied during PCR progression was usually set 4° C lower than the melting temperature of the primer with a lower  $T_M$ . Other PCR conditions, the elongation temperature and elongation time, were adapted to the activity and efficiency of the used polymerases and the length of the amplified fragments, respectively.

- **Preparative PCR:**

For preparative PCRs polymerases with proofreading activity, preferentially *Pwo*, alternatively *Pfu*, were applied as they achieve lower error rates than *Taq* polymerases. As a

template either  $\phi$ Ch1-DNA or plasmid preparations from *E. coli*, both usually diluted 1:30, were used.

**PCR batch *Pwo/Pfu* (100  $\mu$ l):**

68 $\mu$ l	ddH <sub>2</sub> O
10 $\mu$ l	10x <i>Pwo/Pfu</i> buffer
10 $\mu$ l	2 mM dNTPs
5 $\mu$ l	primer forward (0.1 $\mu$ g/ $\mu$ l)
5 $\mu$ l	primer reverse (0.1 $\mu$ g/ $\mu$ l)
1 $\mu$ l	template DNA
2 $\mu$ l	polymerase ( <i>Pwo/Pfu</i> )

**PCR program:**

33 cycles	94° C	5 min	
	94° C	1 min	denaturation
	x° C *	1 min	primer annealing
	y° C *	z min *	elongation
	y° C *	5 min	
	4° C	infinite	

\* x: The annealing temperature was calculated based on the G-C content of the primers used for the approach

y: The elongation temperature was chosen corresponding to the optimal activity of the polymerase

(*Pwo*: 68° C; *Pfu*: 72° C)

z: The elongation time was adapted to the efficiency of the polymerase (*Pwo/Pfu*: 500 bp/min) and the length of the amplified DNA fragment, respectively

• **Analytical PCR:**

Analytical PCRs were often performed to screen for positive clones resulting from transformation of certain plasmids in *Nab. magadii*. For this purpose no proofreading activity was necessary, hence *Taq* polymerases (usually *GoTaq*<sup>®</sup>, alternatively *Dream Taq*<sup>®</sup>) were used. As PCR templates crude extracts were prepared from archaeal cells by centrifugation of 20  $\mu$ l culture (3 min, 10 krpm) and solution of the pellet in 100  $\mu$ l ddH<sub>2</sub>O. In addition, preparations of the transformed plasmids (1:30) and crude extracts from the original culture were tested as positive and negative controls, respectively. Furthermore, in course of this diploma work inversion events on plasmids transformed in *Nab. magadii* were detected by PCR analysis. Since *Taq* polymerases are able to cause inversion of DNA fragments on their own, *Pwo* polymerase was used for these experiments. For preparation of PCR templates, plasmid DNA was isolated from the archaeal cells according to the instructions in section 2.2.3.5.

**PCR batch *GoTaq*<sup>®</sup> (50  $\mu$ l):**

28.5 $\mu$ l	ddH <sub>2</sub> O
10 $\mu$ l	5x <i>GoTaq</i> <sup>®</sup> buffer
5 $\mu$ l	2 mM dNTPs
2.5 $\mu$ l	primer forward (0.1 $\mu$ g/ $\mu$ l)
2.5 $\mu$ l	primer reverse(0.1 $\mu$ g/ $\mu$ l)
1 $\mu$ l	template DNA
0.5 $\mu$ l	polymerase ( <i>GoTaq</i> <sup>®</sup> )

**PCR batch *Dream Taq*<sup>®</sup> (50  $\mu$ l):**

33.5 $\mu$ l	ddH <sub>2</sub> O
5 $\mu$ l	10x <i>Dream Taq</i> buffer
5 $\mu$ l	2 mM dNTPs
2.5 $\mu$ l	primer forward (0.1 $\mu$ g/ $\mu$ l)
2.5 $\mu$ l	primer reverse(0.1 $\mu$ g/ $\mu$ l)
1 $\mu$ l	template DNA
0.5 $\mu$ l	polymerase ( <i>Dream Taq</i> <sup>®</sup> )

**PCR batch *Pwo* (50 µl):**

33 µl	ddH <sub>2</sub> O
5 µl	10x <i>Pwo</i> buffer
5 µl	2 mM dNTPs
2.5 µl	primer forward (0.1 µg/µl)
2.5 µl	primer reverse (0.1 µg/µl)
1 µl	template DNA
1 µl	polymerase ( <i>Pwo</i> )

**PCR program:**

33 cycles	{	94° C	5 min	
		94° C	1 min	denaturation
		x° C *	1 min	primer annealing
		y° C *	z min *	elongation
		y° C *	5 min	
		4° C	infinite	

\* x: The annealing temperature was calculated based on the G-C content of the primers used for the approach

y: The elongation temperature was chosen corresponding to the optimal activity of the polymerase

(*Pwo*: 68° C; *GoTaq*<sup>®</sup>/*Dream Taq*<sup>®</sup>: 72° C)

z: The elongation time was adapted to the efficiency of the polymerase (*Pwo*: 500 bp/min; *GoTaq*<sup>®</sup>/*Dream Taq*<sup>®</sup>: 1000 bp/min) and the length of the amplified DNA fragment, respectively

The results of both, preparative and analytical PCRs were controlled by analysis of DNA probes on agarose and 6 % PAA gels, respectively.

### 2.2.1.3. DNA purification

- **Simple purification:**

In general DNA was purified after PCR and some restriction reactions to get rid of small DNA species (dNTPs, primers, etc.) and chemical components possibly disturbing further reactions. This was performed using the QIAquick PCR purification kit (QIAGEN) according to manufacturer's instructions. Instead of elution buffer, an appropriate volume of ddH<sub>2</sub>O (usually 50 µl) was applied for elution of the purified DNA.

- **Elution from agarose and 6 % PAA gels:**

In the presence of large unwanted PCR or restriction site products, specific DNA fragments could be isolated by extraction from agarose gels and 6 % PAA gels, respectively. The nature of the gel was chosen depending on the size of the fragments (see section 2.2.1.1.). Anyway, for gel elution the whole DNA sample was mixed with 5x DNA loading dye, loaded onto the gel (up to 20 µl per slot) and separated in an electric field as described in section 2.2.1.1. After short staining in an ethidium bromide bath, the bands of interest were cut out of the gel under 70 % UV light and transferred in Eppendorf tubes. DNA isolated from agarose gels was simply purified using the QIAquick Gel Extraction kit (QIAGEN) following the supplied protocol. For extraction from 6 % PAA gels however the gel slices first had to be minced and incubated in 300 µl elution buffer (same kit), shaking at 37° C over night. Finally the DNA was isolated by centrifugation (13.2 krpm, 5 min) and purified from the resulting supernatant, also using the QIAquick Gel Extraction kit (QIAGEN) according to manufacturer's instructions.



Anyway, the purified DNA was eluted from the column with an appropriate volume of ddH<sub>2</sub>O (usually 50 µl). The result of the purification procedure was controlled by analysis of a DNA probe on an agarose or 6 % PAA gel.

#### **2.2.1.4. Restriction of DNA**

Almost all DNA restrictions were performed using restriction enzymes and the appropriate buffers provided by Fermentas. Only for digestion of pUC19 DNA with *Sau3AI* in order to produce a DNA marker, an endonuclease of the company New England BioLabs was applied. For restrictions involved in cloning procedures usually batches with a total volume of 50 µl were mixed, whereas for analytical digests (verifying of positive transformants) smaller batches (20 µl) were sufficient. For cloning approaches the amount of DNA added to the restriction batch was adapted to the estimated DNA concentration in the original probe. The amounts of buffer and enzymes, as well as the sort of buffer, were chosen according to the optimal conditions recommended by the manufacturer. Double digests were performed using the buffers suggested on the Fermentas DoubleDigest™ website (<http://www.fermentas.com/en/tools/doubledigest>). To achieve best restriction results for cloning purpose, the DNA was digested for 3 hours or over night at the appropriate temperature (usually 37° C), whereas analytical restriction batches were incubated for only 1 hour. Anyway, the result of the restriction procedure was analyzed on an agarose gel.

#### **2.2.1.5. Removal of 3' overhangs**

Removal of 3' overhangs was achieved using T4 DNA polymerase from Fermentas in the absence of dNTPs. However, to avoid changing of the buffer system, 1 µl enzyme was added directly to the 50 µl restriction mix after inactivation of the restriction endonucleases (10 min, 65° C) instead of using the supplied buffer. The activity of T4 DNA polymerase in the *KpnI*-buffer was ensured by checking the enzyme informations on the Fermentas website. The blunting reaction was done by incubation at 37° C for 30 min, followed by inactivation of T4 DNA polymerase by heating at 75° C for 10 min.

#### **2.2.1.6. Ligation**

For ligation both, the linearized vector and the DNA fragment to be ligated (insert) were analyzed on an agarose gel in order to estimate the DNA concentration. The ligation reaction was performed using the T4 DNA ligase (Fermentas) in combination with the supplied buffer. The amount

of vector used for ligation was varied by dilution in order to achieve a vector / insert ration of 3 / 1. The batch was mixed as follows:

11.5 µl	insert DNA
1.5 µl	ligase buffer
1 µl	T4 DNA ligase (Fermentas)
1 µl	linearized vector (diluted)

Ligation was performed by incubation for 3 h at room temperature or overnight in a 16° C water bath.

#### **2.2.1.7. Transformation of *E. coli***

- **Generation of CaCl<sub>2</sub> competent *E. coli* cells:**

For generation of competent *E. coli* cells, 400 ml LB \* supplemented with the respective antibiotic were inoculated with an overnight culture of the desired strain (XL-1 Blue and Rosetta, respectively) to an initial optical density (OD<sub>600</sub>) of 0.1. Shaking at 37° C the culture was grown until an OD<sub>600</sub> of approximately 0.6 was reached. The logarithmic growing cells were harvested by centrifugation (15 min, 6000 rpm, 4° C), resuspended in 160 ml MOPS I and incubated on ice for 10 min. Once more, it was centrifuged (15 min, 6000 rpm, 4° C), yielding a pellet which was resuspended in 160 ml MOPS II. This time it was incubated on ice for 30 min and pelletised by centrifugation again. Finally the pellet was solved in 8 ml MOPS IIa, aliquoted to 100 µl per Eppendorf tube and stored at -80° C until final use. To achieve optimal results, all steps were carried out as quickly as possible keeping the cells cooled during the whole procedure and using ice cold solutions.

\* alternatively competent cells were generated from 100 ml culture, using ¼ vol. of the described buffers

- **Heat shock transformation:**

For transformation of a ligation product, the whole 15 µl ligation batch was pipetted to the 100 µl competent *E. coli* cells (thawed on ice). Transformation of plasmid preparations in contrast was performed using 10-200 ng DNA. Anyway, after adding the DNA, the bacterial cells were incubated on ice for 30 min. To enhance the intake of foreign DNA the cells were heat shocked by keeping them on 42° C for 2 min. After short incubation on ice, 300 µl LB were added and the cells were regenerated at 37° C for another 30 min. Finally they were plated on LB agar plates containing the respective antibiotics (120 µl per plate) and incubated at 37° C overnight. The next day single colonies were inoculated in order to screen for positive clones.

### **2.2.1.8. Quick Apply – screening for positive clones**

For quick screening of transformants, numerous single colonies (usually 30) were picked from selective agar plates, inoculated in 5 ml LB medium supplemented with the respective antibiotics and grown at 37° C overnight. The next day 300 µl were taken from each liquid culture and centrifuged at 13.2 krpm for 3 min. The supernatant was removed and the resulting cell pellet was resuspended in 30 µl 5x DNA loading dye. Afterwards the batch was mixed with 14 µl of phenol/chloroform (1:1) by thorough vortexing (approx. 30 sec) and centrifuged again (13.2 krpm, 5 min). 12 µl of the aqueous phase were loaded onto a 0.8 % agarose gel in order to analyze the crude extracted nucleic acids in the probes. The run of the gel and staining were performed as described in section 2.2.1.1. According to the positions of the plasmid bands on the gel, clones containing the religated vector without insert could be distinguished from putative positive clones (containing the vector carrying the insert). The latter were verified by analytical restriction (see section 2.2.1.4.) of prepared plasmids and, if necessary, by analytical PCRs (see section 2.2.1.2.).

### **2.2.1.9. Plasmid preparation from *E. coli***

Plasmid DNA from *E. coli* was prepared from 3 ml liquid culture (2 x 1.5 ml) using the GeneJET™ Plasmid Miniprep Kit from Fermentas according to manufacturer's instructions. However, instead of elution buffer, 50 µl ddH<sub>2</sub>O were used for elution of the plasmid DNA from the silica column.

### **2.2.1.10. Quantification of DNA and lyophilization**

DNA concentrations were calculated based on OD<sub>260/280</sub> using the UV/Vis-Spectrophotometer NanoDrop ND-1000 from PeqLab. Semiquantitative determinations of DNA concentrations were performed by analysis of DNA probes on agarose and 6 % PAA gels, respectively. To increase DNA concentrations by reducing the volume (necessary for some procedures), the speed vac UNIVAPO 100H (UniEquip) was used for lyophilization.

### **2.2.1.11. Alpha complementation**

If an insert was cloned into a vector disrupting the α-fragment of the *lacZ* gene, this method could be used to facilitate the first step of cloning. For that purpose *E. coli* cells (*lacZ*-α deficient *E. coli* strain) transformed with the ligated plasmids were plated on LB agar plates containing 1 mM IPTG and 40 µg/ml X-Gal. As a result, due to the activity of β-galactosidase, two types of colonies

could be distinguished: blue colonies (carrying a functional *lacZ*- $\alpha$ -fragment) and white colonies (containing plasmids carrying the insert). This way, pre-selection of positive clones was enabled.

## 2.2.2. Cloning strategies of current projects

### 2.2.2.1. Strategies for the deletion of $\phi$ Ch1 ORF34

For construction of a  $\phi$ Ch1 deletion mutant lacking the putative tail fibre protein, the regions upstream and downstream of ORF34, interrupted by a novobiocin resistance cassette, were cloned on the suicide vector pKS<sub>II</sub><sup>+</sup>. In a first cloning step the upstream region (nu. 22252 – 23235 of the genome of  $\phi$ Ch1) was amplified by PCR using the primers D34-1 and D34-2. The resulting 1006 bp fragment was digested with *Xba*I and *Kpn*I and ligated with the vector pKS<sub>II</sub><sup>+</sup> (restricted with the same enzymes). After verification of a positive clone, the resulting plasmid (pKS<sub>II</sub><sup>+</sup>  $\Delta$ ORF34-fragment 1) was digested with the restriction endonucleases *Kpn*I and *Hind*III. For cloning of the region downstream of ORF34 (fragment 2, nu. 24625 – 25584 of the genome of  $\phi$ Ch1) another preparative PCR was performed, using the primers D34-3-Sma and D34-4, respectively. However, for amplification of both, fragment 1 and 2,  $\phi$ Ch1 DNA (diluted 1:30) was used as a PCR template. Anyway, just like the vector, the 985 bp product of PCR 2 was restricted with *Kpn*I and *Hind*III and ligated with pKS<sub>II</sub><sup>+</sup>  $\Delta$ ORF34-fragment 1, yielding the plasmid pKS<sub>II</sub><sup>+</sup>  $\Delta$ ORF34-fragment 1+2. Finally, the novobiocin restriction cassette was cloned between fragment 1 and fragment 2. For that purpose the 2453 bp *gyrB* (coding for Nov<sup>R</sup>) was cut out of the plasmid pMDS11 using *Sma*I and *Hind*III and isolated by extraction from a 0.8 % agarose gel. After restriction of pKS<sub>II</sub><sup>+</sup>  $\Delta$ ORF34-fragment 1+2 with *Sma*I and *Hind*III (both restriction sites introduced by primer D34-3-Sma), vector and template were ligated and cloned in *E. coli*. The final construct (pKS<sub>II</sub><sup>+</sup>  $\Delta$ ORF34-deletion cassette) was then used for replacing of ORF34 in the  $\phi$ Ch1 genome by transformation into *Nab. magadii* L11 and screening for positive clones resulting from chromosomal integration.

### 2.2.2.2. Complementation of $\phi$ Ch1- $\Delta$ ORF34

In order to verify the effect caused by deletion of  $\phi$ Ch1 ORF34, the mutation was complemented by introduction of a functional ORF34 on a plasmid. For this purpose, two different variants were tested: the non-inverted fragment ORF34<sub>1</sub> and the inversion product ORF34<sub>52</sub>, carrying the 3' end of ORF36. However, only gene products of constructs comprising ORF34<sub>52</sub> were supposed to complement the function of the putative tail fibre protein gp34, enabling infection of the host cell by the virus  $\phi$ Ch1.

For cloning both variants, ORF34<sub>1</sub> and ORF34<sub>52</sub>, were amplified by preparative PCR and introduced into the vector pRR007. The PCR of ORF34<sub>1</sub> was performed applying the primers 34-3 and 34-Kpn, whereas for the amplification of ORF34<sub>52</sub> the primers 34-Kpn and 36-3 were employed. As templates, the plasmids pBGB1 and pBGB52 respectively, both prepared from *E. coli*, were used. The product of each PCR was restricted with *KpnI* and *HindIII* and ligated with the shuttle vector pRR007 (digested with the same enzymes). The two resulting plasmids, pRR007-ORF34<sub>1</sub> and pRR007-ORF34<sub>52</sub>, were transformed in the *Nab. magadii* strain L11  $\Delta$ ORF34, yet screening did not yield any positive clones. Hence, two further constructs using another shuttle vector (pNB102) were prepared. Again ORF34<sub>1</sub> and ORF34<sub>52</sub> were amplified by preparative PCRs, this time using the primer-sets 34-Kpn / 34-3-Xba and 34-Kpn / 34-3-X, respectively. Both fragments, as well as the vector pNB102 were digested with *KpnI* and *XbaI*. Ligation of pNB102 with ORF34<sub>1</sub> and ORF34<sub>52</sub> respectively yielded two plasmids, pNB102-ORF34<sub>1</sub> and pNB102-ORF34<sub>52</sub>, which were successfully transformed in archaeal strains and used for complementation experiments.

### 2.2.2.3. Construction of eight *int1* clones comprising variations in single repeats

In course of this diploma work, different constructs for further investigation of the inversion reaction were made. All of them were composed of *int1* as well as single repeats of the clusters IR-R and IR-L found within ORF34 and ORF36 of the  $\phi$ Ch1 genome. These repeats were flanking a spacer region resembling the invertible region in its size and G-C content. However, three of the eight clones (#584, #586, #608) were differing in the orientation of the repeats, whereas four clones (#661, #662, #663, #664) were characterized by exchanges of certain nucleotides. The last clone (#615) was used as a negative control as *int1* was lacking, excluding the possibility of inversion of the spacer region. The eight constructs are listed in the table below.

For investigation of the effect of the single repeat variations on the possibility to perform inversion events, all eight *int1*-constructs were cloned on the shuttle vector pRo-5, controlled by the putative strong promoter *fdx* from *H. salinarum*. Hence, as an initial step a cloning vector (pUC19) containing *fdx* had to be produced. For this purpose the 100 bp fragment was amplified by PCR, using the primers *fdx*-1 and *fdx*-2 and pJAS35 (plasmid preparation from *E. coli*) as a template. Both, the produced *fdx*-fragment and the pUC19 vector were digested with *KpnI* and *XbaI*, ligated and transformed into the *E. coli* strain XL-1 Blue. Screening for clones containing the small insert was enhanced by alpha complementation (see section 2.2.1.11.). Positive clones were verified by digestion with *NcoI* (additional restriction site introduced by *fdx*). However, for introduction of the *int1*-constructs, pUC19-*fdx* was digested with *NcoI* and *HindIII*. The eight inserts were isolated by restriction of pBAD24 vectors containing the constructs (pBAD24-584, pBAD24-586, pBAD24-608,

pBAD24-615, pBAD24-661, pBAD24-662, pBAD24-663 and pBAD24-664) and extraction from a 0.8 % agarose gel. All of them were ligated with the digested vector pUC19-fdx and cloned in *E.coli*. The plasmids prepared from positive clones (pUC19-fdx-584, pUC19-fdx-586, pUC19-fdx-608, pUC19-fdx-615, pUC19-fdx-661, pUC19-fdx-662, pUC19-fdx-663 and pUC19-fdx-664) were digested with *HindIII* and *KpnI* in order to isolate the whole fragment comprising the *int1*-construct and the fdx promoter. By gel elution the eight fdx-*int1*-fragments (615: 1200 bp, others: 2000 bp) were separated from the rest vector and finally cloned into the shuttle vector pRo-5. The eight plasmids resulting from these cloning procedures were termed pRo-5-fdx-584, pRo-5-fdx-586, pRo-5-fdx-608, pRo-5-fdx-615, pRo-5-fdx-661, pRo-5-fdx-662, pRo-5-fdx-663 and pRo-5-fdx-664, respectively.

<b>Clone number</b>	<b>Repeat variant</b>	<b>Explanation</b>
#584	Int1- IRLHind IRRXba	spacer region flanked by inverted repeats, positive control
#586	Int1- IRLHind DRRXba	spacer region flanked by direct repeats (IR-L orientation)
#608	IDR IRL int1 (int1 IRRDIRL)	spacer region flanked by direct repeats (IR-R orientation)
#615	ΔIRR IRL	lack of <i>int1</i> , negative control
#661	IRL-IRM1 int1	point mutation within repeat sequence: exchange G3 to A3
#662	IRL-IRM4 int1	point mutation within repeat sequence: exchange G4 to A4
#663	IRL-IRM7 int1	point mutation within repeat sequence: exchange A5 to T5
#664	IRL-IRM11 int1	point mutation within repeat sequence: exchange C6 to A6

#### **2.2.2.4. Cloning of a putative activator of *int1* expression (ORF43/44)**

To investigate the influence of a possible activator on the expression of *int1* and the time point of inversion, the corresponding gene region (ORF43 and ORF44) was cloned onto the shuttle vector pNB102 and introduced in a *Nab. magadii* strain already carrying the invertible region on another vector (pRo-5). The region comprising ORF43 to ORF44 was amplified by PCR using the primers 44-3 and 43-Kpn-5 and φCh1-DNA (diluted 1:30) as a template. The resulting product was restricted with *KpnI* and *XbaI* and ligated with pNB102 (digested with the same enzymes), yielding the plasmid pNB102/43-44.

#### **2.2.2.5. Deletion of the start codon of *int1* (ΔAUG-*int1*)**

Construction of a vector comprising the whole φCh1 invertible region except for the start codon of *int1* was achieved by amplification of the regions upstream and downstream of *int1*-AUG and combination of both fragments on a plasmid. As a first step, the 2323 bp upstream region was cloned using the primers 34-Kpn and 3601-Xba and the plasmid pGB52 as a template for preparative PCR. The product was restricted with *KpnI* and *XbaI* and introduced into a pUC19 cloning vector. Next, the resulting plasmid (pUC19-ΔAUG-int1-fragment1) was digested with *HindIII* and *XbaI*.

In order to prepare the second fragment (region downstream of *AUG-int1*), a PCR was performed using the same template and 36-5-HindIII as well as 3602-Xba as primers. The resulting 2161 bp fragment 2 was digested with *HindIII* and *XbaI* as well and ligated with the linearized vector, yielding the plasmid pUC19- $\Delta$ AUG-int1-fragment1+2. As a third step, the whole  $\Delta$ AUG-construct was transferred to the shuttle vector pRo-5. For this purpose pUC19- $\Delta$ AUG-int1-fragment1+2 was digested with *FspI* (*Nsbl*) and *HindIII*, yielding one *HindIII* restriction site and one blunt end. The 4500 bp  $\Delta$ AUG-fragment was isolated from the rest vector by extraction from a 0.8 % agarose gel. For production of an appropriate pRo-5 vector, a 50  $\mu$ l restriction batch was mixed, digesting with *KpnI* first. Afterwards the enzyme was inactivated and the 3' overhang on the restriction site was removed employing T4 DNA polymerase in the absence of dNTPs (see section 2.2.1.5.), yielding the blunt end. Finally, the DNA was purified in order to remove chemical components of the old buffer-system and pRo-5 was digested with *HindIII* for creation of the appropriate sticky end. To get the plasmid pRo-5- $\Delta$ AUG-int1 which was finally transformed in *Nab. magadii* L13, the resulting pRo-5 vector was ligated with the prepared  $\Delta$ AUG-fragment and cloned in *E. coli*.

### 2.2.3. Methods for *Archaea*

#### 2.2.3.1. Transformation of *Nab. magadii* and screening for positive clones

- **Generation of *Nab. magadii* spheroblast cells:**

For generation of competent *Nab. magadii* cells (spheroblasts), a fresh pre-culture was used for inoculation of three baffled 500 ml flasks, each containing 60 ml NVM+ supplemented with bacitracin (70  $\mu$ g/ml). Usually the batches were completed by the addition of 4 ml, 6 ml, and 8 ml pre-culture, respectively. The cells were grown at 37°C, shaking with a speed of 160 rpm in order to reach an OD<sub>600</sub> of 0.5-0.6 (usually at least after 24h). The culture with the optical density closest to the aimed value was centrifuged at 6000 rpm for 15 min (room temperature), yielding a cell pellet which was resuspended in ½ volume (30 ml) buffered spheroblasting solution with glycerol. After addition of proteinase K to a final concentration of 20  $\mu$ g/ml, the batch was incubated on a 42° C shaker for 1-2 days. When formation of spheroblast cells could be observed by light microscopy, the *Archaea* were supposed to be competent for transformation of foreign DNA.

- **Transformation of competent *Nab. magadii* cells:**

For each transformation batch (incl. neg. control) , spheroblast cells from 1.5 ml culture were harvested by centrifugation (10 krpm, 3 min, room temperature) and resuspended in 150  $\mu$ l

buffered spheroblasting solution (without glycerol). After addition of 15  $\mu\text{l}$  0.5 M EDTA the cells were incubated at room temperature for 10 min. Subsequently the DNA to be transformed (approx. 5  $\mu\text{g}$ ) was added. To prevent dramatic changes of the NaCl concentrations in the transformation batches, a maximal volume of 10  $\mu\text{l}$  DNA was used. Hence, if necessary, the concentration in the DNA solution had to be increased to approx. 500 ng/ $\mu\text{l}$  (at least 300 ng/ $\mu\text{l}$ ) by lyophilization. After addition of the DNA followed by incubation for 5 min, each batch was mixed with 150  $\mu\text{l}$  60 % PEG 600 (see section 2.1.10.5.) and left at room temperature for 30 min. Subsequently 1 ml NVM+ was added and the cells were harvested by centrifugation at 10 krpm for 5 min (room temperature). For regeneration, the pellet was resuspended in 1 ml fresh medium and incubated, shaking at 37° C for 1-2 days. Finally, the transformation batch was plated on agar plates supplemented with the respective antibiotic (120  $\mu\text{l}$  per plate). In addition, a 1:10 dilution was prepared with fresh NVM medium and plated on selective plates too. Single colonies could be observed on the agar plates after incubation at 37° C for at least two weeks.

- **Screening for positive clones:**

To achieve quick screening for transformants, single colonies were picked from agar plates and inoculated in 1ml NVM+ supplemented with the antibiotic needed for selection. Growing in Eppendorf tubes, they had to be aired once a day in order to generate aerobic conditions. After incubation on a 42° C shaker for approx. one week, crude extracts could be prepared as described in section 2.2.1.2. To identify positive transformants, they were used as templates for analytical PCRs. If these test PCRs did not give clear results, southern blot analysis was performed in order to verify putative positive clones.

### **2.2.3.2. Generation and verification of a homozygous deletion mutant**

As described above, a  $\phi\text{Ch1}$  ORF34 deletion mutant was produced by cloning of the neighboring genomic regions as well as the selection marker  $\text{Nov}^{\text{R}}$  on a suicide vector and transformation into *Nab. magadii* L11. Clones showing integration of the deletion cassette into the host chromosome were identified by analytical PCR using the primers D34-1 and Nov-9. However, as *Nab. magadii* is known to contain up to 50 genome copies, the described procedure does probably not yield a homozygous clone completely lacking ORF34. To overcome this problem, wild type variants of ORF34 had to be eliminated by persistent growing, keeping the culture in a logarithmic growth phase, continuously selecting on the antibiotic resistance provided by the deletion cassette. For that purpose the culture was grown until a late logarithmic phase was reached, followed by transfer of 50-500  $\mu\text{l}$  to 20 ml fresh medium containing the selective antibiotic. This procedure, termed passaging was repeated several times. Every fifth passaging cycle, the culture was tested for



both, the presence of the mutant-variant and the wild type gene by analytical PCR. In the case of  $\Delta$ ORF34, the wild type ORF34 was eliminated after a total of 20 passaging cycles (detected by PCR using the primers 34-5 and 36-3).

In addition to PCR analysis, a southern blot was performed in order to verify the homozygous deletion of ORF34. For this purpose chromosomal DNA was isolated from the putative *Nab. magadii* L11- $\Delta$ ORF34 according to the protocol in section 2.2.3.3. and digested with the restriction endonucleases *Bam*HI. As a control, wild type L11 DNA digested with the same enzyme (batches listed below). The fragments resulting from restriction of the mutant DNA on one hand and from the wild type version on the other hand were calculated in theory (listed below). Then their occurrence in the mutant and wild type culture was detected by hybridisation of the separated restriction batches blotted to a membrane with a biotinylated specific DNA probe. However, the absence of wild type fragments in the mutant culture represented a further evidence for the homozygous deletion of ORF34.

Digestion of chr. DNA (batch):

Southern blot – expected fragment lengths:

<i>L11</i>	$\Delta$ ORF34	material	strain	fragments ( <i>Bam</i> HI-digest)
10 $\mu$ l	5 $\mu$ l	chr. DNA	<i>Nab. magadii</i> L11	1847, 586, 361 [bp]
10 $\mu$ l	10 $\mu$ l	Tango Buffer	<i>Nab. magadii</i> L11- $\Delta$ ORF34	3825, 1847, 361 [bp]
4 $\mu$ l	4 $\mu$ l	<i>Bam</i> HI		
26 $\mu$ l	31 $\mu$ l	ddH <sub>2</sub> O		

**2.2.3.3. Isolation of *Nab. magadii* chromosomal DNA**

500 ml of a culture grown to an OD<sub>600</sub> of >0.6 were centrifuged at 8 krpm and 20° C for 20 min. The collected cells (pellet) were resuspended in 5 ml high alkaline salt solution and shared between two SS34 centrifugation tubes. To each tube 2.5 ml 14 mM Desoxycholat were added and carefully mixed with the cell solution by twisting or rolling the tubes in the hands, yielding a slimy liquid. Both batches were supplemented with 7.5 ml ddH<sub>2</sub>O (sterile), thorough mixed as described before and incubated on ice for 30 min. Subsequently 12.5 ml phenol/chloroform (1:1) per tube were added and mixed gently by inverting the tubes. To extract the chromosomal DNA, both batches were centrifuged at 10 krpm for 30 min at 4° C. The supernatant (upper phase) was carefully transferred to a 100 ml flask and overlaid with 0.6x volume Isopropanol. The precipitated DNA was gathered using a bended Pasteur pipette and solved in 5 ml ddH<sub>2</sub>O. Afterwards sterile EDTA was added to a final concentration of 10 mM, followed by supplementation with 1.5 g/ml rigid CsCl and approx. 15  $\mu$ l ethidium bromide (EtBr) solution (10 mg/ml). The rosé-colored liquid was transferred to a Quick-Seal ultracentrifugation tube, sealed and centrifuged at 60 krpm and 20° C for at least 16h. The next day

the resulting DNA bands were collected and transferred to an Eppendorf tube. The EtBr was completely removed by extraction with water saturated butyl alcohol until the solution was completely destained. Finally, the DNA sample was dialyzed against sterile ddH<sub>2</sub>O: first for 4h, then over night, changing the water in between. The result of the chromosomal DNA isolation procedure was controlled by analysis of a small aliquot (2 µl) on a 0.8 % agarose gel.

#### **2.2.3.4. Time course experiments**

Time course experiments were performed for the eight *int1* clones comprising variations in single repeats, L13 cultures containing the invertible region as well as a putative activator of *int1* expression and, moreover, *Nab. magadii* L13 carrying the invertible region but lacking the start codon of *int1* ( $\Delta$ AUG-*int1*). In all three cases the possibility to perform inversion reactions was investigated depending on the time point in *Nab. magadii* life cycle.

For these experiments rich medium (approx. 150 ml) completed with the respective antibiotics was inoculated to an OD<sub>600</sub> of 0.05 – 0.1 and grown at 37° C until the late stationary phase was reached (7-10 days). Every day the optical density was measured and samples were taken for crude extraction of plasmid DNA according to the procedure described in section 2.2.3.5. Appropriate dilutions of these samples were used as templates of analytical PCRs, detecting the non-inverted version on one hand and the inverted fragment on the other hand. In addition, if necessary, southern blot analysis was performed in order to further investigate the presence of the respective fragments in the various samples. For observation of the eight *int1* clones, the primers CH3-8 and p28+ were used for amplification of the non-inverted fragment, whereas the inverted fragment was detected applying CH3-8 and p28-. The negative control lacking *int1* (#615) however was investigated using *fdx1*/p28+ and *fdx1*/p28-, respectively. For the other two experiments ( $\Delta$ AUG-*int1* and supplementation of a possible activator) primers detecting the respective ORF34-variant (1369 bp) were used. In a first approach 34-5 and 34-3 were applied for amplification of ORF34<sub>1</sub> (inversion product) and 34-5/36-3 for detection of ORF34<sub>52</sub> (non-inverted fragment on pBGB52). Later 34-inv1/34-inv2 and 34-inv1/36-inv1 as well as 34-Kpn/34-3 and 34-Kpn/36-3 were tried.

Furthermore in some cases crude protein extracts were prepared from samples taken from the growing cultures and analyzed by western blot using an antibody raised against the His-tag.

#### **2.2.3.5. Extraction of (plasmid) DNA from *Nab. magadii***

3 ml (2 x 1.5 ml) of a growing culture with an OD<sub>600</sub> = 1\* were centrifuged at 13.000 x g for 2 min. The supernatant was removed and the harvested cells were resuspended in 50 µl Solution I

(Resuspension solution). Afterwards they were lysed by addition of 200 µl Solution II (SDS/OH solution) and gently mixing by inversion. The batch was incubated at room temperature for 5 min and supplemented with 150 µl Solution III (K-Acetate solution). Again it was mixed by inversion and centrifuged at 13.000 x g for 3 min. The resulting supernatant was carefully transferred to a new Eppendorf tube without disturbing the pellet. Next the DNA was precipitated by addition of 0.6-1x volume isopropanol, incubation for 2 min and centrifugation at 13.000 x g for 30 min. Immediately after centrifugation had stopped, the supernatant was removed and the DNA-pellet was washed twice with 70 % EtOH (1 ml). After drying, the DNA was solved in 30 µl ddH<sub>2</sub>O. For analyzation, 10 µl of each DNA sample were applied to a 0.8 % agarosegel.

\* For lower optical densities, the volume taken for DNA isolation was adapted

## 2.2.4. Phage methods

### 2.2.4.1. Isolation of phage particles

Phage particles were isolated from the supernatant of a lysated culture, precipitated with PEG 6000 and further purified and concentrated by ultracentrifugation, applying a discontinuous as well as a continuous CsCl gradient.

- As a first step, a dense pre-culture of the *Nab. magadii* culture carrying  $\phi$ Ch1 as a prophage (approx. 250 ml) was used for inoculation of at least 5 l NVM+ to an OD<sub>600</sub> of 0.05-0.1. If necessary, the cultures were supplemented with the appropriate antibiotics. Growth and lysis of the cultures shaking at 37° C was reported by daily determination of the optical density. When complete lysis was observed (stop in decrease of OD<sub>600</sub>), the phage particles were separated from the cell components by centrifugation (20 min, 8 krpm, 20°C).
- The supernatant was poured in fresh flasks, supplemented with 10 % (w/v) PEG 6000 and stirred over night. After precipitation, the phage particles could be collected by centrifugation (20 min, 8 krpm, 20°C) and solved in a reduced volume of high alkaline salt solution (approx. 10 ml / 1 l culture).
- For further purification and concentration, the phage suspension was set on a CsCl gradient and separated by ultracentrifugation. In a first approach, a discontinuous gradient was generated by carefully overlaying of 4 ml Solution 1.5 with 4 ml Solution 1.3, followed by approx. 5 ml phage suspension filling up the tubes (Beckman Ultracentrifuge tubes). After exact balancing,

ultracentrifugation was performed at 30 krpm and 20° C for 20 h using the swinging bucket rotor SW40Ti. The phage particles, usually visible as a defined band located to a certain density, were carefully harvested. After mixing with an equal volume of Solution 1.3., thereby applying a continuous gradient, centrifugation was performed under the same conditions as before. Again the phages particles were collected.

- Finally the resulting fractions were dialyzed against high alkaline salt solution over night and stored at room temperature.

#### **2.2.4.2. Isolation of phage DNA**

- **Quick approach:**

Initially, 100 µl purified phages (section 2.2.4.1.) were mixed with 300 µl ddH<sub>2</sub>O. For extraction of the DNA, 200 µl phenol/chloroform (1:1) were added, followed by thoroughly vortexing and centrifugation at 13.2 krpm for 3 min. Subsequently, the upper (aqueous) phase was carefully transferred to a new Eppendorf tube. The DNA was precipitated by addition of 2x vol. 96 % EtOH and centrifugation at 16.4 krpm and 4° C for 20 min. After removing the supernatant, the pellet was washed twice with 70 % EtOH (1 ml) and dried at 65 ° C. Finally it was solved in 10 µl ddH<sub>2</sub>O and analyzed on an agarose gel.

- **Long approach:**

100 µl phage fraction (section 2.2.4.1.) were combined with 400 µl ddH<sub>2</sub>O as well as 500 µl phenol/chloroform (1:1) and mixed by thoroughly vortexing (approx. 30 sec). Afterwards, the batch was centrifuged (13.2 krpm, 5 min) and the upper (aqueous) phase was transferred to a new Eppendorf tube. If slimy, white junk-elements were observed in the border phase, an additional extraction step had to be performed. For this purpose, like before, the batch was supplemented with 500 µl phenol/chloroform (1:1), vortexed and centrifuged, yielding separation in two phases. However, the isolated aqueous phase was combined with 500 µl chloroform, mixed by vortexing and centrifuged (13.2 krpm, 5 min). Again the upper phase was transferred to a fresh Eppendorf tube and mixed with 2x vol. 96 % EtOH. In order to isolate the precipitated DNA, the batch was centrifuged at 16.4 krpm for 30 min (4° C). The supernatant was removed and the pellet was washed with 70 % EtOH. After drying at 65° C, the viral DNA was solved in 10 µl ddH<sub>2</sub>O. Finally, the result of phage DNA isolation was controlled by analysis of a small aliquot on an agarose gel.

### 2.2.4.3. Precipitation of viral capsid proteins

Capsid proteins were isolated from 200 µl purified phage fractions (section 2.2.4.1.) by precipitation with 5 % TCA. After addition of the TCA, the batch was incubated on ice for 30 min, followed by centrifugation (13 krpm, 30 min, 4° C). The resulting pellet was resuspended in 25 µl 5 mM sodium phosphate buffer and supplemented with 25 µl 2x protein sample buffer (Laemmli). Since precipitation with TCA caused a decrease in pH, the samples had to be neutralized by treatment with gaseous ammoniac until the color turned blue again.

### 2.2.4.4. Phage titre analysis and some applications

For determination of phage titres, a culture of the *Nab. magadii* strain to be infected was grown to the stationary phase. Moreover, different dilutions were prepared from the phage samples to be tested (usually  $10^{-2}$ ,  $10^{-4}$ ,  $10^{-6}$ ,  $10^{-8}$  and  $10^{-10}$ ). For titre analysis, each dilution as well as the undiluted phage fraction was plated twice. For each batch 5 ml soft agar were prepared in a test tube and kept on a heater at 55° C until titre analysis was started. The procedure itself was performed by supplementation of the 5 ml soft agar with 100 µl phages, 300 µl culture and, if necessary, further additives. Quickly the batch was mixed by short vortexing and plated on NVM agar plates (supplemented with antibiotics according to resistances of the infected culture). After one day the rigid plates were put on 37° C and incubated for 7-10 days. Finally, the titre was evaluated by counting the plaques on the respective plates and calculation of an average value.

In general, phage titres are performed in order to determine the concentration of phage particles in fractions resulting from isolation. In course of this diploma work however they were mainly applied as a part of certain experiments:

1) Testing the ability of  $\phi$ Ch1 particles lacking gp34<sub>52</sub> (putative tail fibre) to infect their host:

To enable comparison, titre analysis was performed with both,  $\phi$ Ch1- $\Delta$ ORF34 and the wild type virus. The procedure was carried out according to the protocol described above.

2) Binding assay of purified gp34<sub>52</sub> and gp36<sub>52</sub> to *Nab. magadii* P3:

This experiment was performed in order to investigate a supposed reduction of the titre by binding of gp34<sub>52</sub>. As a result, a *Nab. magadii* strain lacking NEP (*Nab. magadii* P3) had to be used in order to prevent host-regulated digestion of external proteins. Moreover, in addition to the 400 µl culture, different amounts of the purified proteins gp34<sub>52</sub> and gp36<sub>52</sub> (up to 400 µg) were added to the soft agar. 10 µl of the phage fractions in different dilutions ( $10^{-2}$  –  $10^{-8}$ ) were spotted on the respective plates (differing in the amounts of

protein) afterwards. To achieve the required firmness of the soft agar, the amount of agar added to the NVM was adapted if more than 2 ml protein was applied.

3) Quick test to investigate complementation of  $\Delta$ ORF34<sub>52</sub>:

In order to test the complementation of the deletion of ORF34<sub>52</sub>, *Nab. magadii* L13 cultures carrying the plasmids pNB102-ORF34<sub>1</sub>, pNB102-ORF34<sub>52</sub> and pNB102 as well as *Nab. magadii* L13 (control) were transformed with phage DNA isolated from  $\phi$ Ch1- $\Delta$ ORF34. 100  $\mu$ l of the regenerated cells (undiluted, dilutions  $10^{-2}$  and  $10^{-4}$ ) as well as 300  $\mu$ l of the respective culture were added to the 5 ml soft agar and plated on NVM agar / Mev as described above.

## 2.2.5. Protein methods

### 2.2.5.1. Preparation of crude protein extracts

For preparation of crude protein extracts from a growing culture, 1.5 ml were centrifuged at 13.2 krpm for 3 min. The supernatant was removed and the pellet was resuspended in  $OD_{600} \times 75 \mu$ l 5 mM sodium phosphate buffer. Subsequently the same volume of 2x protein sample buffer (Laemmli) was added. Before applying a sample to a protein gel, the extracts were heated at 95° C for 10 min.

### 2.2.5.2. Protein expression in *E. coli*

For production of recombinant proteins in *E. coli*, 4-5 l LB supplemented with the respective antibiotics were inoculated to an  $OD_{600}$  of approx. 0.1 using an overnight culture of the strain carrying the desired gene region on a plasmid. The culture was grown, shaking at 37° C. When an  $OD_{600}$  of approx. 0.3 was reached, expression was induced by addition of IPTG to a final concentration of 0.5 mM (stock: 1 M) and the culture was incubated at 37° C for another 3h. Afterwards the cells were harvested by centrifugation (6000 rpm, 15 min, 4° C) and the supernatant was removed. The pellet could be stored at -20° C until final use.

In order to observe the process of protein expression, crude extracts were prepared from the culture before and after induction with IPTG as described in section 2.2.5.1 and analyzed via SDS-PAGE.

### 2.2.5.3. Protein purification under denaturing conditions

First of all, the cell pellet resulting from protein expression was solved in an appropriate volume of buffer B (100-150 ml for cells resulting from 4-5 l culture) and stirred gently for at least 4h. For complete lysis, the samples were sonicated approx. 5 x 2min (Power 90 %, Cycle 72). Afterwards the lysates were centrifuged at 9000 rpm and 4° C for 20 min and the supernatant containing the proteins was combined with 500 µl – 1 ml Ni-NTA (Quiagen)\*. In order to enable binding of the His-tagged proteins to the Ni<sup>2+</sup> ions, the suspension was stirred over night. For purification of the proteins, the whole lysate was applied to a column provided by Quiagen (QIAexpressionist™ Kit), collecting the flowthrough in an Erlenmeyer flask, whereas the nickel-beads were accumulated on the filter of the column. After washing twice with 4 ml buffer C, the proteins bound to the Ni-NTA were eluted by addition of 6 x 500 µl buffer E. The respective fractions (2 x wash, 6 x elution) were collected in Falcons and Eppendorf tubes, respectively. For analyzation, a small aliquot of each fraction was mixed with an equal volume of 2x protein sample buffer (Laemmli), heated at 95° C for 10 min and applied to a protein gel as described in section 2.2.5.5.

\* The exact conditions were adapted with respect to the results obtained from former attempts

### 2.2.5.4. Dialysis of proteins

For final use, purified proteins were dialyzed in order to remove the urea. Proteins isolated for combination with living *Nab. magadii* cells (e.g. binding assays) were adjusted to high salt concentrations and high pH by dialysis against dialysis buffer 1 and dialysis buffer 2 over night. To achieve better results, both buffers were changed after a few hours. Proteins purified for the production of antibodies in contrast were dialyzed against 1 x PBS, also changing the buffer after one hour, followed by incubation over night.

### 2.2.5.5. SDS-PAGE

For analyzation of protein probes, they were applied to protein gels and separated in electric fields by sodiumdodecylsulfat polyacrylamide gel electrophoresis (SDS-PAGE). This method is based on denaturation of proteins and masking of their net charge by SDS. Hence, they are separated according to their size exclusively.

- **Preparation of protein gels:**

Discontinuous polyacrylamide gels (protein gels) are composed of two parts: a stacking gel and a separation gel. They were cast using the Mini Protean 3 system provided by BioRad

according to manufacturer's instructions. As a first step, the separation gel of the desired percentage was mixed as described below. Immediately after adding APS and TEMED, it was cast between two glass plates separated by a spacer. To prevent generation of a meniscus, it was overlaid with isopropanol. After polymerization, the isopropanol was removed and AA-solution, stacking gel buffer and ddH<sub>2</sub>O were mixed for preparation of the stacking gel. Again, polymerization was started by addition of APS and TEMED. Quickly the gel was poured into the casting apparatus, overlaying the separation gel and a comb was inserted in order to leave space for loading the samples. Completely polymerized gel could be stored at 4°C, rounded by wet paper in order to prevent desiccation.

<u>Separation gel:</u>				<u>Stacking gel:</u>	
<i>material</i>	<i>12 % gel</i>	<i>10 % gel</i>	<i>8 % gel</i>	<i>material</i>	<i>4 % gel</i>
AA-solution (30 %)	2 ml	1.67 ml	1.33 ml	AA-solution (30 %)	267 µl
Separation gel buffer	1.25 ml	1.25 ml	1.25 ml	Stacking gel buffer	500 µl
ddH <sub>2</sub> O	1.75 ml	2.08 ml	2.42 ml	ddH <sub>2</sub> O	1233 µl
APS (10 %)	60 µl	60 µl	60 µl	APS (10 %)	20 µl
TEMED	10 µl	10 µl	10 µl	TEMED	5 µl

- **SDS PAGE – running of protein gels:**

Polymerized protein gels were inserted in a running apparatus provided by BioRad and covered with 1x SDS-PAGE running buffer. Protein samples to be loaded resulting from *E. coli* were mixed with an equal volume of 2x protein sample buffer (Laemmli) and heated at 95° C for 10 min. Afterwards 10 µl were applied to the gel and run was started at 40V in order to enable accumulation in the slots. Then the electric potential was increased to 60V, followed by application of 100V when the samples had reached the separation gel. However, samples resulting from *Archaea* were prepared by either incubation at 37° C over night, or, alternatively, by extensive heating at 65° C to increase liquidity in order to enhance loading. The run was performed by applying a constant electric potential of 40V – 60V during separation.

Anyway, in addition to the protein samples, an appropriate marker was loaded onto the gel. For Coomassie staining 5 µl were applied, whereas 7.5 µl were used for western blot analysis.

### **2.2.5.6. Coomassie staining**

For irreversible staining of proteins separated by SDS-PAGE, the polyacrylamide gels were transferred to a tank filled with Coomassie staining solution and incubated for a few minutes



(depending on the quality of the staining solution). Destaining was performed either in water (o/n) or in destaining solution until the background was removed as well as possible.

#### **2.2.5.7. Western blot analysis**

Western blot analysis is based on the recognition of proteins transferred to a nitrocellulose membrane by a specific antibody or antiserum. Usually this primary antibody is bound by a secondary antibody coupled to a horseradish peroxidase (HRP) which can be detected as it causes emission of light quants in the presence of H<sub>2</sub>O<sub>2</sub> and luminol.

- **Transfer to a nitrocellulose membrane (blotting):**

Proteins to be analyzed by western blot were loaded onto a polyacrylamide gel and separated via SDS-PAGE as described in section 2.2.5.5. If crude extracts prepared from *Archaea* were applied, the corresponding gel was incubated in water for 5 min after running in order to remove sodium chloride. For the transfer procedure one Protran nitrocellulose membrane (Whatman) and six pieces of Whatman paper were cut corresponding to the size of the gel (6.5 x 9 cm). Each of them was rinsed in transblot buffer and the blot was built up in a semi-dry blotting apparatus as follows: 3 layers Whatman paper – nitrocellulose membrane – polyacrylamide gel – further 3 layers Wathman paper. Transfer was performed at 20V for 20 min (one gel) or 30 min (two gels), respectively. To ensure successful blotting, the membrane was shortly incubated in Ponceau S solution, causing reversible staining. After marking visible protein ladder bands, the blot was completely destained again with water.

- **Blocking:**

After blotting, nitrocellulose membranes were blocked by incubation in 1x TBS/TBS-T containing 5 % milk powder at 4° C over night (shaking), in order to prevent unspecific binding of the antibodies.

- **Development of a Western blot:**

The solutions and conditions applied for the development of western blots were adapted to the properties of the antibodies. In course of this diploma work, mainly the primary antibodies  $\alpha$ -gp34 and  $\alpha$ -FlaB1 were used. In both cases, western blot analysis was performed under the same conditions. After blocking, the membrane was washed once by shaking in 1x TBS for 10 min, followed by incubation with the first antibody solution (see section 2.1.8.1.) for 1h. Again, the blot was washed 3 x 10 min with 1x TBS. Subsequently, the second antibody solution ( $\alpha$ -rabbit, 1:5000 in TBS) was applied and the blot was exposed for 1h, shaking at room temperature. Finally the

antibody solution was removed and the blot was washed three times by incubation in 1x TBS for 10 min. For detection of HRP-coupled proteins, the SuperSignal® West Pico Chemiluminescent Substrate kit from Thermo Scientific was applied according to manufacturer's instructions. Immediately afterwards the blot was put in a developing cassette and X-ray hyper films provided by Amersham Biosciences were exposed for different periods of time in the darkroom.

## 2.2.6. Southern blot analysis

In course of this diploma work, southern blot analysis was performed for different purposes:

- 1) Identification of positive clones resulting from transformation of *Nab. magadii*
- 2) Further investigation of inversion events under certain conditions
- 3) Verification of a homozygous  $\phi$ Ch1-  $\Delta$ ORF34 deletion mutant

Anyway, this method was carried out by separation of the respective DNA samples on an agarose gel and blotting to a nylon membrane based on capillary forces. Then the membrane was blocked and the DNA was labeled by hybridisation with a biotinylated DNA probe. This signal was recognized by streptavidine which was bound by another biotin molecule coupled to a horseradish peroxidase (HRP). Hence, finally DNA bands could be visualized by the emission of light quants based on HRP reactions in the presence of H<sub>2</sub>O<sub>2</sub> and luminol, causing blackening of hyperfilms.

### 2.2.6.1. Preparation of biotinylated DNA probes

First of all a biotinylated DNA probe had to be prepared. The respective DNA was amplified by preparative PCR and usually purified by extraction from a gel. For labeling of the probes 34  $\mu$ l DNA were denatured by heating at 95° C for 10 min, followed by incubation on ice for 5 min. Subsequently 10  $\mu$ l 5x labeling mix, 5  $\mu$ l dNTP mix (containing biotinylated ATP) and 1  $\mu$ l Klenow fragments, all of them representing components of the NEBlot® Phototope® Kit provided by New England BioLabs, were added. The labeling reaction was carried out at 37° C for 3h and stopped by the addition of 0.5  $\mu$ l 0.2 M EDTA (pH 8.0). Then the DNA was precipitated by mixing with 10  $\mu$ l 4 M LiCl and 150  $\mu$ l 96 % EtOH, incubation at -20° C for 20 min and centrifugation at 16.4 krpm for 30 min (4° C). The resulting pellet was washed with 1 ml 70 % EtOH and dried at 65° C. Finally it was resolved in 20  $\mu$ l ddH<sub>2</sub>O.

Before adding to the membrane, the DNA probe was denatured for 5 min at 95° C.

### **2.2.6.2. Separation and blotting of DNA samples to a membrane**

Usually the DNA probes to be blotted were mixed with 5 µl 5x DNA loading dye containing 1 mg/ml ethidium bromide (stock: 10 mg/ml). All samples were loaded onto an agarose gel of the desired percentage of agarose (0.8-1.5 %) and separated in an electric field as described in section 2.2.1.1. In addition, 0.5-1 µl biotinylated 2-log DNA Ladder from New England BioLabs was applied. After separation, the DNA was analyzed under UV light and denatured by incubation of the gel in 0.4 M NaOH / 0.5 M NaCl for 30 min. Subsequently, the gel was switched to 1.5 M NaCl / 0.5 M Tris-HCl (pH 7.5) and neutralized for 30 min. Then the DNA was transferred to an Amersham Hybond™ nylon membrane (GE Healthcare) by capillary blotting over night. For this purpose, a piece of membrane corresponding to the size of the gel was rinsed in water and equilibrated in 10x SSC. The blot was built up on a potest placed inside a tank as follows: 3 layers Whatman paper (the lowest extended to the ground of the tank) – gel – membrane – further 3 layers Whatman paper – one stack of adsorbent paper of an appropriate size. Finally the tank was filled with 10x SSC and the whole blot was stably weighted in order to enhance transfer to the membrane. The next day successful blotting was ensured by staining of the gel with ethidium bromide. Finally the membrane was shortly incubated in 0.4 M NaOH and 0.2 M Tris/HCl (1 min each) and the DNA was fixed by UV-cross linking using the Stratalink cross-linker provided by Stratagene.

### **2.2.6.3. Blocking and hybridisation**

For blocking, the membrane was transferred to a southern blot tube which was filled with 12 ml hybridisation buffer and 120 salmon sperm DNA (100 µg/ml), placed to a hybridisation oven and incubated at 65° C for at least 3h (rotating). Afterwards the labeled DNA probe (20 µl) was added and incubation was continued over night.

### **2.2.6.4. Developing of a southern blot**

Left in the southern blot tube, the membrane was washed 2 x 5 min at room temperature using either 4x SSC / 0.1 % SDS (PCR samples) or 2x SSC / 0.1 % SDS (chromosomal DNA samples). Then it was incubated with 0.1x SSC / 0.1 % SDS at 65° C for 2 x 15 min.

Afterwards the membrane was transferred to a small basin and developed using the Phototope®-Star detection Kit provided by New England BioLabs. As a first step, the membrane was washed 1 x 5 min in blocking solution (shaking), followed by 5 min incubation with a streptavidin solution (7 ml blocking solution supplemented with 7 µl streptavidin) . Afterwards it was washed 3 x 5 min with 1x Wash solution I and exposed to biotinylated alkaline phosphatase solution (7ml

blocking solution supplemented with 7  $\mu$ l alkaline phosphatase) for 5 min. Finally the blot was washed 1 x 5 min with blocking solution and 3 x 5 min with 1x Wash solution II. For detection, peroxidase reaction was started by mixing of 3 ml 1x CDP-Star<sup>®</sup> dilution buffer with 6 $\mu$ l CDP-Star<sup>®</sup> reagent and pipetting over the membrane for 5 min. Immediately afterwards the blot was put in a developing cassette and X-ray hyper films provided by Amersham Biosciences were exposed for different periods of time in the darkroom.

## 3. Results and Discussion

---

### 3.1. Deletion of $\phi$ Ch1 ORF34

Deletion mutants had already successfully been constructed of both,  $\phi$ Ch1 and its host *Nab. magadii*. The method applied for this purpose was established in 2009 in the laboratory of Angela Witte when Christian Derntl managed to delete the extracellular protease (NEP) of *Nab. magadii* L13 (Derntl, 2009). It was based on transformation of a suicide vector carrying a deletion cassette composed of the upstream and downstream regions of the desired open reading frame as well as a selection marker working in *Nab. magadii*. Integration of this deletion cassette into the archaeal genome yielded a *Nab. magadii* strain lacking NEP, termed P3, representing the first ever deletion mutant of a haloalcaliphilic archaeon (Derntl, 2009). In 2010 the same method was successfully applied for the construction of different deletion mutants of the virus  $\phi$ Ch1, namely  $\Delta$ ORF79,  $\Delta$ ORF11 (structural protein E) and  $\Delta$ ORF93 (holin) (Selb, 2010). For this purpose the *Nab. magadii* strain L11 carrying  $\phi$ Ch1 as a prophage was used, enabling recombination events between the deletion cassette and the corresponding regions on the phage DNA integrated into the host chromosome. In order to eliminate the wild type variants of the desired genes in the resulting clones, the phage particles were harvested from lysated cultures and used for reinfection of a cured *Nab. magadii* strain L13. Grown on agar plates containing novobiocin, it was selected for archaeal cells infected by mutant viruses exclusively, yielding a homozygous lysogenic *Nab. magadii* culture. The corresponding phage particles could then be isolated and purified from the supernatant of lysated cultures.

Within the course of this diploma work a deletion mutant of  $\phi$ Ch1 ORF34 was constructed according to the well-tried strategy described above. Yet, since a  $\phi$ Ch1 strain lacking ORF34 and thus the putative tail fibre protein was supposed to be characterized by a loss of infectivity, production of a homozygous lysogenic strain could not be achieved by reinfection with a mixture of wild type and mutant phage particles. Instead of this, wild type variants of ORF34 were removed by passaging of the heterozygous culture and selection for the mutant version.

### 3.1.1. Aim of the study and prognosis

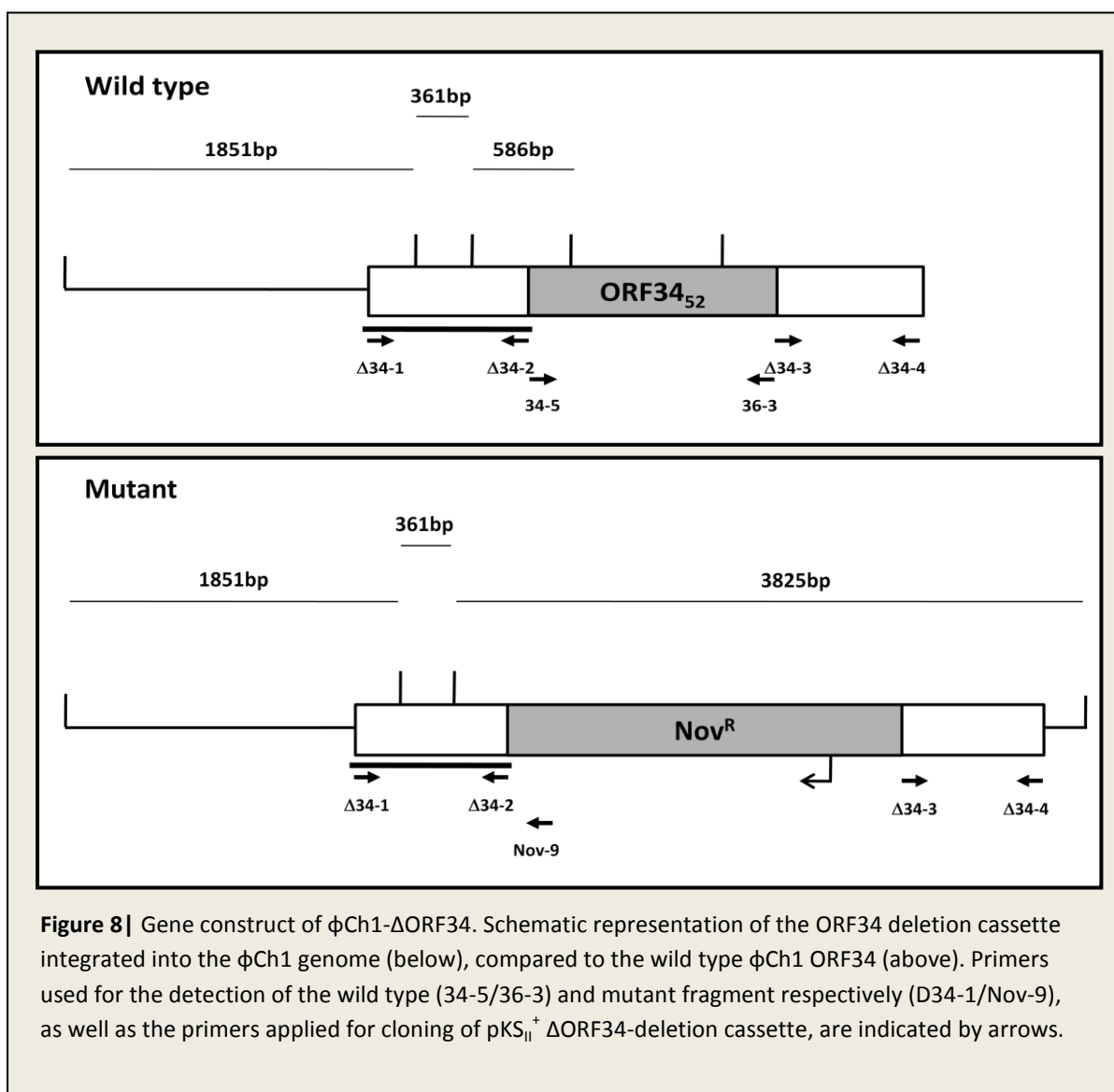
As described in section 1.2.3.5., binding assays clearly demonstrated that the protein resulting from inversion within ORF34 and ORF36, gp34<sub>52</sub>, but not the non-inverted version gp34<sub>1</sub>, binds to the surface of *Nab. magadii* cells (Rössler *et al.*, in prep). Moreover the C-terminus of gp34, the striking part for attachment to the archaeal cells, was shown to comprise a galactose like binding domain which may be involved in interaction with glycosylated structures on the surface of the archaeal cells (e.g. flagella, S-layer). These facts indicated that gp34 represents the tail fibre protein of  $\phi$ Ch1, a structural element which is often involved in binding of head tail viruses to their hosts during initiation of infection. However, only gp34<sub>52</sub> was supposed to be required for attachment to the surface of *Nab. magadii*, the only known host of  $\phi$ Ch1. Moreover a crucial role of the putative tail fibre protein gp34<sub>52</sub> for infection of the host cell could be assumed, as the addition of  $\alpha$ -D-galactose to the growth medium was shown to inhibit  $\phi$ Ch1 infectivity (Rössler *et al.*, in prep).

Anyway, to present evidence for the supposed function of gp34<sub>52</sub> and its importance for infectivity of the halophage  $\phi$ Ch1, this diploma thesis aimed to produce a mutant virus lacking the putative tail fibre protein encoded by ORF34<sub>52</sub>. In contrast to the wild type, the resulting mutant virus was expected to be unable to infect cured *Nab. magadii* L13 cells due to the absence of the structure required for binding to the host. Supposed changes concerning phenotypic features were intended to be visualized by electron microscopy.

### 3.1.2. Production of a homozygous ORF34 deletion mutant

For the production of an ORF34 deletion mutant, a deletion cassette was cloned onto the suicide vector pKS<sub>II</sub><sup>+</sup> according to procedure described in section 2.2.2.1. As illustrated in figure 8, this cassette is composed of the 983 bp upstream (nu. 22252 – 23235 of the genome of  $\phi$ Ch1) and the 959 bp downstream (nu. 24625 – 25584 of the genome of  $\phi$ Ch1) regions of ORF34, interrupted by a novobiocin resistance cassette (Nov<sup>R</sup>). The plasmid carrying this construct (pKS<sub>II</sub><sup>+</sup>  $\Delta$ ORF34-deletion cassette) was transformed into *Nab. magadii* L11 and it was selected for novobiocin resistant clones. However, due to the absence of an origin of replication working in *Archaea*, the vector construct itself was not able to persist within the cells. Hence, clones showing resistance against the selective antibiotic could not result from the presence of pKS<sub>II</sub><sup>+</sup>  $\Delta$ ORF34-deletion cassette, but only from integration of the deletion cassette into the archaeal genome. This event was the consequence of recombination between the upstream and downstream regions of ORF34 on the vector and the

corresponding wild type sequences on the  $\phi$ Ch1 genome during the lysogenic cycle of the virus. This way, the original ORF34 could be replaced by Nov<sup>R</sup> (see figure 8).



Positive clones resulting from integration of the ORF34 deletion construct into the chromosome were identified by PCR analysis using the primers D34-1 and Nov-9. Anyway, due to the presence of up to 50 genome copies in *Nab. magadii* cells, this procedure did not yield clones comprising the mutant version of ORF34 exclusively. Hence, wild type variants had to be eliminated by passaging as described in section 2.2.3.2. The homozygous deletion mutant resulting from 20 passaging cycles was verified both, by PCR and by southern blot analysis. Analytical PCRs were performed according to the protocol in section 2.2.1.2. using the primers 34-5 and 36-3 for the amplification of the wild type ORF34 fragment and D34-1/Nov-9 for the detection of the mutant version. In both cases a positive and a negative control was applied in addition to the culture to be

tested (L11- $\Delta$ ORF34, passage 20). As illustrated in figure 9a, amplification of the  $\Delta$ ORF34-fragment gave an approx. 1000 bp product using either the vector pKS<sub>II</sub><sup>+</sup>  $\Delta$ ORF34-deletion cassette (positive control, lane 5) or L11- $\Delta$ ORF34-DNA (lane 7) as a template. However, no product of the desired size resulted from PCR analysis of the wt *Nab. magadii* L11-DNA (negative control, lane 6). The approx. 1390 bp ORF34 wild type fragment in contrast could be detected in the positive control exclusively (*Nab. magadii* L11-DNA, lane 2), but not in the negative control (pKS<sub>II</sub><sup>+</sup>  $\Delta$ ORF34-deletion cassette, lane 3) or the deletion mutant (lane 4). Hence, according to these results, the wild type ORF34 had been completely removed from *Nab. magadii* L11- $\Delta$ ORF34. Anyway, in order to verify this assumption, southern blot analysis was performed.

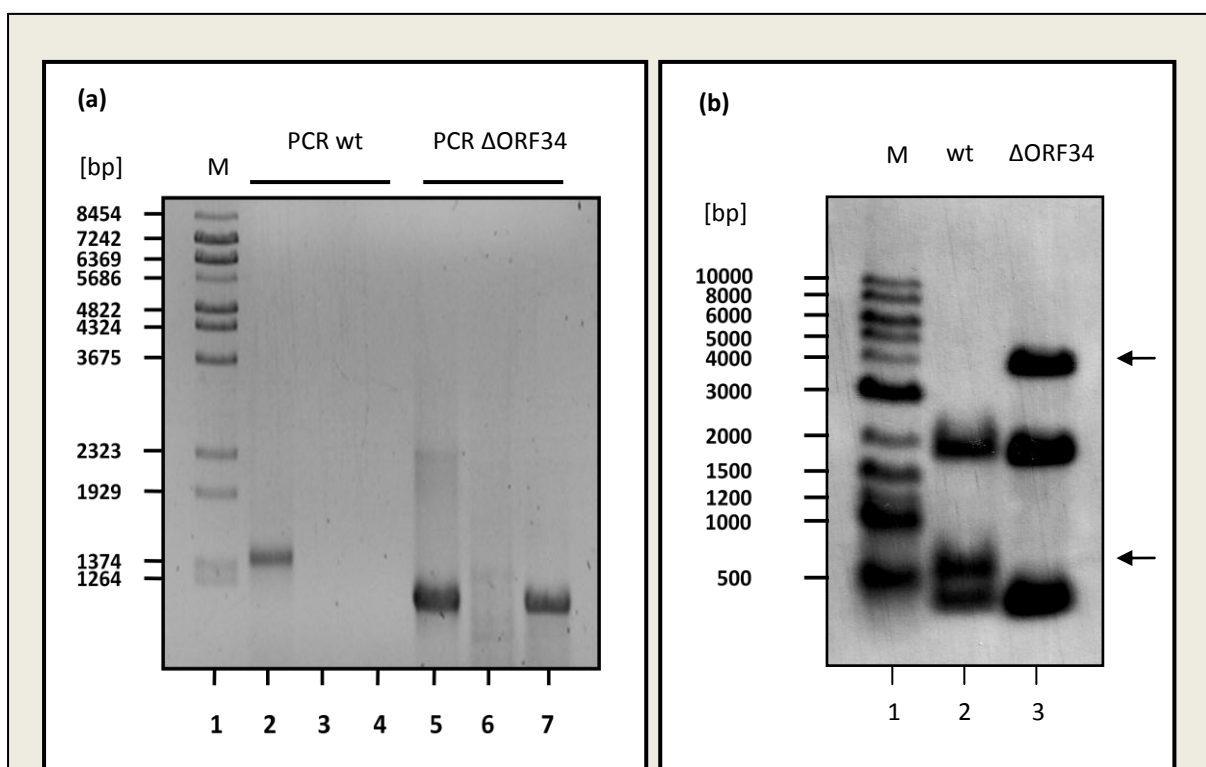


**Figure 9 |** Verification of a homozygous *Nab. magadii* L11- $\Delta$ ORF34 deletion mutant. **(a)** PCR analysis: Detection of the ~1390 bp wild type ORF34 fragment in L11 (positive control, lane 2), pKS<sub>II</sub><sup>+</sup>  $\Delta$ ORF34 deletion cassette (negative control, lane 3) and L11- $\Delta$ ORF34 passage 20 (lane 4) was performed using the primers 34-5/36-3. Detection of the ~1000 bp  $\Delta$ ORF34 fragment in pKS<sub>II</sub><sup>+</sup>  $\Delta$ ORF34 deletion cassette (positive control, lane 5), L11 (negative control, lane 6) and L11- $\Delta$ ORF34 passage 20 (lane 7) was performed using the primers D34-1/Nov-9. **(b)** Southern blot analysis: Chromosomal DNA of *Nab. magadii* L11 and *Nab. magadii* L11- $\Delta$ ORF34 passage 20 was digested with *Bam*HI and the resulting fragments were detected by hybridisation with a specific DNA probe. The 586 bp fragment specific for wt-DNA was only present in the wt (lane 2), but not in the  $\Delta$ ORF34 mutant (lane 3), whereas the mutant specific 3825 bp fragment could be detected in  $\Delta$ ORF34 exclusively.



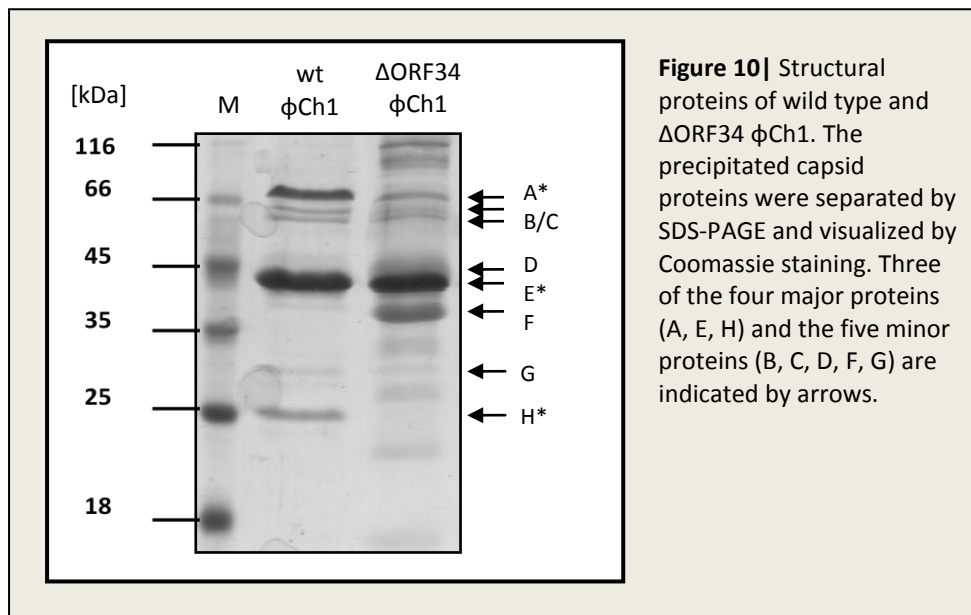
For southern blot analysis, chromosomal DNA was isolated from *Nab. magadii* L11 and *Nab. magadii* L11- $\Delta$ ORF34 passage 20 (see section 2.2.3.3.) and digested with *Bam*HI as stated in section 2.2.3.2. Aliquots of both batches were separated on a 0.8 % agarose gel, blotted to a nylon membrane (see section 2.2.6.) and hybridized with a biotinylated DNA probe specific for the 983 bp upstream region of ORF34. The restriction pattern of *Nab. magadii* L11- $\Delta$ ORF34 passage 20 completely correlated with the expected fragment lengths calculated for a homozygous deletion mutant (see section 2.2.3.2), since the 361 bp, 1847 bp as well as the mutant specific 3825 bp fragments could be detected, whereas the wt-specific 586 bp fragment was not visible (see figure 9b). Hence, it was concluded that a homozygous *Nab. magadii* L11 strain lacking any wt ORF34 variants had been prepared.

### 3.1.3. Isolation and quantification of phage particles

In a first attempt, mutant phage particles were isolated from the corresponding culture (*Nab. magadii* L11- $\Delta$ ORF34) according to the protocol in section 2.2.4.1. However, in contrast to the wild type, purification of  $\phi$ Ch1- $\Delta$ ORF34 via CsCl gradients yielded several fractions of different densities. None of them was correlating with the usual position of the wild type phages. In order to exclude that this fact was due to long time passaging of the culture used for purification of phage particles, phage DNA was isolated from one fraction according to the instructions in section 2.2.4.2. and retransformed in the cured *Nab. magadii* strain L13. Again a positive clone was identified by PCR analysis using the primers D34-1 and Nov-9. The resulting culture apparently carrying  $\phi$ Ch1- $\Delta$ ORF34 as a prophage was grown to a pre-culture and used for isolation of phage particles. Again ultracentrifugation yielded different fractions, yet application of a continuous gradient gave rise to one fraction correlating to the position of wild type  $\phi$ Ch1 (buoyant density  $n = 1.4$ ).

Since  $\phi$ Ch1- $\Delta$ ORF34 was supposed to be characterized by a loss of infectivity, the phage particles isolated from this deletion mutant could not be quantified by determination of the phage titre. Hence, the presence of phage particles in the respective purification fractions was observed by loading of an aliquot (5  $\mu$ l) on an agarose gel in order to detect viral DNA (data not shown). Moreover capsid proteins could be precipitated with TCA and analyzed by SDS-PAGE and Coomassie staining (see section 2.2.4.3.). It has to be noted, that the numerous fractions resulting from phage isolation yielded quite different protein patterns. Compared to the wild type  $\phi$ Ch1, some fractions were characterized by a reduced amount or complete lack of certain structural proteins, whereas on the other hand in some cases additional bands were present. For example the fraction illustrated in figure 10 seemed to lack protein H, whereas all other structural proteins were present, albeit varying

in their concentrations compared to the wild type. Anyway, all fractions contained a protein with a size corresponding to the main capsid protein E, the crucial element for the formation of the viral heads. In some cases these signals were more than ten-fold stronger than the signal resulting from precipitated structural proteins of the wild type  $\phi$ Ch1. Hence it was concluded that the different fractions now and then may contain very high amounts of viral particles, but also an excess of some additional proteins which can not be detected in purification fractions of the unmodified phages. Moreover, a unique morphotype of  $\phi$ Ch1- $\Delta$ ORF34 could be assumed.



### 3.1.4. Characteristics of $\phi$ Ch1- $\Delta$ ORF34 particles and the lysogenic culture

#### 3.1.4.1. Growth and lysis behaviour of *Nab. magadii* L11- $\Delta$ ORF34

First of all the growth and lysis behaviour of *Nab. magadii* L11- $\Delta$ ORF34 was analyzed in comparison to the wild type lysogenic strain *Nab. magadii* L11. For this purpose both cultures were grown to a late stationary phase, starting with an initial  $OD_{600}$  of approx. 0.1. Every day the optical density was measured, in order to enable construction of growth and lysis curves. As it can be seen in the graph of figure 11, no relevant differences of *Nab. magadii* L11- $\Delta$ ORF34 concerning growth and lysis behaviour could be observed compared to the wild type.

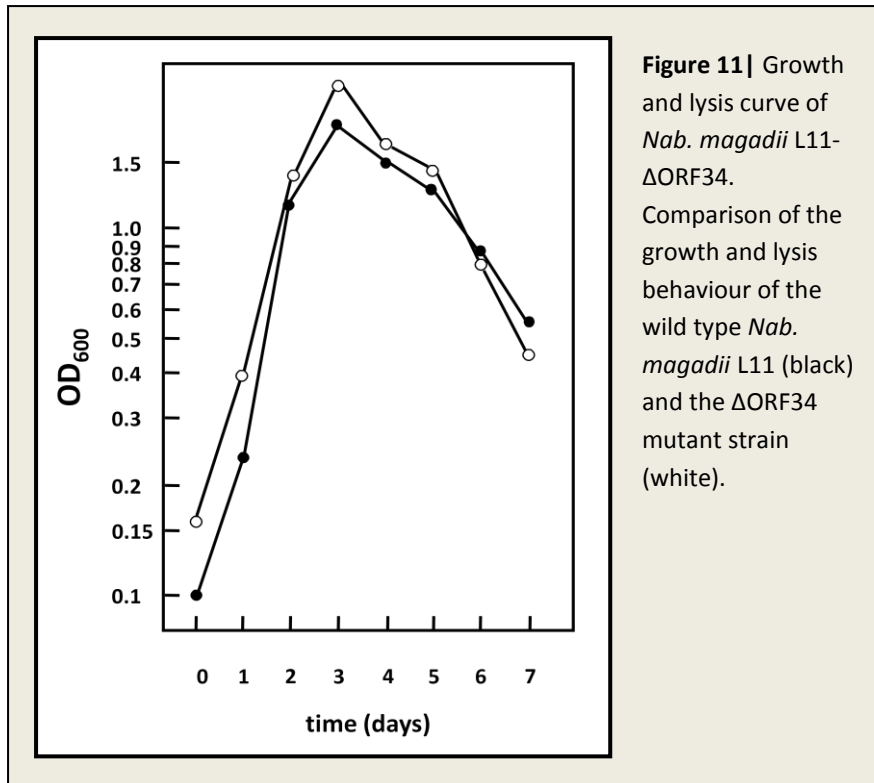
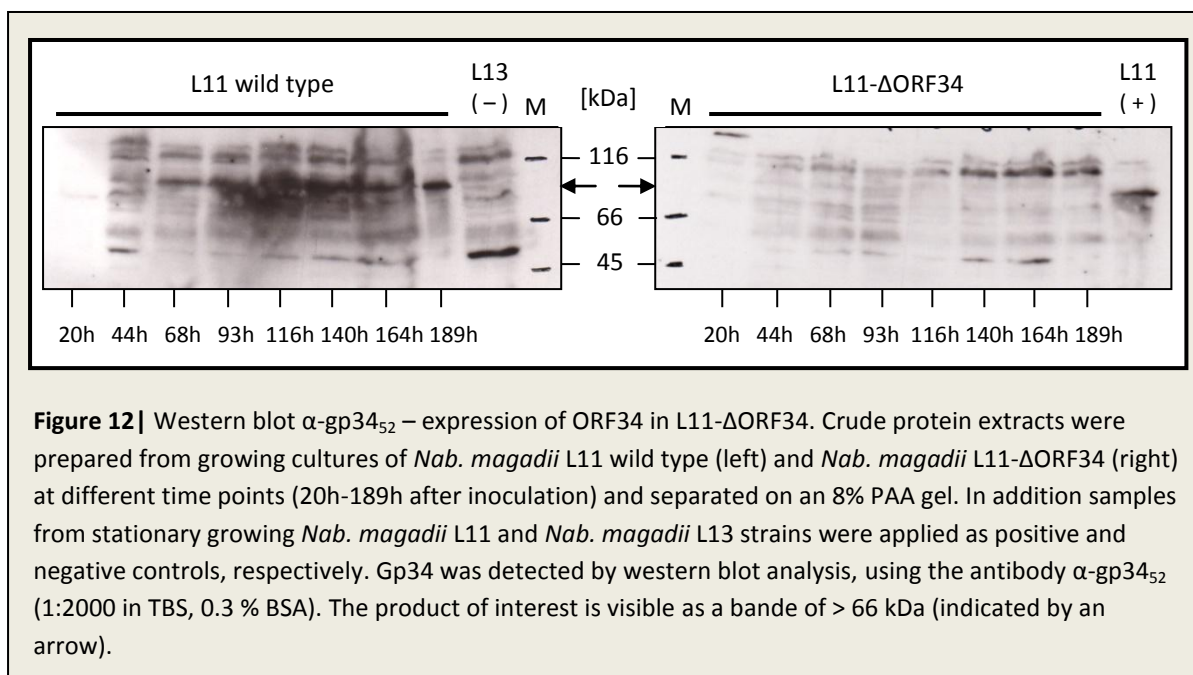


**Figure 11** | Growth and lysis curve of *Nab. magadii* L11- $\Delta$ ORF34. Comparison of the growth and lysis behaviour of the wild type *Nab. magadii* L11 (black) and the  $\Delta$ ORF34 mutant strain (white).

### 3.1.4.2. Expression of ORF34 in *Nab. magadii* L11- $\Delta$ ORF34 – Western blot analysis

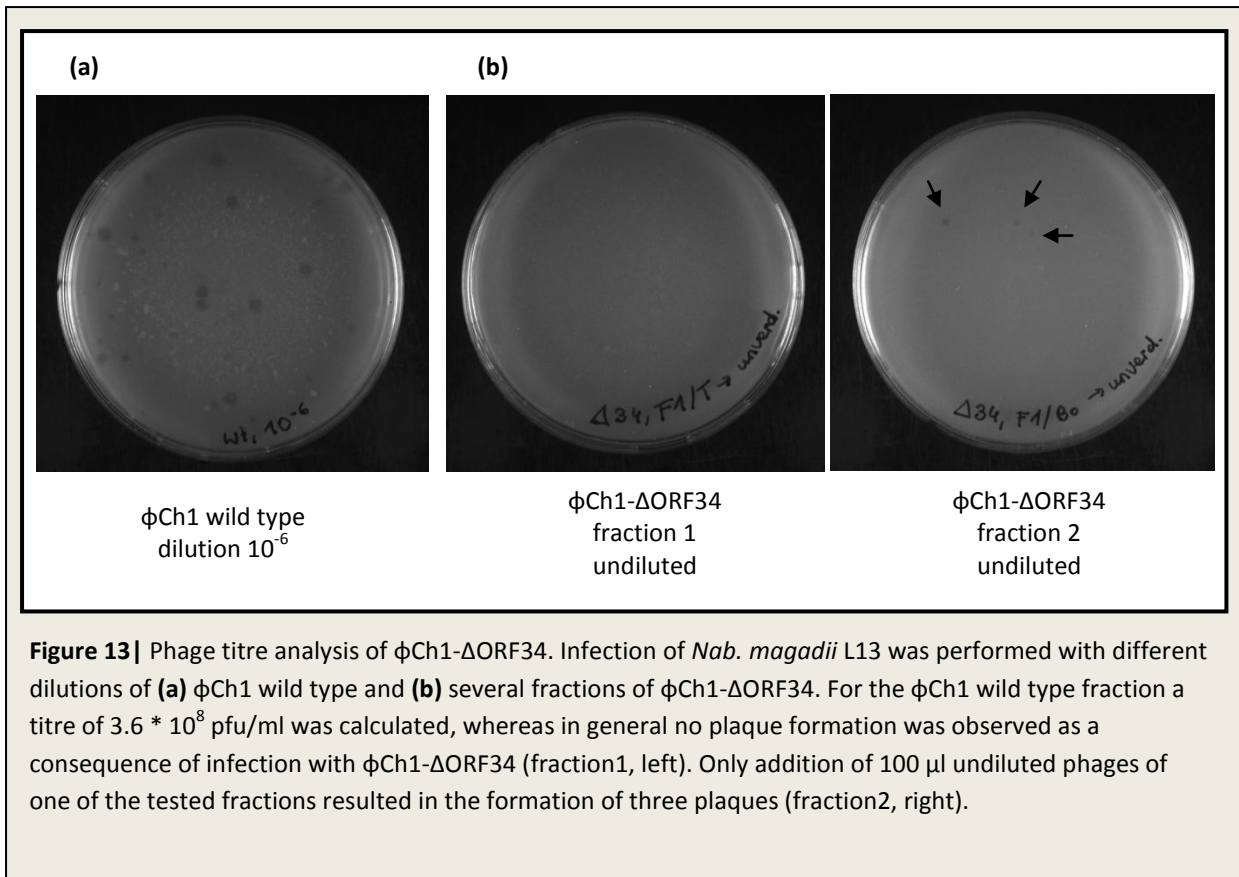
The expression of ORF34 in the *Nab. magadii* mutant strain L11- $\Delta$ ORF34 was reported by western blot analysis, using an antibody raised against gp34<sub>52</sub>. For this purpose, a culture was inoculated to an initial OD<sub>600</sub> of approx. 0.05 and incubated at 37°C for eight days (late stationary growth phase). Every day the optical density was measured and crude protein extracts were prepared as described in section 2.2.5.1. To enable comparison, the same procedure was performed with a *Nab. magadii* L11 wild type strain. All samples were loaded onto an 8% PAA gel. In addition, crude extracts from stationary growing L11 and L13 strains were applied as positive and negative controls, respectively. The proteins were separated by SDS-PAGE (see section 2.2.5.5) and analyzed by western blotting, using an antibody directed against gp34<sub>52</sub> ( $\alpha$ -gp34<sub>52</sub>) according to the instructions described in section 2.2.5.7. As illustrated in figure 12, a signal of a protein with a molecular mass of > 66 kDa is present in the positive control (L11 stationary growing), but absent in the crude extract of the cured strain *Nab. magadii* L13 (negative control). Moreover, this protein is present in the samples taken from a growing culture of *Nab. magadii* L11 (wild type strain) at different time points. Expression can first be detected 44h after inoculation (logarithmic growth phase) and strongly increases during stationary growth, persisting until completion of lysis. However, in the mutant strain *Nab. magadii* L11- $\Delta$ ORF34, a bande of the desired size is not visible at any point in the viral life cycle (see figure

12). Hence, it could be concluded, that ORF34 had successfully been deleted and that its gene product, the putative tail fibre protein, is not produced in this strain. Thus, the corresponding phage particles were supposed to lack the terminal structural elements of their contractile tails probably involved in interaction with the host cell during infection.



### 3.1.4.3. Infectivity of $\phi$ Ch1- $\Delta$ ORF34 – phage titre analysis

To present evidence for the supposed function of gp34<sub>52</sub>, the ability of the mutant phage  $\phi$ Ch1- $\Delta$ ORF34 to infect its host *Nab. magadii* was observed by phage titre analysis (see section 2.2.4.4.). Since phage isolation yielded several fractions possibly containing mature virus particles, the different fractions were tested separately. Moreover, the same procedure was carried out with the wild type  $\phi$ Ch1 as a control. The titres were analyzed after incubation at 37° C for 7 days. For the  $\phi$ Ch1 wild type fraction, a titre of  $3.6 \cdot 10^8$  pfu/ml was calculated by counting the plaques on the plates resulting from infection with 100  $\mu$ l phage fraction diluted  $10^{-6}$ . Lower dilutions and infection with the undiluted phage fraction however caused more or less complete lysis of the plated host cells. In contrast to this, as illustrated in figure 13, infection with any dilution of  $\phi$ Ch1- $\Delta$ ORF34 and even with undiluted particles did not result in formation of plaques in most cases (titre <  $10^1$  pfu/ml). Only three plaques were observed as a consequence of addition of 100  $\mu$ l undiluted phages from one of the tested fractions (fraction 2, figure 13b right). However, compared to the  $\phi$ Ch1 wild type phages yielding complete lysis in dilutions lower than  $10^{-6}$ , plaque formation of  $\phi$ Ch1- $\Delta$ ORF34 has to be considered as almost eliminated. As a result it can be concluded that the ability of  $\phi$ Ch1 to infect its host *Nab. magadii* strongly depends on the presence of the putative tail fibre protein gp34<sub>52</sub>.



#### 3.1.4.4. Visualization of $\phi$ Ch1- $\Delta$ ORF34 – electron microscopy

To observe the morphological characteristics of the mutant virus  $\phi$ Ch1- $\Delta$ ORF34, the mature particles contained in different fractions resulting from phage isolation (see section 3.1.3.) were visualized by electron microscopy. The samples were prepared and negatively stained with uranyl acetate as described in Witte *et al.*, 1990.

As illustrated in figure 14 the resulting electron micrographs clearly demonstrate that the particles of the mutant virus  $\phi$ Ch1- $\Delta$ ORF34 show significant differences compared to the  $\phi$ Ch1 wild type. As described above, the latter are composed of icosahedral heads and contractile tails (figure 14a). Phage fractions of the mutant  $\phi$ Ch1 in contrast contain a high number of probably intact heads completely lacking the contractile tails (figure 14b). However, the heads shown in figure 14 seem to be empty; yet viral DNA could successfully be isolated from the mutant phage particles in most purification fractions (data not shown). Hence it is very likely that this effect had been caused by the preparation of the samples for microscopic examination.

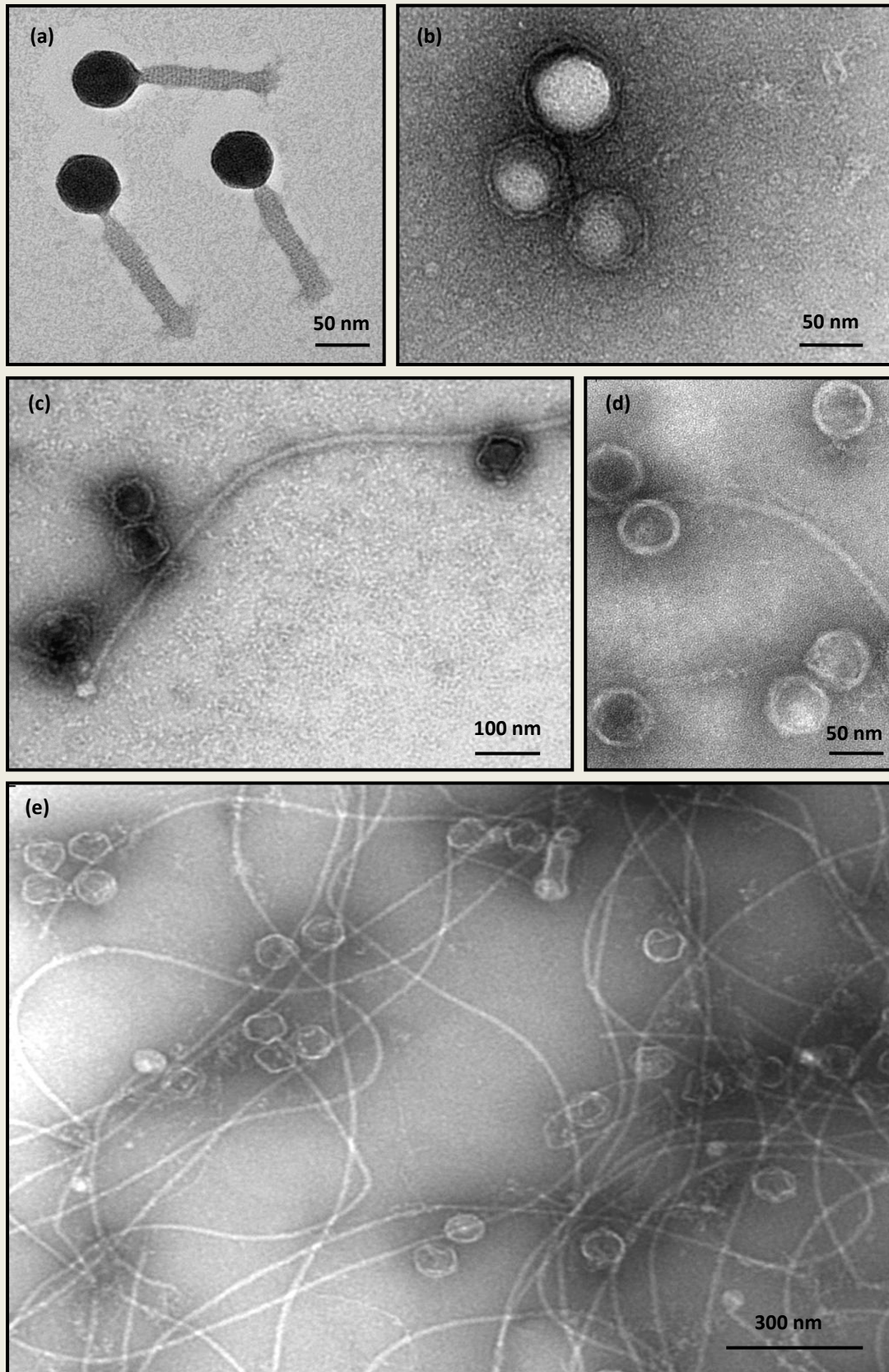
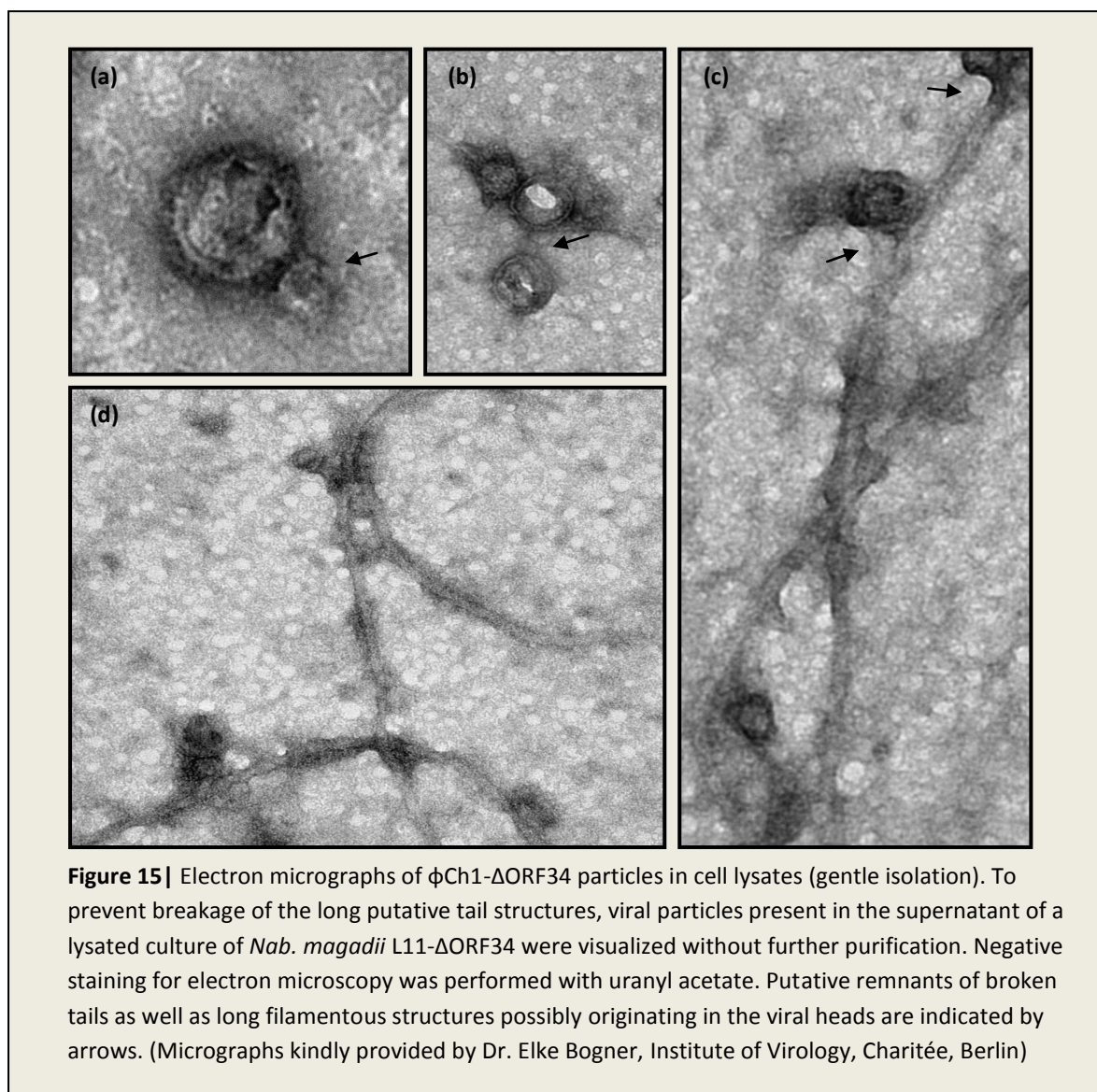


**Figure 14** | Electron micrographs of purified  $\phi$ Ch1- $\Delta$ ORF34 particles. This figure shows electron micrographs of (a)  $\phi$ Ch1 wild type and (b – e)  $\phi$ Ch1- $\Delta$ ORF34 particles resulting from isolation via a CsCl gradient, negatively stained with uranyl acetate. (Micrographs kindly provided by Dr. Elke Bogner, Institute of Virology, Charité, Berlin)



In addition to the heads, long filamentous structures extending over the whole electron micrographs are present (figure 14c – e). In most cases the start- and end points of these structures are not visible. The nature of the long structures was not clear, yet it was taken into consideration that they may be tails of the halophage  $\phi$ Ch1 which, during assemblage of the mutant phage particles, might have been extended more and more due to the lack of the protein needed for finalization. This theory would also explain the presence of heads without tails, since the lysates had been exposed to high shearing forces during purification of phage particles via ultracentrifugation. Hence, this method might have easily led to the breakage of long, instable tail structures.

For this reason, in a second approach, mutant phage particles were harvested from a lysated culture by centrifugation (6000 rpm, 15 min) and visualized without any further purification steps. Preparation of the samples and negative staining with uranyl acetate was performed as described above. The resulting micrographs are illustrated in figure 15.



Like the mutant particles isolated via CsCl gradient (ultracentrifugation), gently prepared  $\phi$ Ch1- $\Delta$ ORF34 samples comprise several virion heads without tails. As illustrated in figure 15a and b however, some short structures originating in viral heads, resembling the basis of the tails are visible (indicated by arrows). They may be remains of broken tails. Furthermore, again long structural elements are found in the lysates (see figure 15c and d). In some cases a connection to viral heads can be assumed (indicated by arrows), yet a definite statement is difficult as, due to microscopic examination of unpurified samples, qualitative resolution is reduced.

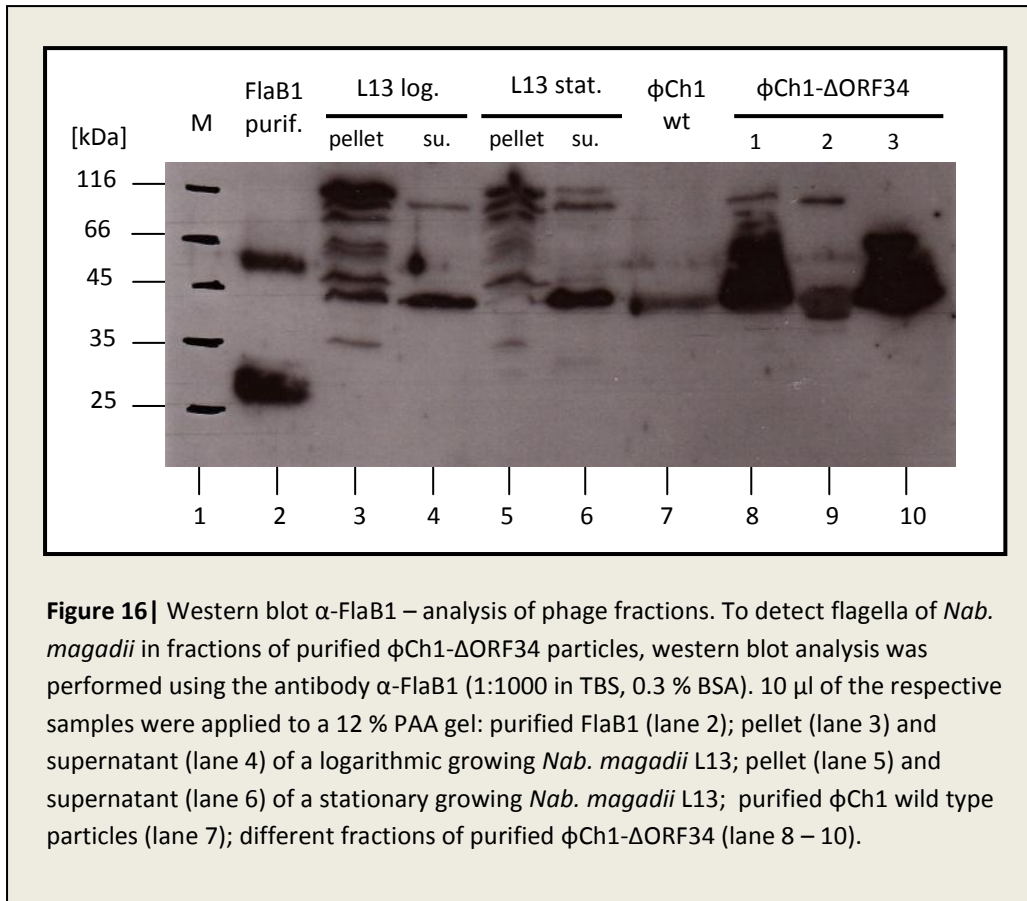
Anyway, another possible explanation for these long structures is the presence of *Nab. magadii* flagella in the observed samples. They are normally found in the supernatant of a lysated culture, but they can be separated from phage particles by application of a discontinuous CsCl gradient. Thus, usually they are not present in purified phage fractions. Yet, in this case, ultracentrifugation yielded several fractions of different densities, none of them correlating to the position of wild type  $\phi$ Ch1. Hence it can not be excluded that the fractions resulting from isolation of  $\phi$ Ch1- $\Delta$ ORF34 may also contain flagella of *Nab. magadii*. Moreover flagella and the tails of  $\phi$ Ch1 are of a quite similar width and therefore can hardly be discriminated on electron micrographs.

However, to further observe if the filamentous structures in the purified phage fractions were flagella of the archaeal cells, an antiserum detecting the *Nab. magadii* flagellar protein FlaB1 was raised in a rabbit and used for western blot analysis as described in the next section.

#### **3.1.4.5. Detection of flagella (protein FlaB1) in fractions of purified $\phi$ Ch1- $\Delta$ ORF34**

To test for the presence of flagella in fractions resulting from purification of  $\phi$ Ch1- $\Delta$ ORF34 mutant phage particles, western blot analysis was performed using an antibody raised against the *Nab. magadii* flagellar protein FlaB1 (see figure 16). Three different purification fractions of the mutant virus (lane 8 – 10) as well as  $\phi$ Ch1 wild type particles (lane 7) were analyzed. In addition several controls were applied: the purified protein FlaB1 expressed in *E. coli* (lane 2), logarithmic growing *Nab. magadii* L13 (lane 3 + 4) and *Nab. magadii* L13 in a stationary growth phase (lane 5 + 6). The samples resulting from the logarithmic and stationary growing L13 were prepared from pelleted cells as described in section 2.2.5.1. In addition, the proteins present in the supernatant (1.5 ml) were precipitated with 5 % TCA (see section 2.2.4.3.) and solved in the same volume of 5 mM sodium phosphate buffer and 2x protein sample buffer (Laemmli) just like those resulting from the pellet. 10  $\mu$ l of each sample were separated on a 12 % PAA gel and transferred to a nitrocellulose membrane (see section 2.2.5.5. and 2.2.5.7.). Development of the western blot was performed as described in section 2.2.5.7., using the antibody  $\alpha$ -FlaB1 (1:1000 in TBS, 0.3 % BSA).





As illustrated in figure 16, a bande corresponding to the approx. 30 kDa protein FlaB1 is caused by the sample resulting from expression in *E. coli* (lane 2). No signal of this size can be found in the phage fractions, yet it is also missing in archaeal protein extracts, both, the ones resulting from the pellets (lanes 3 + 5), and those from the supernatants (lanes 4 + 6). Hence, it has to be assumed that the FlaB1 expressed in *Archaea* differs in its properties and thus is changed in its mobility. As the flagella are supposed to predominate in the supernatant, rather than in the pellet after centrifugation, they are probably represented by the approx. 43 kDa bande visible in the samples from *Nab. magadii* L13 (lane 4 + 6). A product of an equal size is also found in samples resulting from purification of  $\phi$ Ch1- $\Delta$ ORF34 particles (lane 8 – 10). Yet, also separation of wild type  $\phi$ Ch1 particles yields a signal at a similar position (lane 7). As a result, based on this approach the presence of *Nab. magadii* flagella in purification fractions of  $\phi$ Ch1- $\Delta$ ORF34 particles can neither be excluded nor definitely verified. However, further studies are necessary to present evidence for the nature of the long filamentous structures visible on the electron micrographs.

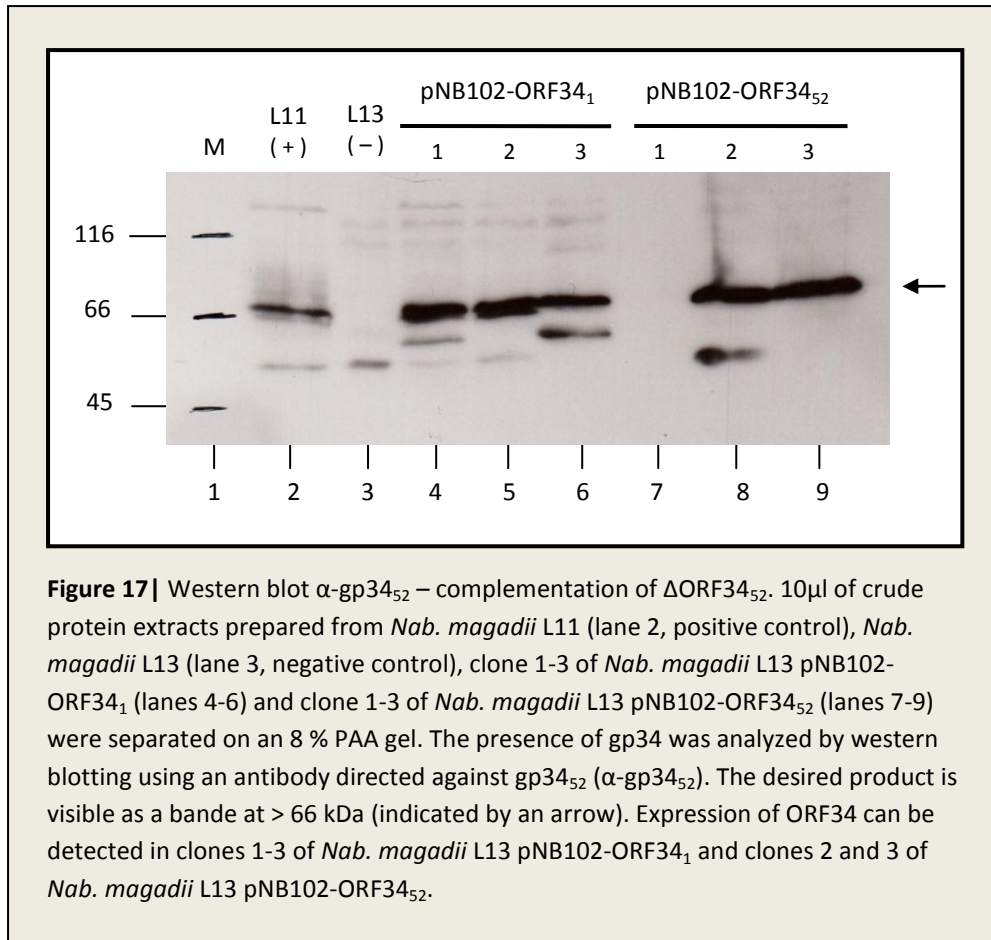
### 3.1.5. Complementation of $\phi$ Ch1- $\Delta$ ORF34

#### 3.1.5.1. Retransformation with pRR007-ORF34<sub>1/52</sub> and pNB102-ORF34<sub>1/52</sub>

In order to verify the effect caused by deletion of  $\phi$ Ch1 ORF34, the mutation was aimed to be complemented by introduction of a functional ORF34 on a plasmid. For this purpose, in a first attempt, two variants of ORF34, the non-inverted fragment ORF34<sub>1</sub> and the inversion product ORF34<sub>52</sub> were cloned on a pRR007 vector as described in section 2.2.2.2. However, transformation into *Nab. magadii* L11- $\Delta$ ORF34 did not yield positive clones. Hence both, ORF34<sub>1</sub> and ORF34<sub>52</sub> were introduced into the mutant strain using another shuttle vector system, namely pNB102 (see section 2.2.2.2.). Positive transformants carrying pNB102-ORF34<sub>1</sub> and pNB102-ORF34<sub>52</sub> could be verified by PCR and southern blot analysis, yet growing cultures of the corresponding strains tended to lose the phage-DNA integrated into the host genome before onset of lysis. As a result, phage particles complemented with gp34<sub>1</sub> and gp34<sub>52</sub> could not be isolated from these cultures. For this reason, another strategy to enable investigation of the infectivity of mutant phage particles complemented with gp34<sub>1</sub> and gp34<sub>52</sub>, respectively, was applied.

#### 3.1.5.2. Quick test – investigation of $\Delta$ ORF34<sub>52</sub> complementation

As retransformation of *Nab. magadii* L11- $\Delta$ ORF34 with pNB102-ORF34<sub>1</sub> and pNB102-ORF34<sub>52</sub> did not yield mature phage particles which could be tested for their ability to infect *Nab. magadii* cells, the same plasmids as well as the original pNB102 vector were transformed into *Nab. magadii* L13. Positive clones of the resulting cultures (L13 pNB102, L13 pNB102-ORF34<sub>1</sub> and L13 pNB102-ORF34<sub>52</sub>) were verified by PCR analysis using the primers NB-1 and NB-2. Moreover, to pre-select for clones showing well expression of the foreign genes introduced via shuttle vector, crude protein extracts were prepared from three different clones of the respective cultures (pNB102-ORF34<sub>1</sub> and L13 pNB102-ORF34<sub>52</sub>) as described in section 2.2.5.1. The samples were separated on an 8 % PAA gel (see section 2.2.5.5.) and analyzed by western blotting using the  $\alpha$ -ORF34<sub>52</sub> antibody as described in section 2.2.5.7. In addition, protein extracts of L11 and L13 were applied as positive and negative controls, respectively. The resulting blot illustrated in figure 17 clearly proves well expression of ORF34 in all three L13 pNB102-ORF34<sub>1</sub> clones, as well as clones 2 and 3 of L13 pNB102-ORF34<sub>52</sub>. The desired product is visible as a band at > 66 kDa in the positive control (L11) as well as in the respective clones, but not in the negative control (L13).



Based on the western blot analysis described above clone 1 of *Nab. magadii* L13 pNB102-ORF34<sub>1</sub> and clone 2 of L13 pNB102-ORF34<sub>52</sub>, both showing well expression of the respective genes, as well as clone 1 of *Nab. magadii* L13 pNB102 were chosen for further work. In order to test for the ability of the respective constructs to cause complementation of the deleted ORF34, DNA of  $\phi$ Ch1- $\Delta$ ORF34 was transformed into these cultures and a quick test was performed for determination of the phage titre without screening for positive clones and isolation of the complemented phage particles (see section 2.2.4.4.). For this purpose in a first step DNA was extracted from purified  $\phi$ Ch1- $\Delta$ ORF34 particles according to the long approach described in section 2.2.4.2. The result of this procedure was examined by separation of a small aliquot on a 0.8 % DNA gel (data not shown). Moreover for the transformation of this DNA, competent cells of all clones had to be prepared. Initially this was tried to be achieved by the standard procedure implying removal of the S-layer with bacitracin followed by treatment with proteinase K (see section 2.2.3.1). Yet, since growth of the cultures was quite problematical in general, especially in the presence of bacitracin, spheroblast cells were generated without treatment with bacitracin. For the final approach cultures of all clones, *Nab. magadii* L13 pNB102-ORF34<sub>1</sub>(clone 1), *Nab. magadii* L13 pNB102-ORF34<sub>52</sub> (clone 2) and *Nab. magadii* L13 pNB102 (clone 1) as well as *Nab. magadii* L13 (control) were inoculated in NVM and grown to a logarithmic phase (OD<sub>600</sub> approx. 0.5-0.6). Though *Nab. magadii* L13 and L13 pNB102 showed lower

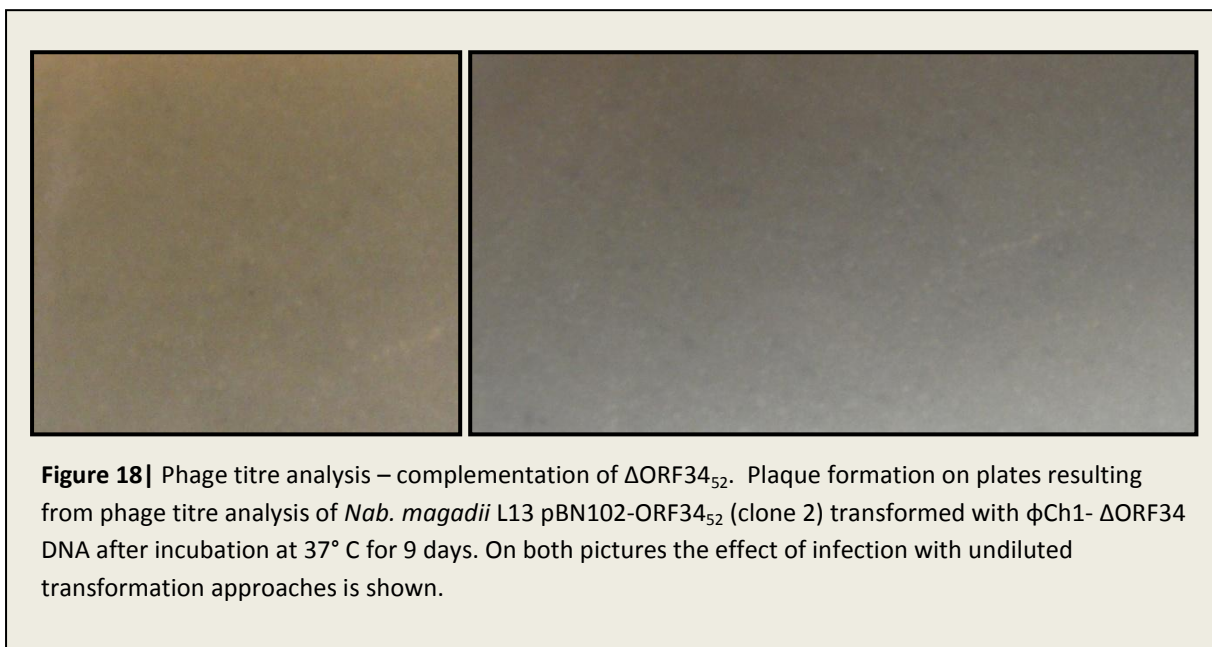
optical densities ( $OD_{600} = 0.352$  and  $0.409$ , respectively) they were definitely logarithmic growing at that time. Anyway, the cells were harvested and the further procedure was carried out as described in section 2.2.3.1. Subsequently each culture was transformed with  $10 \mu\text{l}$   $\phi\text{Ch1-}\Delta\text{ORF34}$  DNA and the cells were regenerated in rich medium at  $37^\circ\text{C}$ . Finally both, after one and after two days, phage titre analysis was performed according to the protocol in section 2.2.4.4. As described above, three different dilutions of the transformation approaches were tested: undiluted,  $10^{-2}$  and  $10^{-4}$ .

The phage titres were evaluated after incubation at  $37^\circ\text{C}$  for 7 and 8 days, respectively. By that time no plaques were visible on the plates resulting from infection of *Nab. magadii* L13. However, single plaques were present at some plates of *Nab. magadii* L13 supplemented with the respective pNB102 constructs. This effect had already been described for infection of *Nab. magadii* L13 with  $\phi\text{Ch1-}\Delta\text{ORF34}$  (see section 3.1.4.3.). Yet, since it was independent from the applied dilution it is also possible that the plaques resulted from contamination with wild type phages. Anyway, in addition to these apparent plaques, a high number of small and very weak plaques was visible on the plates achieved by complementation with gp34<sub>52</sub> (clone *Nab. magadii* L13 pNB102-ORF34<sub>52</sub>). This effect could neither be observed as a consequence of infection of *Nab. magadii* L13, nor in approaches of *Nab. magadii* L13 supplemented with pNB102 or pNB102-ORF34<sub>1</sub>. Moreover the highest number of plaques was achieved by infection with the undiluted transformation approach of *Nab. magadii* L13 pNB102-ORF34<sub>52</sub>, whereas none were visible in the case of a dilution of  $10^{-4}$ . Furthermore an increase of this effect could be observed after further incubation at  $37^\circ\text{C}$ . The numbers of plaques finally resulting from one of the two phage titre approaches as well as the calculated phage titres are listed in table 2. Since the other approach yielded similar results, they are not shown.

		Clone			
		L13	L13 pNB102	L13 pNB102-ORF34 <sub>1</sub>	L13 pNB102-ORF34 <sub>52</sub>
Plaques	undiluted	0	0	0	> 100
	$10^{-2}$	0	0 / 2	0	> 10
	$10^{-4}$	0	0	0	0
Phage titre [pfu/ml]		< $10^1$	< $10^1$	< $10^1$	$10^3 - 10^5$

**Table 2** | Phage titres of  $\phi\text{Ch1-}\Delta\text{ORF34}$  in complemented and control cultures. This table shows the number of plaques resulting from infection of *Nab. magadii* L13, L13 pNB102, L13 pNB102-ORF34<sub>1</sub> and L13 pNB102-ORF34<sub>52</sub> with  $100 \mu\text{l}$   $\phi\text{Ch1-}\Delta\text{ORF34}$  transformation approach (undiluted,  $10^{-2}$  and  $10^{-4}$  diluted) as well as the calculated phage titres. Since the plaques on plates supplemented with gp34<sup>52</sup> (clone L13 pNB102-ORF34<sub>52</sub>) were quite weak and small, clear quantification was not possible. Nevertheless, to figure out differences to the controls, the minimal plaque numbers are stated. Though 2 plaques were visible on one plate resulting from infection with phage particles from a  $10^{-2}$  diluted transformation approach, this result was not taken into consideration for calculation of the phage titre as no plaques were found on the other plates, especially those supplemented with the undiluted approaches.

Plaque formation resulting from incubation for 9 days is illustrated in figure 18. Though the plaques are smaller and weaker than those usually yielded by phage titre analysis, they are clearly visible. Since they are present in a high number (titre:  $10^3 - 10^5$ ), successful retrieval of the infectivity of  $\phi\text{Ch1-}\Delta\text{ORF34}$  by complementation with  $\text{gp34}_{52}$  can be concluded based on these results.



### 3.1.6. Discussion

In the course of this diploma work, a homozygous ORF34 deletion mutant of the halophage  $\phi\text{Ch1}$  was constructed and verified both, by PCR and southern blot analysis. Moreover, the fail in expression of the desired gene, was definitely confirmed by western blot analysis using an antibody directed against  $\text{gp34}_{52}$  (see figure 12). However, as  $\text{gp34}_{52}$  was supposed to represent the tail fibre protein of  $\phi\text{Ch1}$ , morphological differences of the mutant particles compared to the wild type were expected. Indeed, the absence of tail fibre proteins could be demonstrated by electron microscopic analysis of purified phage fractions. Yet, the mutant particles visible on the micrographs were completely lacking the entire tails, consisting of the viral heads exclusively (see figure 14). This fact also explains changes in the density of the mutant phage particles and hence a different position of the purified phages resulting from application of a discontinuous CsCl gradient. However, the presence of long filamentous structural elements in the purification fractions (see figure 14) supported the idea, that in the absence of the final tail element in this mutant virus, the tails may get extended more and more during assemblage of the phage particles. The resulting tail structures can be supposed to be very instable and hence susceptible to break when they are exposed to high shearing forces during purification of phage particles. Finally breakage of the tails may leave intact

viral heads as well as long filamentous structures, yielding a situation similar to that observed by electron microscopic analysis. This theory was also supported by visualization of phage particles resulting from the supernatant of a lysated culture (see figure 15). In this case some of the long, filamentous structures actually seem to originate in the viral heads. Nevertheless a high number of viral heads definitely lacking tails as well as heads with short structures resembling remains of broken tails are visible on the micrographs. Hence it has to be concluded that, though gentle isolation of viral particles without further purification, most tails are not associated to the heads of the mutant virions. Breakage of the tails may have happen immediately after release from the corresponding *Nab. magadii* culture while shaking in a baffled flask or during harvesting by centrifugation. Anyway, based on these results it is very likely that the long structures visible on electron micrographs indeed represent broken tails of the mutant phage particles.

However, other explanations for the presence of structures like those found in the samples examined in the electron microscope are possible. Flagella of the archaeal host *Nab. magadii* are of an equal size and look very similar, hence they could hardly be distinguished from elongated tails. Moreover, they are very likely to occur in both, the supernatant of a lysated culture as well as the fractions resulting from isolation of the mutant phage particles. Furthermore, due to a western blot detecting the flagellar protein FlaB1 (figure 17), the presence of flagella in the observed samples is quite possible. Yet, even if the fractions analyzed by electron microscopy actually contained *Nab. magadii* flagella, the presence of broken viral tails cannot be excluded. It has to be kept in mind, that, in fact, some of the viral heads are associated with putative remnants of broken tails. So finally it can be concluded that, anyway, the lack of viral tails can be explained by the deletion of the putative tail fibre protein gp34<sub>52</sub>. Hence, the observed results clearly indicate that ORF34 encodes for the tail fibre protein of  $\phi$ Ch1.

In addition, the supposed function of the putative tail fibre protein gp34<sub>52</sub> was investigated by phage titre analysis. As described in section 3.1.4.3., in contrast to the  $\phi$ Ch1 wild type, the mutant virus lacking gp34<sub>52</sub> was shown to be at least strongly reduced in its ability to infect cells of the cured strain *Nab. magadii* L13. The addition of 100  $\mu$ l of only one of the phage fractions resulted in the formation of three plaques. However, contamination with the wild type virus which was used as a control at the same time can not be excluded. Anyway, most of the observed phage fractions did not cause plaque formation at all. Thus, the titre of the mutant virus determined from the results of phage infection is  $< 10^1$  pfu/ml, although, based on analysis of precipitated structural phage proteins, the respective phage fractions did not contain less particles than the  $\phi$ Ch1 wild type (titre  $3.6 * 10^8$  pfu/ml). Hence, the ability of the isolated  $\phi$ Ch1- $\Delta$ ORF34 particles to infect *Nab. magadii* has to be considered as almost eliminated. Yet, it has to be noted that the particles resulting from isolation of

the mutant virus were not lacking the tail fibres exclusively, but the entire tail structures (see figure 14). Thus, the loss of infectivity of these particles does not necessarily have to be traced back to the absence of the tail fibre proteins, albeit this effect is not observed with particles of the  $\phi$ Ch1 wild type. Anyway, based on the present results, a key role of the gene product of ORF34 in the initiation of infection can be supposed. This assumption could also be supported since complementation with the gene region encoding for gp34<sub>52</sub> resulted in the retrieval of the infectivity of the mutant virus. Yet, supplementation with gp34<sub>1</sub> did not yield any effect on plaque formation. This finding also correlates to the fact that gp34<sub>52</sub>, but not gp34<sub>1</sub> or any variants of gp36 binds to the surface of  $\phi$ Ch1 host *Nab. magadii* (Rössler *et al.*, in prep). However, further experiments may be performed to definitely confirm the function of the putative tail fibre protein gp34<sub>52</sub>.

## 3.2. Int1-mediated Inversion of $\phi$ Ch1 ORF34 and ORF36

As described in detail in section 1.2.3.5., the region on the  $\phi$ Ch1 genome comprising ORF34 to ORF36 gets inverted by the viral encoded site-specific recombinase Int1. This event leads to an exchange of the 3' ends of ORF34 and ORF36 and hence gives rise to different gene products of ORF34: the original protein gp34<sub>1</sub> and the inversion product carrying the C-terminus of gp36, gp34<sub>52</sub> (Rössler *et al.*, 2004). In the last chapter the function of the putative tail fibre protein gp34<sub>52</sub> and its importance for infectivity of  $\phi$ Ch1 were discussed. This chapter however is focused on the mechanism of inversion within its gene locus as well as the enzyme performing this reaction, the site-specific recombinase Int1.

### 3.2.1. Analysis of eight *int1* clones comprising variations in single repeats

#### 3.2.1.1. Aim of the study and prognosis

The importance and sufficiency of Int1 to perform inversion of ORF34 and ORF36 had already been confirmed in course of previous projects. In 2008 two different cultures of *Nab. magadii* L13 were analyzed: *Nab. magadii* L13 (pRo-5 52-2) supplemented with the whole invertible region and *Nab. magadii* L13 (pRo-5 52-3), carrying a plasmid comprising ORF34 and ORF36 but lacking ORF35 (*int1*). However, inversion products could only be detected in *Nab. magadii* L13 (pRo-5 52-2), but not in the clone lacking the gene region encoding for Int1. Hence it could be concluded that the ability to

perform inversion reactions within ORF34 and ORF36 totally depends on the presence of this enzyme (Ladurner, 2008).

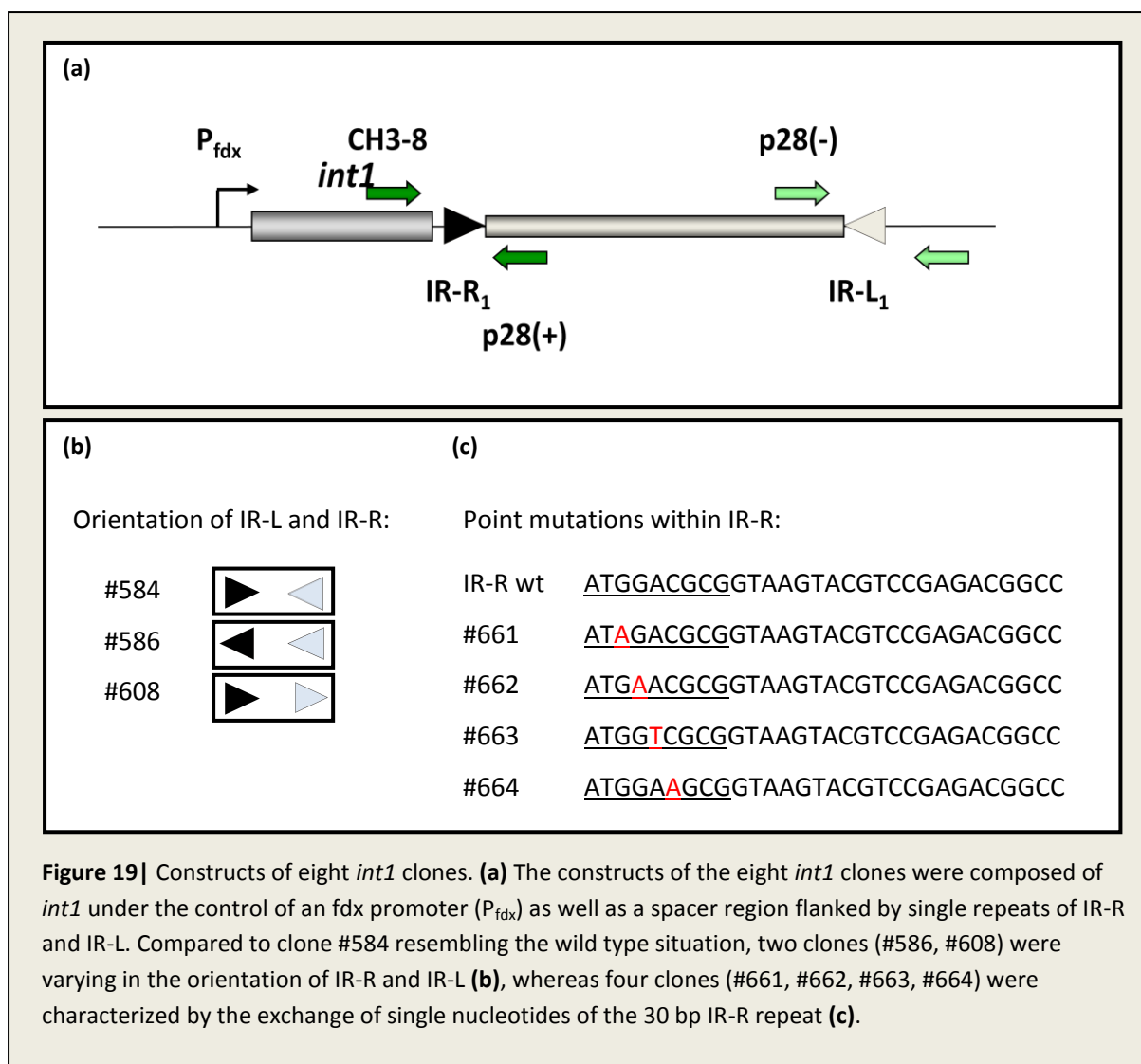
Yet, since the activity of Int1 on the entire invertible region was observed, this experiment did not yield informations about the crucial characteristics of the genetic target sites of Int1. In its natural situation site-specific recombination occurs at two clusters of 30 bp direct repeats located to ORF34 and ORF36, respectively. These clusters, designated as IR-L and IR-R, are arranged in an inverted orientation with respect to each other. This orientation is supposed to be crucial in order to enable inversion of the region flanked by IR-L and IR-R (Rössler et al., 2004).

However, in the project described above, just like in the natural situation on the  $\phi$ Ch1 genome, the whole IR-R and IR-L clusters and hence a high number of repeats were present on the invertible region. Yet, to work out certain characteristics of the repeats crucial for the ability to perform inversion, different constructs comprising *int1* under the control of an *fdx* promoter as well as a spacer region flanked by single repeats of IR-L and IR-R were cloned on the shuttle vector pRo-5 and analyzed in *Nab. magadii* L13. Three of these constructs were varying in the orientation of the repeats, whereas four clones were characterized by the exchange of single nucleotides of the 30 bp repeat sequence. So on one hand it was aimed to confirm the importance of an inverted arrangement of the repeat clusters with respect to each other. However, no inversion products were expected in the case of direct repeats flanking the spacer region. On the other hand it was intended to figure out which of the conserved nucleic acid residues are totally required to enable recognition by Int1. Anyway, as previously only the entire invertible region had been tested, it was not clear if one set of single repeats was actually sufficient to cause inversion of the flanked region.

### **3.2.1.2. Construction of the eight *int1* clones**

As a first step the ferredoxin (*fdx*) promoter derived from *H. salinarum* was cloned onto the vector pUC19, yielding pUC19-*fdx*. Based on this plasmid, eight different *int1* constructs were prepared as described in section 2.2.2.3. Each construct was composed of the gene encoding for  $\phi$ Ch1 integrase 1 (*int1*) under control of the *fdx* promoter as well as a spacer region flanked by single repeats of IR-L and IR-R, respectively. The arrangement is illustrated in figure 19a.





As described above, the constructs of the eight *int1* clones were varied in certain characteristics of the single repeats. In contrast to #584 resembling the wild type situation, the repeats of #586 and #608 were arranged in a direct orientation with respect to each other (see figure 20b). Like #584 the constructs of the clones #661, #662, #663 and #664 comprised inverted repeats, yet they were characterized by exchanges of certain nucleotides of the most conserved region of the IR-R repeat sequence (see figure 20c). In addition to these seven variants, clone #615 lacking *int1* was prepared as a negative control.

Transferred to the shuttle vector pRo-5, these eight *int1* constructs were transformed into *Nab. magadii* L13 and positive clones were verified by PCR analysis using the primers D54-2 and p28-, yielding an 1856 bp product. Furthermore the presence of the *fdx* promoter was confirmed by amplification of corresponding fragment using the primers *fdx*-1 and p28+ (product: 1058 bp) and contamination with  $\phi$ Ch1 was excluded by application of 34-XbaI-a and 36-3 (product: 1600 bp).

### 3.2.1.3. Inversion – time course experiment

In order to observe if inversion was possible under the respective conditions, a time course experiment was performed as described in section 2.2.3.4. For this purpose verified clones of each strain (*Nab. magadii* L13 #584, #586, #608, #615, #661, #662, #663 and 664)\* were grown to a late stationary phase. Every day the optical density was measured and DNA samples were prepared according to the instructions in section 2.2.3.5. To estimate the concentration of the DNA, 10 µl of the respective samples were applied to a 0.8 % agarose gel (data not shown). Based on this information, appropriate dilutions were prepared (1:5 or 1:10) and used as templates for PCR analysis. To get a first insight, only two samples taken at a stationary growth phase (6 and 7 days after inoculation) were investigated. In addition, approaches with the respective plasmid preparations from *E. coli* (1:30) as well as a crude DNA extract of *Nab. magadii* L13 were analyzed as positive and negative controls, respectively. The presence of products resulting from inversion of the spacer region was detected using the primers CH3-8 and p28-. As a positive control CH3-8 and p28+ were applied in order to amplify the 420 bp non-inverted fragments. For observation of the clone lacking *int1* (#615) in contrast, the primers fdx1/p28- and fdx1/p28+ would have been used\*. 10 µl of each sample were applied to a 6 % PAA gel and separated as described in section 2.2.1.1.

The results of PCR analysis of the samples from the clones #584 and #664 are illustrated in figure 21. However, the gels resulting from examination of the clones #608, #661, #662 and #663 look very similar; hence they are not shown. In all these cases a strong signal is visible at 420 bp as a consequence of amplification of the non-inverted fragment (PCR positive). Thus it can be concluded that the concentration of plasmid DNA in the two observed samples of each clone (day 6 and 7 after inoculation) was sufficient to enable PCR analysis in general. In contrast to this, due to poor growth of the corresponding culture resulting in low amounts of DNA in the prepared samples, no non-inverted fragments could be detected in the samples of clone #586. Hence it is not surprising that, in this case, the analysis of possible inversion products did not yield any signals either. Anyway, in PCR approaches for detection of possible inversion products (PCR inversion) of the other clones, 420 bp fragments are completely lacking as well. Yet, in the samples taken from stationary growing *Nab. magadii* cultures of the respective clones, several more or less weak bands are visible at other positions (samples 6 and 7). Some of them correlate to the unspecific fragments detected in the control batches (amplification of *Nab. magadii* L13 DNA and plasmid preparations from *E. coli*), whereas others may have resulted from inversion. Since the mechanism of inversion is not completely known, possible products of other sizes resulting from e.g. deletion or duplication of the inverted region can not be excluded. However, all signals resulting from amplification of inversion products are quite similar in clone #584 resembling the natural situation and the modified clones

(#608, #661, #662, #663 and #664). Hence it is quite unlikely that these bands represent products of inversion of the spacer region.

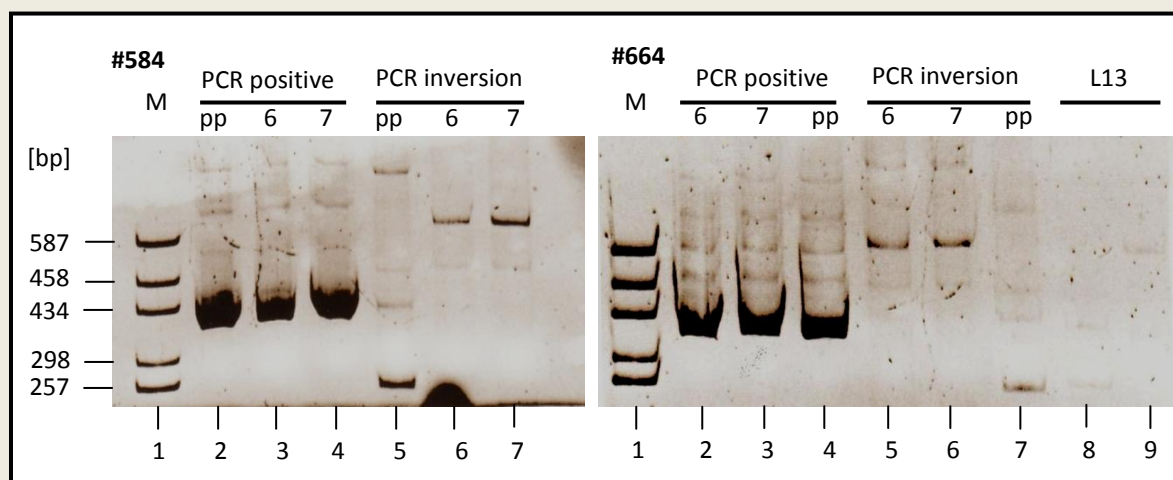
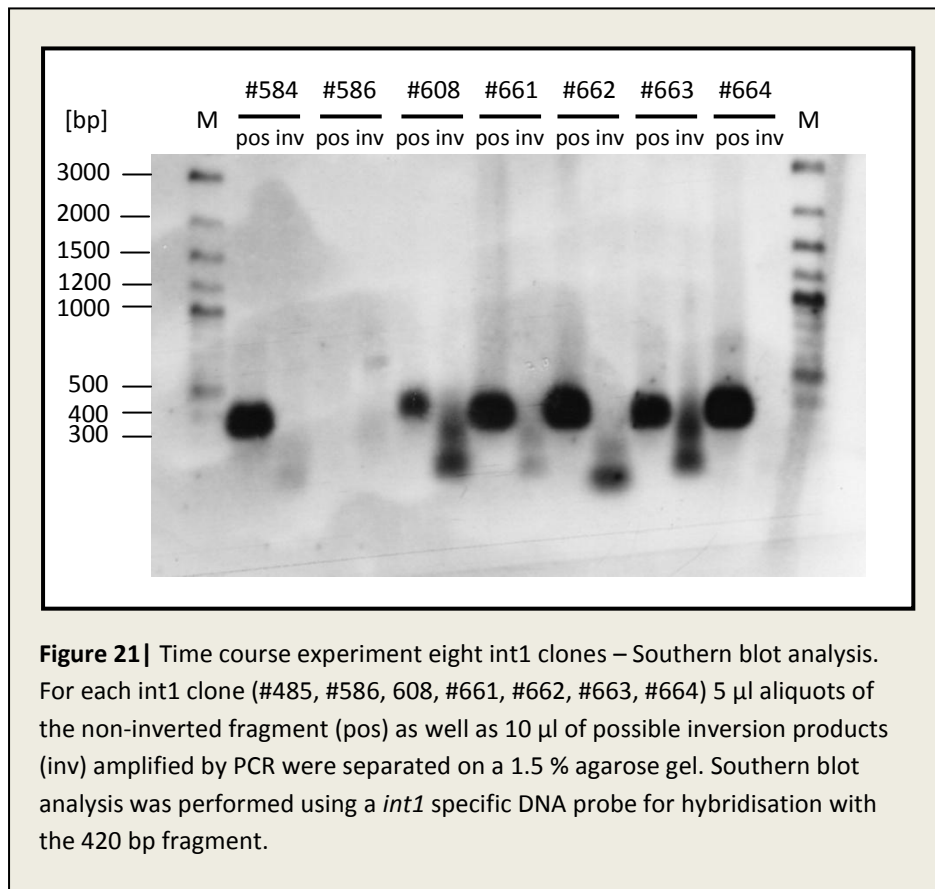


**Figure 20** | Time course experiment eight *int1* clones – PCR analysis. For analysis of the DNA samples taken from growing cultures of the different *int1* clones (*Nab. magadii* L13 #584, #586, #608, #661, #662, #663, #664), the 420 bp non-inverted fragment (PCR positive) as well as inversion products (PCR inversion) were amplified using the primers CH3-8/p28+ and CH3-8/p28-, respectively. Samples from stationary cultures (6 and 7 days after inoculation) as well as plasmid preparations from *E. coli* (pp) of the respective clones were investigated. Moreover, as a control, both PCRs (PCR positive: lane 8, PCR inversion: lane 9) were performed using crude DNA extracts of *Nab. magadii* L13 as a template. This figure shows the results of the PCR of clones #584 (left) and #664 (right) separated on 6 % PAA gels.

\* Since positive transformants of clone #615 were verified much later than those of other clones, the time course experiment was carried out with #584, #586, #608, #661, #662, #663 and #664 first. However, as PCR and southern blot analysis of these clones did not yield any useful results, the samples taken from growing cultures of the clone #615 were not further examined.

Anyway, to further investigate if inversion products of different sizes were present in the respective samples, southern blot analysis was performed (see section 2.2.6.). For this purpose two samples of each clone were applied to a 1.5 % agarose gel: 5  $\mu$ l of the amplified non-inverted fragment (PCR positive) and 10  $\mu$ l of one batch for detection of inversion products (PCR inversion), both of them resulting from sample 7 (template: sample taken seven days after inoculation). All samples as well as an aliquot of the biotinylated 2-Log DNA ladder were separated and transferred to a nylon membrane as described in section 2.2.6.2. For detection of the 420 bp non-inverted fragment as well as possible inversion products, a DNA probe complementary to a part of *int1* was prepared by PCR using the primers Jas Int5 and Int13-Xba and  $\phi$ Ch1 DNA as a template. The 693 bp fragment was purified by elution from a 6 % PAA gel and labeled as described in section 2.2.6.1. After hybridisation, the blot was developed according to the instructions in section 2.2.6.4.



As illustrated in figure 21, the resulting blot is quite similar to the 6 % PAA gels shown in figure 20. Again the 420 bp non-inverted fragments (pos) of the clones #584, #608, #661, #662, #663 and #664 are visible, whereas concrete bands of this size are lacking in the samples resulting from amplification of possible inversion products (inv). Instead of this, in clones #584, #608, #661, #662 and #663 more or less strong signals are present at a lower position on the gel, extending towards approx. 420 bp. Yet, it is very surprising that this effect is found in all clones except for one, namely #664. (Like before, the sample isolated from clone #586 did not yield any bands in general.) Moreover, it has to be noted that these signals are of the lowest intensity in #584, the clone resembling the wild type situation of the invertible region. Hence, as it is quite unlikely that the exchange of certain nucleotides within the repeat sequence has an enhancing effect on the inversion events, these signals are more probably the result of unspecific binding of the DNA probe, rather than amplified inversion products.

### 3.2.1.4. Discussion

The results presented above raise the question if the amplified fragments differing in their size compared to the 420 bp non-inverted version indeed were caused by inversion of the spacer region in the respective clones. However, as mentioned above this is very unlikely, since it would imply that inversion was possible or even enhanced by the changes in the orientation (#608) or sequence (#661, #662 and #663) of the single repeats compared to natural situation resembled by clone #584. Yet, it has to be noted that this effect was not observed in clone #664, comprising an exchange of cytosine<sub>6</sub> to an adenine. Hence if the observed fragments in fact were inversion products it would lead to the conclusion that only the nucleotide at position six, but not those at the positions three, four and five is crucial to enable targeting by Int1.

Anyway, probably the observed signals were not the result of inversion performed by Int1, but the consequence of unspecific binding of the primers CH3-8 and p28- as well as the DNA probe used for southern blot analysis. In this case the failure of clone #584 to perform inversion of the spacer region flanked by single repeats may be explained by the necessity of a high number of repeats. Previously, inversion had only been investigated at the natural invertible region comprising large clusters of the repeats within ORF34 and ORF36 (IR-R and IR-L), respectively. Hence, it can not be excluded that this arrangement is crucial for the ability of Int1 to perform inversion and that, as a result, targeting of the construct illustrated in figure 19 is not possible.

Another possible explanation for a general absence of inversion events is the failure of *int1* expression due to the used promoter. However, though  $P_{fdx}$  represents a strong promoter for ferredoxin in *H. salinarum* and is also expected to cause well expression of foreign genes introduced into *Nab. magadii*, its function in the latter archaeon has not been confirmed so far. Hence to further observe this possibility, this experiment may be repeated using another control element for the expression of *int1*. Also the application of an inducible promoter constructed in course of recent work (Alte, 2011) may open up new possibilities to shed light on this topic.

## 3.2.2. Investigation of a possible activator of *int1* expression

### 3.2.2.1. Aim of the study and prognosis

As described in section 1.2.3.4. previous studies indicate that inversion happens in the late stationary growth phase (78 h after inoculation) of a *Nab. magadii* L13 culture supplemented with the  $\phi$ Ch1 invertible region (Ladurner, 2008). Yet, in the wild type strain L11, expression of *int1* was

shown to occur in an early logarithmic growth phase (Rössler *et al.*, in prep). This effect may be explained by the activity of an activator of *int1* expression, a protein encoded by  $\phi$ Ch1 and hence only present in the lysogenic strain L11, but not in the cured strain supplemented with the  $\phi$ Ch1 invertible region.

In course of this diploma work the effect of one possible activator encoded by the  $\phi$ Ch1 region comprising ORF43 and ORF44 was investigated. Both sequences were known to be highly identical (90 % and 94 %, respectively) to regulatory elements of the plasmid p $\phi$ HL providing immunity of *H. salinarum* towards infection with halophage  $\phi$ H. In addition, detailed studies had clearly confirmed a role of gp43 and/or gp44 as a transcriptional activator, since an enhancing effect on the expression of *bgaH* in the presence of ORF48 (*rep*), a gene encoding for a putative repressor, could be observed in *Hfx. volcanii* (Iro *et al.*, 2007). Hence, an influence on *int1* resulting in an earlier production of the corresponding protein was conceivable. To investigate this possibility, a *Nab. magadii* culture supplemented with both, the whole invertible region of  $\phi$ Ch1 (implying *int1*) and ORF43/44 was observed. However, if one of the concerned gene products indeed was acting on the gene locus of *Int1*, inversion events were supposed to be detectable at earlier time points compared to a strain lacking ORF43/44.

### 3.2.2.2. Cloning of the putative activator (ORF43/44)

For preparation of clones supplemented with the putative activator gp43/gp44, a pNB102 shuttle vector containing the corresponding gene region was constructed as described in section 2.2.2.4 and transformed in two different strains of *Nab. magadii* L13. Both of them were carrying the invertible region on a pRo-5 shuttle vector, yet one construct was comprising the whole - orientated fragment (pRo-5-52-2) while the other one was lacking *int1* (pRo-5-52-3). Positive clones carrying pNB102/43-44 were verified by PCR analysis using the primers applied for cloning of the concerned gene region: 44-3 and 43-Kpn-5. In addition the presence of pRo-5-52-2 and pRo-5-52-3 was confirmed by amplification of a 916 bp pRo-5 specific fragment using TR-2 and Nov-6 as primers.

### 3.2.2.3. Inversion – time course experiment

In order to observe inversion of ORF34 and ORF36 in the two cultures carrying the possible activator of *int1* expression, *Nab. magadii* L13 (pRo-5-52-2) and *Nab. magadii* L13 (pRo-5-52-3), a time course experiment was carried out as described in section 2.2.3.4. However, samples for crude extraction of plasmid DNA were not taken every day, but at certain time points depending on the growth phase of the cultures (at least lag-, early logarithmic-, late logarithmic- and stationary phase).

In order to confirm successful extraction of plasmid DNA, the respective samples were separated on a 0.8 % agarose gel (data not shown). Finally appropriate dilutions of all samples were analyzed by PCR using the primers 34-5 and 36-3 for the detection of the 1369 bp non-inverted fragment ORF34<sub>52</sub> (orientation corresponding to the - oriented fragment in pRo-5-52-2/3). On the other hand possible inversion products were amplified by application of the primers 34-5 and 34-3. In addition to the samples taken from the growing cultures at different time points, PCR batches containing either crude DNA extracts of *Nab. magadii* L11 or the plasmids pRo-5-52-2 and pRo-5-52-3 prepared from *E. coli* were examined as controls. The result of this PCR was analyzed on a 0.8 agarose gel.

Both, the growth curves of *Nab. magadii* L13 (pRo-5-52-3) and *Nab. magadii* L13 (pRo-5-52-2) #1 and #2, all supplemented with pNB102/43-44, as well as PCR analysis of the respective samples are illustrated in figure 22. In general amplified ORF34<sub>52</sub> (non-inverted) fragments are visible as concrete bands at 1369 bp in batches containing the plasmids prepared from *E. coli* (pp *E. coli*, figure 22 b) as well as most of the samples taken from growing *Nab. magadii* cultures (figure 22 b + c, left). In approaches for the detection of inversion products in contrast, the present signals are weaker and blurred due to variation of the lengths of the fragments resulting from inversion (figure 22 b + c, right). In this case, no inversion products can be detected by amplification of pRo-5-52-2 isolated from *E. coli*, but, surprisingly, in the sample containing pRo-5-52-3. Furthermore, for unknown reasons neither ORF34<sub>1</sub>, nor ORF34<sub>52</sub> can be amplified from the crude extract of *Nab. magadii* L11. However, in samples taken from one clone carrying the whole invertible region as well as the putative activator (*Nab. magadii* L13 (pRo-5-52-2 pNB102/43-44 #1)), PCR products of the non-inverted fragment ORF34<sub>52</sub> (resembling the orientation of pRo-5-52-2) are present in samples prepared 50, 147 and 197 hours after inoculation, but not in those taken from early lag- (6h, 32h) or stationary phase (266h). Inversion products are found in the samples taken during logarithmic (147h, 197h) and stationary growth (266h), but they can not be amplified from the sample prepared 50h after inoculation, albeit this sample yields a signal for detection of ORF34<sub>52</sub>. Hence, it may be concluded that at this time point the non-inverted fragment is present exclusively, whereas inversion occurs afterwards and thus can be detected at an early logarithmic growth phase for the first time. In this respect, an effect of gp43/gp44 on *int1* expression could be supposed.

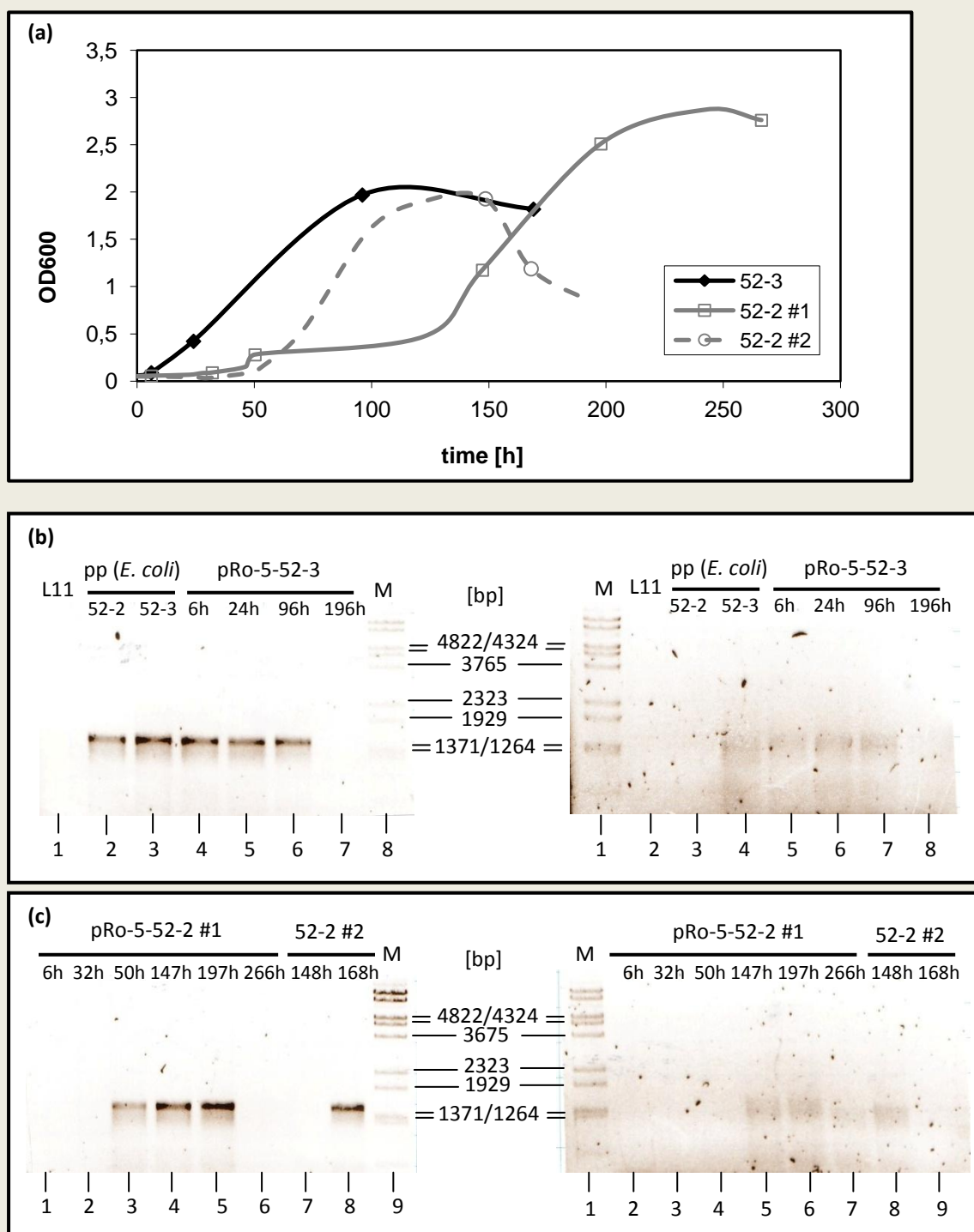


**Figure 22** | Time course experiment activator – PCR analysis. **(a)** Growth curves of cultures *Nab. magadii* L13 (pRo-5-52-2) and *Nab. magadii* L13 (pRo-5-52-3), both supplemented with pNB102/43-44 (possible activator of *int1*). OD<sub>600</sub> was determined every day and samples were taken at certain time points (indicated by squares and circles). **(b)** PCR analysis of controls (crude extract of L11 DNA; plasmids prepared from *E. coli*) and samples taken from a growing culture of *Nab. magadii* L13 (pRo-5-52-3 pNB102/43-44). Amplification of the 1369 bp non-inverted fragment was performed using the primers 34-5/36-3 (left); inversion products were detected by application of 34-5/34-3 (right). **(c)** PCR analysis of the samples taken from clone #1 and #2 of *Nab. magadii* L13 (pRo-5-52-3 pNB102/43-44). Amplification of the 1369 bp non-inverted fragment was performed using the primers 34-5/36-3 (left); inversion products were detected by application of 34-5/34-3 (right).



However, it has to be noted that the clone lacking *int1* (*Nab. magadii* L13 (pRo-5-52-3/pNB102/43-44)) also yields signals correlating to inversion products (figure 22b, right). Like the non-inverted fragments (figure 22b, left), they can be detected in samples taken at a lag- (6h), early logarithmic (24h) and late logarithmic growth phase (96h), while both fragments are lacking in the last sample (169h), probably due to low DNA concentrations of in the analyzed sample. Yet, since PCR analysis of the original plasmid prepared from *E. coli* causes the amplification of inversion products as well, this effect does not present evidence for inversion events occurring independently of the presence of *Int1* in *Nab. magadii*.

Anyway, in general the occurrence of PCR products resulting from amplification with the primers 34-5/36-3 and 34-5/34-3 seems to be quite random. In several samples amplification of the non-inverted fragment could not be observed, even though the applied templates definitely contained sufficient amounts of DNA and, in some cases, even inversion products could be detected. Moreover, the results of control batches (L11 and plasmids prepared from *E. coli*) were not clear. Even further PCR analysis using the same or alternative primers (34-inv1/36-inv1 and 34-inv1/34-inv2, respectively) did not enable to shed light on this project (data not shown).

#### 3.2.2.4. Discussion

Based on the results described above, a definite conclusion about a regulatory effect of gp43/gp44 on the expression of *int1* is not possible. Though analysis of the samples prepared from *Nab. magadii* L13 (pRo-5-52-2 pNB102/43-44) #1 may indicate that inversion occurs at the early logarithmic grow phase in the presence of gp43/gp44, amplification of both, ORF34<sub>1</sub> and ORF34<sub>52</sub>, seems to be quite random. However, the lack of a signal in approaches quantifying possible inversion products does not necessarily mean that in fact no corresponding fragments were present. On the contrary, detection of inversion products could be observed independently from the presence of *Int1* in clone *Nab. magadii* L13 (pRo-5-52-3 pNB102/43-44). This finding does not correlate to previous studies, definitely confirming the necessity of this enzyme to perform inversion of the concerned gene region (Ladurner, 2008). Furthermore, inversion products also resulted from addition of the original plasmid pRo-5-52-3. This fact implies that either the construct itself does not contain the - oriented version of the invertible region lacking *int1* exclusively, or that PCR analysis using the primers 34-5/36-3 may yield a signal of an appropriate size anyway. However, inversion events performed by the polymerase were intended to be prevented since the proofreading polymerase *Pwo* was applied instead of *Taq*. As metioned above, in contrast to *Pwo*, the later enzyme is known to cause inversion within DNA fragments on its own. This mechanism would, of course, have also resulted in the occurrence of inversion products independently from the activity of *Int1*.

### 3.2.3. Deletion of the start codon of *int1* ( $\Delta$ AUG-*int1*)

#### 3.2.3.1. Aim of the study and prognosis

In previous work, a failure of inversion in the absence of Int1 had only been demonstrated in *Nab. magadii* L13 (pRo-5-52-3), a strain supplemented with the invertible region but completely lacking the corresponding gene of Int1 (Ladurner, 2008). Hence, it could not be excluded that this effect was caused by the shortening of the invertible region resulting from removing of *int1*, but not by the absence of Int1. For this reason, a clone carrying the whole invertible region including *int1*, but though lacking the corresponding protein due to deletion of the start codon ( $\Delta$ AUG-*int1*) was prepared in course of this work. If indeed Int1 was required for inversion of the region comprising ORF34 – ORF36, a total lack of inversion products was expected to be demonstrable by PCR analysis.

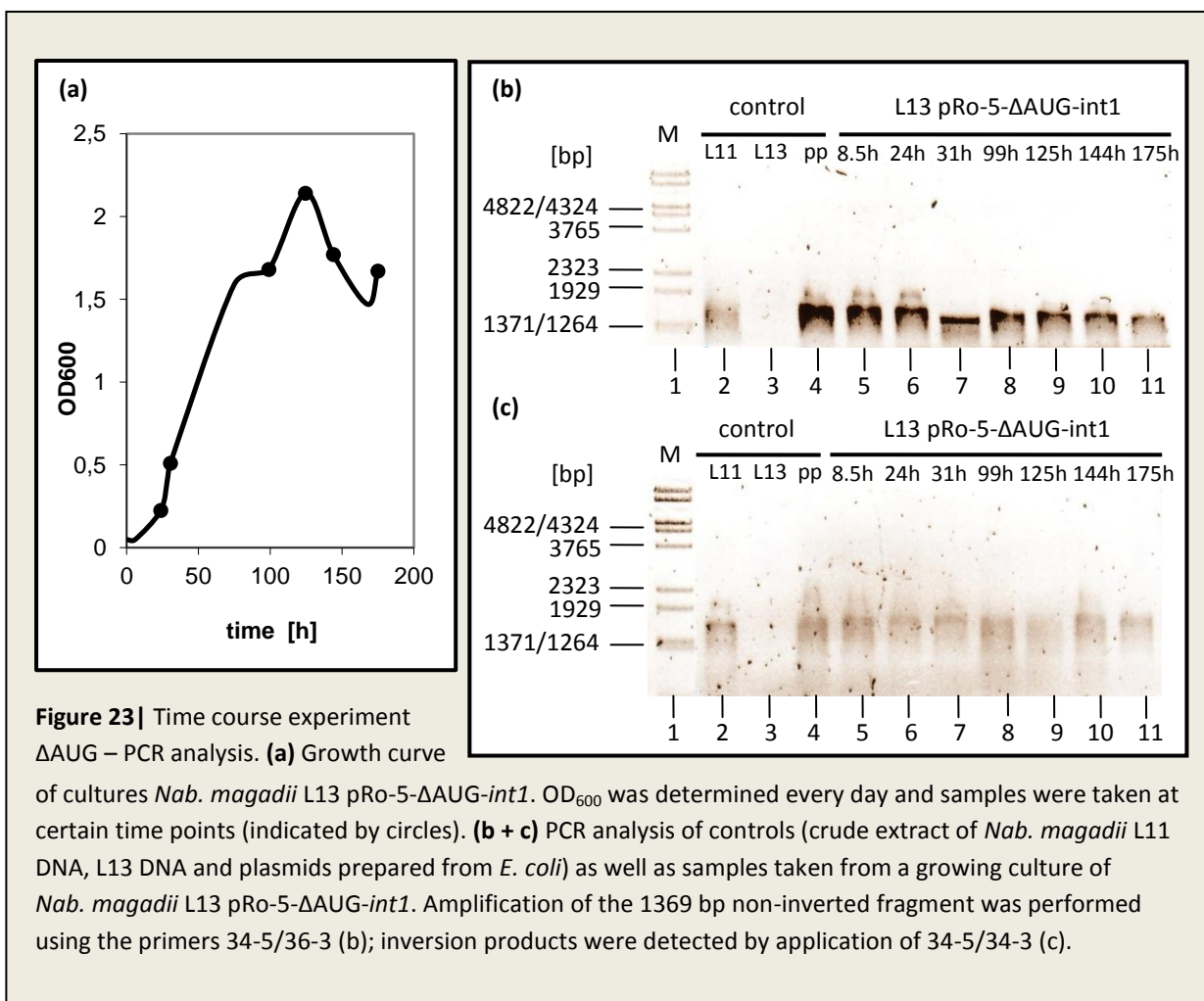
#### 3.2.3.2. Cloning of *Nab. magadii* L13 $\Delta$ AUG-*int1*

Construction of the plasmid pRo5- $\Delta$ AUG-*int1* comprising the whole invertible region except for the start codon of *int1* was performed as described in section 2.2.2.5. Subsequently the vector was transformed into *Nab. magadii* L13 and positive clones were verified by PCR analysis, detecting both, the fragments upstream (2323 bp) and downstream (2161 bp) of *int1*-AUG. For amplification of both fragments the primers applied for cloning of pRo-5- $\Delta$ AUG-*int1*, 34-Kpn/3601-XbaI (fragment 1) and 36-5-HindIII/3602-Xba (fragment 2), were used.

#### 3.2.3.3. Inversion – time course experiment

To examine the ability of verified clones to perform inversion reactions, a time course experiment was carried out as described in section 2.2.3.4. Periodical (almost every day) samples were taken and plasmid DNA was extracted according to the instructions in section 2.2.3.5. Since in a first approach a sample resulting from the lag phase of the growing culture was missing, a fresh culture was inoculated and an additional sample was taken after 8.5 hours. In order to estimate the DNA concentrations, all resulting samples were analyzed on a 0.8 % agarose gel. Finally, appropriate dilutions of the samples were analyzed by PCR. As described in the previous section (investigation of a possible activator of *int1* expression), two different PCRs were performed: one for detection of the non-inverted fragment (ORF34<sub>52</sub>) and one for detection of possible inversion products. Again for amplification of ORF34<sub>52</sub> the primers 34-5 and 36-3 were applied, whereas the presence of inversion products was investigated using 34-5 and 34-3. In addition to the samples taken from the growing culture, different controls were applied: batches containing crudely extracted DNA of *Nab. magadii*

L11 (positive control), *Nab. magadii* L13 (negative control) and the plasmid resulting from cloning in *E. coli*. Finally, all PCR batches were analyzed by separation on a 0.8 agarose gel. The growth curve of *Nab. magadii* L13 pRo-5- $\Delta$ AUG-*int1* as well as the results of analysis of the respective samples are shown in figure 23.



As already described for *Nab. magadii* L13 supplemented with the invertible region and the possible activator of *int1* expression (see section 3.2.2.3.), amplification of non-inverted fragments yields signals at 1369 bp (figure 23b), whereas inversion products are visible as weaker, blurred bands (figure 23c). Both, non-inverted and inverted fragments seem to be present in all samples taken from growing cultures of *Nab. magadii* L13 pRo-5- $\Delta$ AUG-*int1*. Moreover, they can be detected in DNA extracts prepared from *Nab. magadii* L11, but are lacking in the negative control (L13). However, a signal indicating the presence of inversion products also results from analysis of the original plasmid prepared from *E. coli*. Hence, a conclusion about the occurrence of inversion events in the *Nab. magadii* culture supplemented with the invertible region but lacking *Int1* due to deletion of the start codon of the corresponding gene is not possible.

#### 3.2.3.4. Discussion

In general, the presence of inversion products in samples prepared from a growing culture of *Nab. magadii* L13 pRo-5- $\Delta$ AUG-*int1* would indicate, that inversion is possible in the absence of Int1. However, since the plasmid prepared from *E. coli* yielded a signal as well, inversion products can be expected to occur in the concerned *Nab. magadii* culture, independently from the activity of Int1. As described for clone *Nab. magadii* L13 pRo-5-52-3 pNB102/43-44 supplemented with a possible activator of *int1* expression (see section 3.2.2.), the application of the primers 34-5/36-3 may yield a signal of an appropriate size anyway. Yet, this explanation does not correlate to the results of previous studies confirming the occurrence of inversion products only in the presence of Int1 based on this PCR (Ladurner, 2008). Anyway, a conclusion about the ability to perform inversion reactions in the absence of the gene product Int1, but in the presence of the whole invertible region on a genetic level is not possible based on these results.

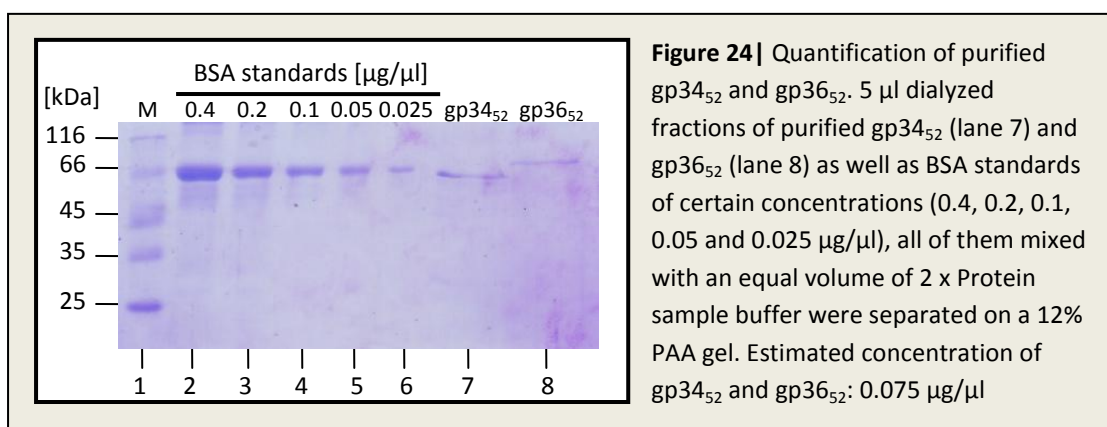
### 3.3. Binding of gp34 to *Nab. magadii* P3

#### 3.3.1. Aim of the study and prognosis

Since the gene product of  $\phi$ Ch1 ORF34<sub>52</sub> was shown to bind to the surface of *Nab. magadii*, this protein was supposed to be crucial for the infectivity of the virus (Rössler *et al.*, in prep). In course of this diploma work this assumption was supported, as deletion of the putative tail fibre protein resulted in a loss of infectivity (see section 3.1.). Based on this idea, purified gp34<sub>52</sub> bound to the surface of the archaeal cell was supposed to compete with the tail fibre protein of mature phage particles of  $\phi$ Ch1, thus leading to a reduction of the phage titre. Hence, as a further project for examination of gp34<sub>52</sub>, a phage titre analysis was performed adding both, the  $\phi$ Ch1 particles and varying amounts of the purified protein gp34<sub>52</sub> expressed in *E. coli*. Yet, since *Nab. magadii* was known to produce a protease which gets segregated to the exterior of the cell (NEP) and thus causes degradation of foreign proteins in the surrounding medium (Derntl, 2009), a *Nab. magadii* strain lacking NEP (*Nab. magadii* P3) was used. However, the presence of gp34<sub>52</sub> was expected to result in a reduction of the phage titre compared to equal approaches including the inverted version of gp36 (gp36<sub>52</sub>) or lacking any of these proteins, respectively.

### 3.3.2. Purification of gp34<sub>52</sub>/gp36<sub>52</sub> and quantification

In order to investigate the effect of gp34<sub>52</sub> and gp36<sub>52</sub> on the phage titre of  $\phi$ Ch1, first of all both proteins had to be purified. For this purpose the corresponding genes introduced via the cloning vector pQE30 (pQE-34<sub>52</sub> and pQE-36<sub>52</sub>) were expressed in the *E. coli* strain XL-1 Blue as described in section 2.2.5.2. After expression for 3 hours, the cells were harvested and the pellet resulting from 5 liter culture was solved in 100 ml (gp36<sub>52</sub>) and 150 ml (gp34<sub>52</sub>) buffer B, respectively. After lysis of the cells, the proteins were collected by centrifugation and incubated with 900 $\mu$ l (gp36<sub>52</sub>) / 1 ml (gp34<sub>52</sub>) Ni-NTA in order to enable binding based on the affinity of the His-tag to the Ni<sup>2+</sup> ions (see section 2.1.10.4.). Finally they were purified under denaturing conditions according to the instructions in section 2.1.10.4. The different fractions resulting from this procedure (flowthrough, 2 x wash, 6 x elution) as well as crude protein extracts prepared from the respective *E.coli* cultures for and after induction of expression of the concerned genes were analyzed on protein gels as described in section 2.2.5.5. (data not shown). For the binding assays, samples containing appropriate amounts of quite pure gp34<sub>52</sub> and gp36<sub>52</sub> were dialyzed against buffer 1 and buffer 2 in order to adapt them to high salt concentrations and hypersaline conditions (see section 2.2.5.4.). Afterwards, an aliquot of each sample was mixed with an equal volume of 2 x Protein sample buffer (Laemmli) and separated on a protein gel as described in section 2.2.5.5. In order to estimate the protein concentration in the samples, BSA standards of certain concentrations (0.025, 0.05, 0.1, 0.2 and 0.4  $\mu$ g/ $\mu$ l) were applied. Based on the resulting gel (see figure 24), a concentration of 0.075  $\mu$ g/ $\mu$ l was determined for the dialyzed fractions of both proteins.

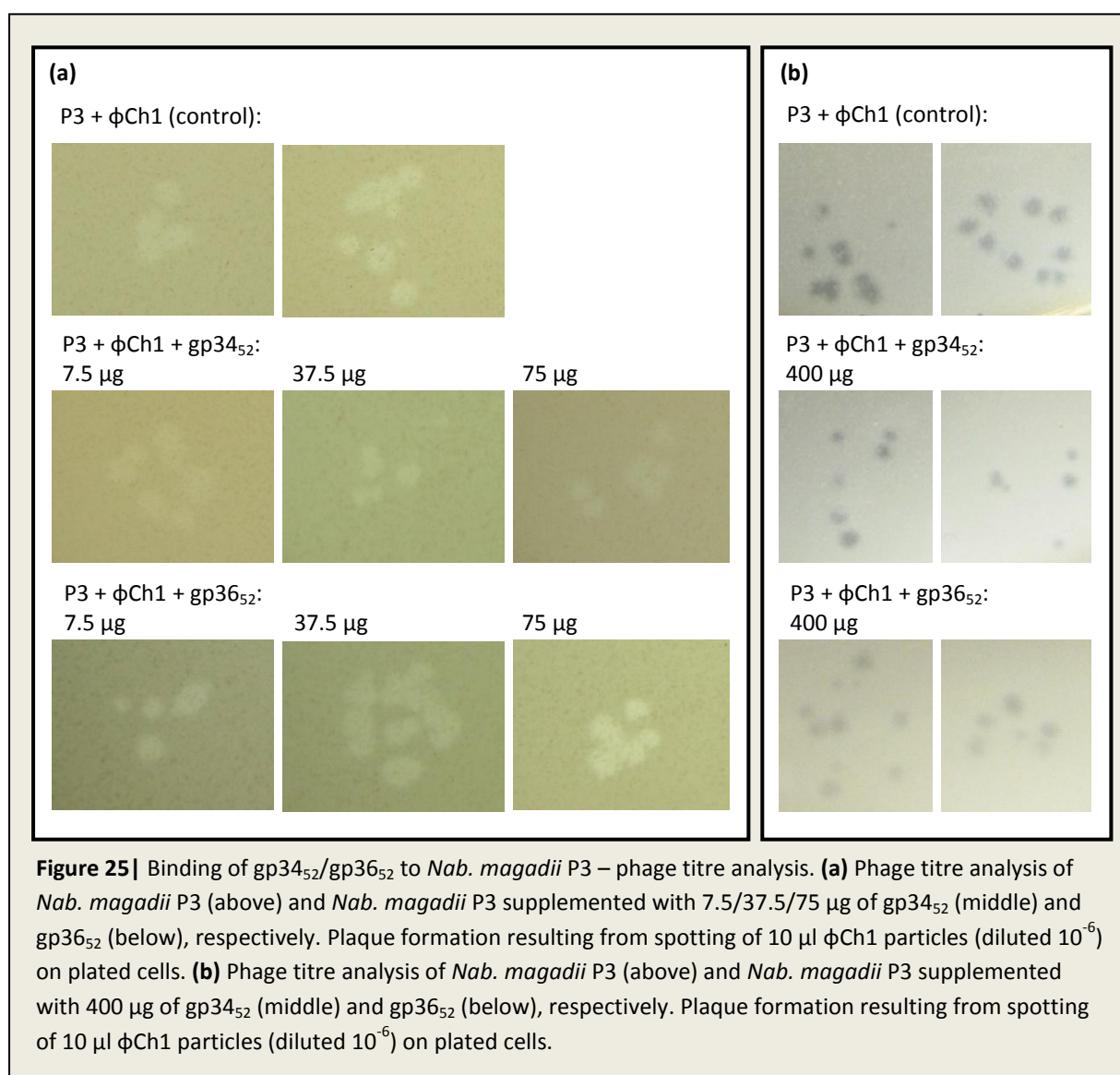


### 3.3.3. Phage titre analysis

In order to investigate a possible reduction in the plaque formation caused by the addition of gp34<sub>52</sub> or gp36<sub>52</sub>, phage titre analysis was performed. As described in section 2.2.4.4., in addition to 400  $\mu$ l stationary culture of *Nab. magadii* P3, varying amounts of the purified proteins gp34<sub>52</sub> and

gp36<sub>52</sub> were added to 5 ml soft agar and plated on NVM agar plates. In a first approach, three different amounts were tested: 7.5 µg, 37.5 µg and 75 µg (contained in 100 µl, 500 µl and 1ml protein fraction, respectively). As a control, the same procedure was performed twice in the absence of gp34<sub>52</sub> and gp36<sub>52</sub>, only adding *Nab. magadii* P3. However, after hardening of the plated soft agar, 10 µl of purified φCh1 particles in different dilutions (10<sup>-2</sup>, 10<sup>-4</sup>, 10<sup>-6</sup> and 10<sup>-8</sup>) were spotted in an appropriate distance with respect to each other. The titre was evaluated after incubation at 37° C for 7 days.

In all three cases (phage titre analysis of *Nab. magadii* P3 and *Nab. magadii* P3 supplemented with gp34<sub>52</sub> and gp36<sub>52</sub>, respectively) spotting of 10<sup>-2</sup> and 10<sup>-4</sup> diluted φCh1 particles resulted in complete lysis of the cells, whereas a dilution of 10<sup>-8</sup> did not cause plaque formation at all (data not shown). However, single plaques could be counted as a consequence of infection with 10<sup>-6</sup> diluted phages. The results are illustrated below (see figure 25a).

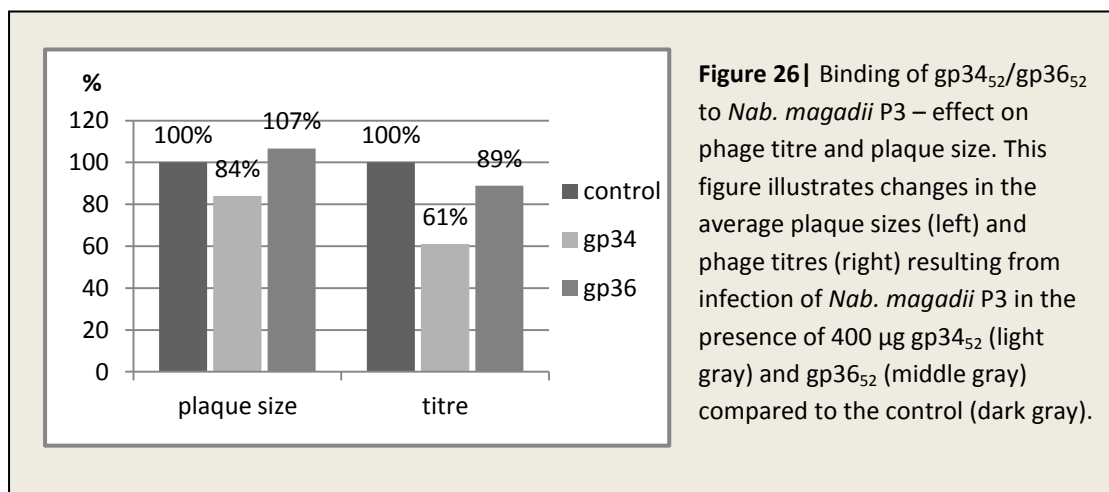


In both, the titres additionally containing gp34<sub>52</sub> and those supplemented with gp36<sub>52</sub>, the number of plaques did not differ significantly from the one observed on plates resulting from infection with  $\phi$ Ch1 in the absence of the concerned proteins. Yet, as visible on the pictures illustrated in figure 25a, the plaques resulting from addition of 37.5 and 75  $\mu$ g gp34<sub>52</sub> respectively (P3 +  $\phi$ Ch1 + gp34<sub>52</sub>) were reduced in their size compared to approaches containing gp36<sub>52</sub> (P3 +  $\phi$ Ch1 + gp36<sub>52</sub>) or lacking both proteins (P3 +  $\phi$ Ch1). For the titre supplemented with 75  $\mu$ g gp34<sub>52</sub> an average plaque size of 1.13 mm was calculated, which is approx. 68.5 % of the total plaque size of P3 infected with  $\phi$ Ch1 without any additives ( $\emptyset$ : 1.65 mm). In contrast to this, the plaques resulting from addition of up to 75  $\mu$ g gp36<sub>52</sub> exhibited an average size of 1.67 mm and thus did not differ in their size compared to the control approach. Hence it can be excluded that the observed effect had been caused by changes in the agar content due to addition of up to 1 ml liquid to the soft agar. Instead of this, these results rather indicate, that the competition of purified gp34<sub>52</sub> with mature  $\phi$ Ch1 particles had resulted in a delay in infection. However, since a reduction of the phage titre could not be observed as a consequence of addition of up to 75  $\mu$ g gp34<sub>52</sub>, further phage titres were performed applying higher amounts of the respective proteins. For this purpose appropriate fractions of purified gp34<sub>52</sub> and gp36<sub>52</sub> were dialyzed as described before (section 3.3.2.). Again the protein concentrations in the resulting fractions were estimated by SDS-PAGE, applying BSA standards in addition.

First the effect of addition of 150  $\mu$ g gp34<sub>52</sub> / gp36<sub>52</sub> contained in 1546.7  $\mu$ l (gp34<sub>52</sub>) and 1500  $\mu$ l (gp36<sub>52</sub>) protein fraction, respectively, was investigated. Yet, like before no decrease in the titre could be observed as a consequence of supplementation with gp34<sub>52</sub>, while the size of the present plaques was slightly reduced (data not shown). Surprisingly, in this case a small reduction in both, the number and size of the plaques was detectable in the approach containing gp36<sub>52</sub>. However, since this titre analysis yielded formation of only few plaques in general (max. 5 plaques in one control approach), a conclusion based on this data is not possible anyway.

Finally, a last titre analysis was performed applying 400  $\mu$ g gp34<sub>52</sub> and gp36<sub>52</sub>, respectively. However, since a total volume of 2390  $\mu$ l protein fraction was added to the 5 ml approach, the agar content of the soft agar was adapted in order to enable hardening after plating (6 g agar / liter NVM). To achieve better comparison, the control approach was supplemented with an equal volume of high salt alkaline solution. Furthermore, in contrast to the phage titres performed before, phage dilutions of  $10^{-4}$ ,  $10^{-5}$  and  $10^{-6}$  were applied and spotted twice this time on all three plates. The plaques resulting from this procedure are illustrated in figure 25b. Like in the first attempt, a reduction in the plaque size caused by the addition of gp34<sub>52</sub> could be observed. Compared to the approx. 2.01 mm control plaques, the plaques of approaches supplemented with 400  $\mu$ g gp34<sub>52</sub> showed an average

size of 1.69 mm (84.1 % of the control size) whereas no effect on the plaque size could be detected in the presence of gp36<sub>52</sub>. In addition to the plaque size, a reduction in the plaque number could be observed. In contrast to the control approaches yielding 9 plaques each, 5 and 6 plaques respectively were present on the plate supplemented with gp34<sub>52</sub>. This represents a decrease in plaque formation of 38.9 %. However, since infection with 10 µl φCh1 particles spotted on plated cells caused only few plaques in general, a definite statement based on these results is difficult. Yet, a tendency to a negative effect on the infection with φCh1 in the presence of gp34<sub>52</sub> may be supposed.



### 3.3.4. Discussion

In general an effect on plaque formation could be observed in the presence of gp34<sub>52</sub>. Compared to the plaques resulting from phage infection in the absence of the protein, the plaques of approaches supplemented with at least 37.5 µg gp34<sub>52</sub> were reduced in their size. However, the effect on the plaque size did not increase with increasing amounts of protein added to the cells. Moreover a similar extend in the reduction of the plaque size was observed in the presence of 150 µg gp36<sub>52</sub>. Yet, in the case of gp36<sub>52</sub> neither a tendency to formation of smaller plaques nor a reduction in the titre was observed as a consequence of supplementation with lower or higher amounts of the protein. Hence it is unlikely that this protein indeed has an influence infection of *Nab. magadii* by the virus φCh1. Approaches containing gp34<sub>52</sub> in contrast yielded a constant reduction in plaque size, indicating that this effect can actually be traced back to the presence of the protein. It may have been caused by a delay in infection resulting from competition of φCh1 and gp34<sub>52</sub>. However, complete prevention of infection causing a decrease in the phage titre was definitely not observed in the presence of up to 150 µg of the concerned protein. Approaches supplemented with 400 µg in contrast yielded a reduced number of plaques, yet it is not clear weather this effect indeed resulted from competition with the protein. In general spotting of 10 µl phage particles caused the formation



of only few plaques, varying in the number even under the same conditions. Anyway, a tendency to a reduction in the titre resulting from competition with gp34<sub>52</sub> may be supposed. To come to a definite conclusion, determination of the phage titre may be performed applying 100 µl phage particles. Yet, since in this case on one plate only one phage dilution could be tested, high amounts of gp34<sub>52</sub> would be required for extensive studies.

Finally, based on the data presented above, an effect of gp34<sub>52</sub> on the ability of φCh1 to infect its host *Nab. magadii* is quite likely, but still has to be confirmed in course of further work. For this purpose, even higher amounts of gp34<sub>52</sub> may be applied in order to increase the observed effect.



## 4. References

---

- Abremski, K.E. and Hoess, R.H. (1992) Evidence for a second conserved arginine residue in the integrase family of recombination proteins. *Protein engineering* **5**: 87-91
- Allers, T. and Mevarech, M. (2005) Archaeal genetics – the third way. *Nature Reviews Genetics* **6**: 58-73
- Alte, B. (2011) Konstruktion einer Flagellum-Deletionsmutante in *Natrialba magdii* und Charakterisierung bestehender *Natrialba magdii* Mutanten. *Diploma thesis, University of Vienna*
- Aravind, L. and Koonin, E.V. (1999) DNA-binding proteins and evolution of transcription regulation in the *Archaea*. *Nucleic acids research* **27**: 4658-70
- Argos, P. *et al.* (1986) The integrase family of site-specific recombinases: regional similarities and global diversity. *The EMBO journal* **5**: 433-40
- Arnold, H. P., Ziese, U. & Zillig, W. (2000a) SNDV, a novel virus of the extremely thermophilic and acidophilic archaeon *Sulfolobus*. *Virology* **272**: 409-16
- Arnold, H. P. *et al.* (2000b) A novel lipothrixvirus, SIFV, of the extremely thermophilic crenarchaeon *Sulfolobus*. *Virology* **267**: 252-66
- Barns, S.M., Delwiche, C.F., Palmer, J.D. and Pace, N.R. (1996) Perspectives on archaeal diversity, thermophily and monophyly from environmental rRNA sequences. *Proceedings of the National Academy of Science of the United States of America* **93**: 9188-93
- Baranyi, U., Klein, R., Lubitz, W., Krüger, D.H. and Witte, A. (2000) The archaeal halophilic virus encoded dam-like methyltransferase M.ϕCh1-I methylates adenine residues and complements dam mutants in the low salt environment of *Escherichia coli*. *Molecular Microbiology* **35**: 1168-79
- Bath, C., Cukalaca, T., Portera, K., Dyall-Smith, M.L. (2006) His1 and His2 are distantly related, spindle shaped haloviruses belonging to the novel virus group, *Salterprovirus*. *Virology* **350**: 228-39
- Bath, C. and Dyall-Smith, M.L. (1998) His1, an archaeal virus of the *Fuselloviridae* family that infects *Haloarcula hispanica*. *Journal of Virology* **72**: 9392-5
- Baumann, P. and Jackson, S.P. (1996) An archaeobacterial homologue of the essential eubacterial cell division protein FtsZ. *Proceedings of the National Academy of Science of the United States of America* **93**: 6726-30
- Bell, S.D, Jackson, S.P. (1998) Transcription and translation in *Archaea*: a mosaic of eukaryal and bacterial features. *Trends in Microbiology* **6**:222-8
- Blakely, G.W. and Sherratt, D.J. (1996) *Cis* and *trans* in site-specific recombination. *Molecular Microbiology* **20**: 233-8
- Boone, D. R. and Castenholz, R. W. (2001) *Bergey's manual of systematic bacteriology*. New York: Springer

Brown, J.R., Doolittle, W.F. (1997) *Archaea* and the prokaryote-to-eukaryote transition. *Microbiology And Molecular Biology Reviews* **61**: 456-502

Cline, S.W., Doolittle, W.F. (1987) Efficient transfection of the archaebacterium *Halobacterium halobium*. *Journal of Bacteriology* **169**: 1341-4

Chatton, E. (1938) Titre et travaux scientifique (1906-1937) de Edouard Chatton. *E. Sottano, Sète, France*

Charbonnier, F. and Forterre, P. (1994) Comparison of plasmid DNA topology among mesophilic and thermophilic *Eubacteria* and archaebacteria. *Journal of bacteriology* **176**: 1251-9

Copeland, H.F. (1938) The kingdoms of organisms. *The Quarterly Review of Biology* **13**: 383-420

DeLong, E.F. and Pace, N.R. (2001) Environmental diversity of *Bacteria* and *Archaea*. *Systematic biology* **50**: 470-8

Dennis, P.P. (1997) Ancient Ciphers: translation in *Archaea*. *Cell* **89**: 1007-10

Derntl, C. (2009) Construction of the first deletion mutant of a haloalkaliphilic archaeon and analysis of gene expression of the methyltransferase M.Nma $\phi$ Ch1I of the halophage  $\phi$ Ch1. *Diploma thesis, University of Vienna*

Dyall-Smith, M. (2009) The Halohandbook - protocols for haloarchaeal genetics (version 7). [http://www.haloarchaea.com/resources/halohandbook/Halohandbook\\_2008\\_v7.pdf](http://www.haloarchaea.com/resources/halohandbook/Halohandbook_2008_v7.pdf).

Dyall-Smith, M., Tang, S.-L. and Bath, C. (2003) Haloarchaeal viruses: how diverse are they? *Research in Microbiology* **154**: 309-13

Fendrihan, S., Legat, A., Pfaffenhuemer, M., Gruber, C., Weidler, G., Gerbl, F., Stan-Lotter, H. (2006) Extremely halophilic *Archaea* and the issue of long-term microbial survival. *Reviews in Environmental Science and Biotechnology* **5**: 203-18

Forterre, P., Brochier, C. and Philippe, H. (2002) Evolution of the *Archaea*. *Theoretical Population Biology* **61**: 409-22

Fox, G.E., Pechman, K.R. and Woese, C.R. (1977) Conservation of primary structure in 16S ribosomal RNA. *International Journal of Systematic Bacteriology* **27**: 44-57

Glansdorff, N., Xu, Y. and Labedan, B. (2008) The last universal common ancestor: emergence, constitution and genetic legacy of an elusive forerunner. *Biology Direct* **3**: 29

Glasgow, A.C., Hughes, K.T., and Simon, M.I. (1989) Bacterial DNA inversion systems. In: *Mobile DNA*. Berg, D.E., and Howe, M.M. (eds). Washington, DC: *American Society for Microbiology Press*, pp. 637-659

- Gribaldo, S. and Brochier-Armanet, C. (2006) The origin and evolution of *Archaea*: a state of the art. *Philosophical Transactions of the Royal Society* **361**: 1007-22
- Gropp, F., Grampp, B., Stolt, P., Palm, P. and Zillig, W. (1992) The immunity-conferring plasmid p $\phi$ HL from the *Halobacterium salinarium* phage  $\phi$ H: nucleotide sequence and transcription. *Virology* **190**: 45-54
- Guzman, L.M., Belin, D., Carson M.J., Beckwith, J. (1995) Tight regulation, modulation, and high-level expression by vectors containing the arabinose PBAD promoter. *Journal of Bacteriology* **177**: 4121-30
- Haeckel, E. (1866) *Generelle Morphologie der Organismen*. Reimer, Berlin
- Hallet, B., and Sherratt, D.J. (1997) Transposition and site-specific recombination: adapting. DNA cut-and-paste mechanisms to a variety of genetic rearrangements. *FEMS microbiology reviews* **21**: 157-178
- Häring, M., Xu, P., Brügger, K., Rachel, R., Stetter, K.O., Garrett, R.A., Prangishvili, D. (2004) Morphology and genome organization of the virus PSV of the hyperthermophilic archaeal genera *Pyrobaculum* and *Thermoproteus*: a novel virus family, the *Globuloviridae*. *Virology* **323**: 233-42
- Häring, M., Rachel, R., Peng, X., Garrett, R. and Prangishvili, D. (2005a) Viral diversity in hot springs of Pozzuoli, Italy, and characterization of a unique archaeal virus, *Acidianus* bottle-shaped virus, from a new family, the *Ampullaviridae*. *Journal of Virology* **79**: 9904-11
- Häring, M., Vestergaard, G., Rachel, R., Lanming, C. and Prangishvili, D. (2005b) Independent virus development outside a host *Nature* **436**: 1101-2
- Holmes, M.L. and Dyall-Smith, M.L. (1991) Mutations in DNA gyrase result in novobiocin resistance in halophilic archaeobacteria. *Journal of Bacteriology* **173**: 642-8
- Holmes, M., Nuttall, S. and Dyall-Smith, M. (1991) Construction and use of halobacterial shuttle vectors and further studies on *Haloferax* DNA gyrase. *Journal of Bacteriology* **173**: 3807-13
- Horikoshi, K. (1999) Alkaliphiles: some applications of their products for biotechnology. *Microbiology and Molecular Biology Reviews* **63**: 735-50
- Huber, H., Hohn, M.J., Rachel, R., Fuchs, T., Wimmer, V.C. and Stetter, K.O. (2002) A new phylum of *Archaea* represented by a nanosized hyperthermophilic symbiont. *Nature* **417**: 63-7
- Huber, H., Hohn, M.J., Stetter, K.O., Rachel, R. (2003) The phylum *Nanoarchaeota*: present knowledge and future perspectives of a unique form of life. *Research in Microbiology* **154**: 165-71
- Huet, J., Schnabel, R., Sentenac, A. and Zillig, W. (1983) Archaeobacteria and eukaryotes possess DNA dependent RNA polymerases of a common type. *The EMBO journal* **2**: 1291-4

Iro, M., Klein, R., Gálos, B., Baranyi, U., Rössler, N., Witte, A. (2007) The lysogenic region of virus  $\phi$ Ch1: identification of a repressor-operator system and determination of its activity in halophilic *Archaea*. *Extremophiles* **11**: 383-96

Iro, M., Ladurner, A., Meissner, C., Derntl, C., Reiter, M., Haider, F., Rössler, N., Klein, R., Baranyi, U., H, S. and Witte, A. (in prep.) Transformation of *Natrialba magadii*: application of  $\phi$ Ch1 elements for a shuttle vector system for haloalkaliphilic *Archaea*

Jain, R., Rivera, M.C. and Lake, J.A. (1999) Horizontal gene transfer among genomes: the complexity hypothesis. *Proceedings of the National Academy of Science of the United States of America* **96**: 3801-6

Jones, B.E., Grant, W.D., Duckworth, A.W. and Owenson, G.G. (1998) Microbial diversity of soda lakes. *Extremophiles* **2**: 191-200

Kamekura, M., Dyall-Smith, M.L., Upasani, V., Ventosa, A., Kates, M. (1997) Diversity of alkaliphilic halobacteria: proposals for transfer of *Natronobacterium vacuolatum*, *Natronobacterium magadii*, and *Natronobacterium pharaonis* to *Halorubrum*, *Natrialba*, and *Natronomonas* gen. nov., respectively, as *Halorubrum vacuolatum* comb. nov., *Natrialba magadii* comb. nov., and *Natronomonas pharaonis* comb. nov., respectively. *International Journal of Systematic Bacteriology* **47**: 853-7

Kandler, O. and König, H. (1998) Cell wall polymers in *Archaea* (archaeobacteria). *Cellular and Molecular Life Science* **54**: 305-8

Keeling, P.J., Doolittle, W.F (1995) *Archaea*: narrowing the gap between prokaryotes and eukaryotes. *Proceedings of the National Academy of Science of the United States of America* **92**: 5761-4

Klein, R., Baranyi, U., Rössler, N., Greineder, B., Scholz, H. and Witte, A. (2002) *Natrialba magadii* virus  $\phi$ Ch1: first complete nucleotide sequence and functional organization of a virus infecting a haloalkaliphilic archaeon. *Molecular Microbiology* **45**: 851-63

Klein, R., Greineder, B., Baranyi, U. and Witte, A. (2000) The structural protein E of the archaeal virus  $\phi$ Ch1: evidence for processing in *Natrialba magadii* during virus maturation. *Virology* **276**: 376-87

Klenk, H-P. *et al.* (1997) The complete genome sequence of the hyperthermophilic, sulphate-reducing archaeon *Archaeoglobus fulgidus*. *Nature* **390**: 364-70

Lam, W.L. and Doolittle, W.F. (1992) Mevinolin-resistant mutations identify a promoter and the gene for a eukaryote-like 3-hydroxy-3-methylglutaryl-coenzymeA reductase in the archaeobacterium *Haloferax volcanii*. *The Journal of Biological Chemistry* **267**: 5829-34

Ladurner, A. (2008) Characterization of the inversion reaction of  $\phi$ Ch1 and the establishment of a transformation system for *Natrialba magadii*. *Diploma thesis, University of Vienna*

- Lanyi, J.K. (1974) Salt-dependent properties of proteins from extremely halophilic *Bacteria*. *Bacteriological Reviews* **38**: 272-90
- Lopez, P., Philippe, H., Myllykallio, H., and Forterre, P. (1999) Identification of putative chromosomal origins of replication in *Archaea*. *Molecular microbiology* **32**: 883-6
- Luo, Y., Pfister, P., Leisinger, T., and Wasserfallen, A. (2001) The genome of archaeal prophage  $\Psi$ M100 encodes the lytic enzyme responsible for autolysis of *Methanothermobacter wolfeii*. *Journal of bacteriology* **183**: 5788-92
- Machida, Y.J., Hamlin, J.L. and Dutta, A. (2005) Right place, right time and only once: replication initiation in metazoans. *Cell* **123**: 13-24
- Madern, D., Pfister, C., Zaccai, G. (1995) A single acidic amino acid mutation enhances the halophilic behaviour of malate dehydrogenase from *Haloarcula marismortui*. *European journal of biochemistry/ FEBS* **230**: 1088-95
- Marteinsson, V.T., Birrien, J.-L., Reysenbach, A.-L., Vernet, M., Marie, D., Gambacorta, A., Messner, P., Sleytr, U.B. and Prieur, D. (1999) *Thermococcus barophilus* sp. nov., a new barophilic and hyperthermophilic archaeon isolated under high hydrostatic pressure from a deep-sea hydrothermal vent. *International Journal of Systematic Bacteriology* **49**: 351-9
- Markhof, A.M., Trus, B.L., Conway, J.F., Simon, M.N., Zurabishvili, T.G., Mesyanzhinov, V.V. and Steven, A.C. (1993) The short tail-fibre of the bacteriophages T4: molecular structure and a mechanism for its conformational translation. *Virology* **194**: 117-27
- Ng, W.L., DasSarma, S. (1993) Minimal replication origin of the 200-kilobase *Halobacterium* plasmid pNRC100. *Journal of Bacteriology* **175**: 4584-96
- Nuttall, S.D., Dyall-Smith, M.L. (1993) HF1 and HF2: novel bacteriophages of halophilic *Archaea*. *Virology* **197**: 678-84
- Olsen, G.J. (1994) *Archaea, Archaea, everywhere*. *Nature* **371**: 657-8
- Oren, A. (1999) Bioenergetic aspects of halophilism. *Microbiology and Molecular Biology Reviews* **63**: 334-48
- Oren, A. (2002) Diversity of halophilic microorganisms: environments, phylogeny, physiology, and applications. *Journal of Industrial Microbiology and Biotechnology* **28**: 56-63
- Oren, A. (2008a) Microbial life at high salt concentrations: phylogenetic and metabolic diversity. *Saline Systems* **4**
- Oren A (2008b) Bergey's Manual of Systematic Bacteriology, 2nd edn, <http://www.the-icsp.org/taxa/halobacterlist.htm>
- Oren, A., Bratbak, G., Haldal, M. (1997) Occurrence of virus-like particles in the Dead Sea. *Extremophiles* **1**: 143-9

Pace, N.R., Stahl, D.A., Lane, D.J. and Olsen, G.J. (1986) The analysis of natural microbial populations by ribosomal RNA sequences. *Advances in microbial Ecology* **9**: 1-55

Pfeifer, F., Offner, S., Krüger, K., Ghahraman, P. and Englert, C. (1994) Transformation of halophilic *Archaea* and investigation of gas-vesicle synthesis. *Systematic and Applied Microbiology* **16**: 569-77

Pfister, P., Wasserfallen, A., Stettler, R. and Leisinger, T. (1998) Molecular analysis of *Methanobacterium* phage  $\Psi$ M2. *Molecular microbiology* **30**: 233-44

Prangishvili, D., Arnold, H.B., Götz, D., Ziese, U., Holz, I., Kristjansson, J.K., Zillig, W. (1999) A novel virus family, the *Rudiviridae*: structure, virus-host interactions and genome variability of the *Sulfolobus* viruses SIRV1 and SIRV2. *Genetics* **152**: 1387-96

Prangishvili, D. (2003) Evolutionary insights from studies on viruses of hyperthermophilic *Archaea*. *Research in Microbiology* **154**: 289-94

Prangishvili, D., Forterre, P. and Garrett, R.A. (2006a) Viruses of the *Archaea*: a unifying view. *Nature* **4**: 837-48

Prangishvili, D., Garrett, R.A. and Koonin, E.V. (2006b) Evolutionary genomics of archaeal viruses: unique viral genomes in the third domain of life. *Virus Research* **117**: 52-67

Reistad, R. (1970) On the composition and nature of the bulk protein of the extremely halophilic *Bacteria*. *Archiv für Microbiologie* **71**: 353-60

Rivera, M.C., Jain, R., Moore, J.E. and Lake, J.A. (1998) Genomic evidence for two functionally distinct gene classes. *Proceedings of the National Academy of Science of the United States of America* **95**: 6239-44

Rivera, M.C., Lake, J.A. (2004) The ring of life provides evidence for a genome fusion origin of eukaryotes. *Nature* **431**: 152-5

Robinson, N.P., Dionne, I., Lundgren, M., Marsh, V.L., Bernander, R. and Bell, S.D. (2004) Identification of two origin of replication in the single chromosome of the archaeon *Sulfolobus solfataricus*. *Cell* **116**: 25-38

Rössler, N., Klein, R., Scholz, H., Witte, A. (2004) Inversion within the haloalkaliphilic virus  $\phi$ Ch1 DNA results in differential expression of structural proteins. *Molecular Microbiology* **52**: 413-26

Rössler, N., Kögl, K., Hofstätter, H., Iro, M., Scholz, H., Klein, R. and Witte, A. (in prep) ORF34 encodes the tail fibre protein of virus  $\phi$ Ch1.

Rothschild, L.J. and Mancinelli, R.L. (2001) Life in extreme environments. *Nature* **409**: 1092-101

Sandmeier, H. (1994) Acquisition and rearrangement of sequence motifs in the evolution of bacteriophage tail fibers. *Molecular microbiology* **12**: 343-50



Schnabel, H. (1984) An immune strain of *Halobacterium halobium* carries the invertible L segment of phage  $\phi$ H as a plasmid. *Proceedings of the National Academy of Sciences of the United States of America* **81**: 1017-20

Schnabel, H., Zillig, W., Pfaffle, M., Schnabel, R., Michel, H. and Delius, H. (1982) *Halobacterium halobium* phage  $\phi$ H. *EMBO Journal* **1**: 87-92

Selb, R. (2010) Construction of mutants of *Natrialba magadii* and  $\phi$ Ch1. *Diploma thesis, University of Vienna*

Shirai, T., Kobayashi, T., Ito, S., Horikoshi, K. (2008) Alkaline adaptation of proteins. In: *Protein adaptation in extremophiles (molecular anatomy and physiology of proteins)*. Siddiqui, K.S., Thomas, T., (eds). *Nova Publishers*, pp. 105-141

Svoboda, T. (2011) Characterization of putative repressors of the temperate phage  $\phi$ Ch1 and analysis of the flagellum operon as a putative receptor of  $\phi$ Ch1. *Diploma thesis, University of Vienna*

Tindall, B., Ross, H. and Grant, W. (1984) *Natronobacterium* gen. nov. and *Natronococcus* gen. nov., two new genera of haloalkaliphilic archaebacteria. *Systematic and Applied Microbiology* **5**: 41-57

Torsvik, T. and Dundas, I.D. (1974) Bacteriophage of *Halobacterium salinarum*. *Nature* **248**: 680-1

Torsvik, T. and Dundas, I.D. (1980) Persisting phage infection in *Halobacterium salinarum* str. 1. *Journal of General Virology* **47**: 29-36

van de Vossenberg, J.L.C.M., Driessen, A.J.M., Grant, D., Konings, W.N. (1999) Lipid membranes from halophilic and alkali-halophilic *Archaea* have a low H<sup>+</sup> and Na<sup>+</sup> permeability at high salt concentration. *Extremophiles* **3**: 253-7

Wais, A.C., Kon, M., MacDonald, R.E., Stollar, B.D. (1975) Salt-dependent bacteriophages infecting *Halobacterium cutirubrum* and *H. halobium*. *Nature* **256**: 314-5

White, M.F., Bell, S.D. (2002) Holding it together: chromatin in the *Archaea*. *Trends in Genetics* **18**: 621-6

Whittaker, R.H. (1959) On the broad classification of organisms. *The Quarterly Review of Biology* **34**: 210-26

Whittaker, R.H. and Margulis, L. (1978) Protist classification and the kingdoms of organisms. *Biosystems* **10**: 3-18

Witte, A., Baranyi, U., Klein, R., Sulzner, M., Luo, C., Wanner, G., Krüger, D. and Lubitz, W. (1997) Characterization of *Natronobacterium magadii* phage  $\phi$ Ch1, a unique archaeal phage containing DNA and RNA. *Molecular Microbiology* **23**: 603-16

- Witte, A., Wanner, G., Bläsi, U., Halfmann, G., Szostak, M. and Lubitz, W. (1990) Endogenous transmembrane tunnel formation mediated by  $\phi$ X174 Lysis Protein E. *Journal of Bacteriology* **172**: 4109-14
- Woese, C.R. (1998) The universal ancestor. *Proceedings of the National Academy of Science of the United States of America* **95**: 6854-9
- Woese, C.R. and Fox, G.E. (1977) Phylogenetic structure of the prokaryotic domain: The primary kingdoms. *Proceedings of the National Academy of Science of the United States of America* **11**: 5088-90
- Woese, C.R., Kandler, O. and Wheelis, M. L. (1990) Towards a natural system of organisms: proposal for the domains *Archaea*, *Bacteria*, and *Eucarya*. *Proceedings of the National Academy of Science of the United States of America* **87**: 4576-9
- Wolf, Y.I., Aravind, L., Grishin, N.V., Koonin, E.V. (1999) Evolution of aminoacyl-tRNA-synthetase-analysis of unique domain architectures and phylogeny trees reveals a complex history of horizontal gene transfer events. *Genome Research* **9**: 689-710
- Yanisch-Perron, C., Vieira, J., Messing, J. (1985) Improved M13 phage cloning vectors and host strains: nucleotide sequences of the M13mp18 and pUC19 vectors. *Gene* **33**: 103-19
- Zhang, R. and Zhang, C.T. (2003) Multiple replication origins of the archaeon *Halobacterium* species NRC-1. *Biochemical and biophysical research communication* **302**: 728-34
- Zhou, M., Xiang, H., Sun, C. and Tan, H. (2004) Construction of a novel shuttle vector based on an RCR-plasmid from a haloalkaliphilic archaeon and transformation into other haloarchaea. *Biotechnology letters* **26**: 1107-13
- Zivanovic, Y., Armengaud, J., Lagorce, A., Leplat, C., Guérin, P., Dutertre, M., Anthouard, V., Forterre, P., Wincker, P. and Confalonieri, F. (2009) Genome analysis and genome-wide proteomics of *Thermococcus gammatolerans*, the most radioresistant organism known amongst the *Archaea*. *Genome Biology* **10**: R70

# 5. Appendix

---

## Index of Figures and Tables

Figure 1  Phylogenetic tree	12
Figure 2  <i>Natrialba magadii</i>	27
Figure 3  Morphotypes of archaeal viruses	32
Figure 4  Morphology of $\phi$ Ch1	35
Figure 5  Linear representation of the $\phi$ Ch1 genome	38
Figure 6  The invertible region of $\phi$ Ch1	41
Figure 7  The function of Int1 – time course experiment in <i>Nab. magadii</i>	43
Figure 8  Gene construct of $\phi$ Ch1- $\Delta$ ORF34	87
Figure 9  Verification of a homozygous L11- $\Delta$ ORF34 deletion mutant	88
Figure 10  Structural proteins of wild type and $\Delta$ ORF34 $\phi$ Ch1	90
Figure 11  Growth and lysis curve of L11- $\Delta$ ORF34	91
Figure 12  Western blot $\alpha$ -gp34 <sub>52</sub> – expression of ORF34 in L11- $\Delta$ ORF34	92
Figure 13  Phage titre analysis of $\phi$ Ch1- $\Delta$ ORF34	93
Figure 14  Electron micrographs of purified $\phi$ Ch1- $\Delta$ ORF34 particles	94
Figure 15  Electron micrographs of $\phi$ Ch1- $\Delta$ ORF34 particles in cell lysates (gentle isolation)	95
Figure 16  Western blot $\alpha$ -FlaB1 – analysis of phage fractions	97
Figure 17  Western blot $\alpha$ -gp34 <sub>52</sub> – complementation of $\Delta$ ORF34 <sub>52</sub>	99
Figure 18  Phage titre analysis – complementation of $\Delta$ ORF34 <sub>52</sub> .	101
Figure 19  Constructs of eight <i>int1</i> clones	105
Figure 20  Time course experiment eight <i>int1</i> clones – PCR analysis	107
Figure 21  Time course experiment eight <i>int1</i> clones – Southern blot analysis	108
Figure 22  Time course experiment activator – PCR analysis	112
Figure 23  Time course experiment $\Delta$ AUG – PCR analysis	115
Figure 24  Quantification of purified gp34 <sub>52</sub> and gp36 <sub>52</sub>	117
Figure 25  Binding of gp34 <sub>52</sub> /gp36 <sub>52</sub> to <i>Nab. magadii</i> P3 – phage titre analysis	118
Figure 26  Binding of gp34 <sub>52</sub> /gp36 <sub>52</sub> to <i>Nab. magadii</i> P3 – effect on phage titre and plaque size	120
Table 1  Repeat clusters within gp34 and gp36	42
Table 2  Phage titres of $\phi$ Ch1- $\Delta$ ORF34 in complemented and control cultures.	100



## Acknowledgements

First of all I want to say that I really enjoyed working on my diploma thesis since social intercourse of all members of the “halolab” generated a great atmosphere for both, scientific work and relaxed conversation.

In this respect the first person I want to thank is Prof. Dr. Angela Witte. She gave me the opportunity to work in her team and raised my enthusiasm for the fascinating world of *Archaea*. Her impressive knowledge and working experience in several fields was a great help for the introduction into scientific work. As a supervisor she always provided advises and support, not only for me, but for all members of her team. All requests were treated with incredible composure and patience. In addition, I want to express my especial appreciation for the help during my work as a tutor of student practical trainings. This time was an important experience for me.

Furthermore I want to thank my colleagues of the “halolab”. During the last year they became friends of mine rather than co-workers. Especial gratitude goes to my place mate Mag. Tatjana Svoboda who provided “*mental and creative support during my diploma thesis*” (Svoboda, 2011), but also to Beatrix Alte, my main contact person during the last months. In addition I want to thank Daniel Kiesenhofer as well as our newcomers Katharina Dimmel and Judith Beraha who were very helpful during the final period of my work. Further thank goes to all Bachelor students who assisted my work, especially Alexander Leithner, Julia Biebl and Natascha Hruschka. Moreover I am deeply grateful for the kind and patient introduction into scientific working by the former members of the “halolab”, Mag. Michael Reiter and Mag. Regina Selb.

Gratitude goes also to all workers of the neighbouring labs as well as the group leaders Prof. Dr. Udo Bläsi and Mag. Dr. Isabella Moll. Especially I want to thank Dr. Armin Resch and Dr. Elisabeth Sonnleitner for providing technical support and helpful hints.

Furthermore, especial thank goes to my mother Mag. Renate Till and my father Hubert Till, who supported me during the whole time of my study, both, financially and emotionally. Their help was no matter of course, but a gift and enabled realization of my work. Moreover I am very grateful for every scientific discussion with my mother. But gratitude goes also to all other members of my family, in particular my sister Mirjam Till. Furthermore I want to thank my closest friends, especially my best friend Inanna Palikrushew but also Tina Kern and Jan Navara. The contact to them was very important for my inner balance and represented a good contrast to my scientific work.

Last but not least I want to thank Dr. Elke Bogner for providing the grate electron micrographs.



## Abstract

One special characteristic of the haloalkaliphilic virus  $\phi$ Ch1 is the presence of a genomic region which gets inverted by the virus encoded site-specific recombinase Int1 during the lysogenic life cycle of the temperate phage. Since this inversion event results in an exchange of the 3' ends of ORF34 and ORF36, this event gives rise to the formation of different gene products of ORF34: the non-inverted variant (gp34<sub>1</sub>) and the variant comprising the C-terminus of gp36 (gp34<sub>52</sub>). Both of them represent putative tail fibre proteins of  $\phi$ Ch1, structural elements which are often involved in interaction with the host cell during initiation of infection. Yet, based on previous studies only gp34<sub>52</sub> was supposed to be crucial for infection of *Natrialba magadii*, the only known host of  $\phi$ Ch1.

To confirm the putative function of gp34<sub>52</sub>, this work aimed to produce an ORF34 deletion mutant by replacing of the concerned gene region with a novobiocin resistance cassette (Nov<sup>R</sup>). The absence of gp34 in the resulting lysogenic culture *Nab. magadii* L11- $\Delta$ ORF34 was demonstrated by western blot analysis. In addition certain phenotypic characteristics of the corresponding mutant phage particles could be pointed out. On one hand morphological changes which can be explained by the absence of tail fibre structure could be visualized by electron microscopy. On the other hand  $\phi$ Ch1- $\Delta$ ORF34 was shown to be at least strongly reduced in its ability to infect *Nab. magadii* L13. Based on these results, this work could present evidence for both, the function of gp34<sub>52</sub> as the tail fibre protein of  $\phi$ Ch1 as well as its crucial role in infection of *Nab. magadii*.

In addition to deletion of the putative tail fibre protein gp34, this work describes an attempt to cause a reduction in the phage titre by competition of  $\phi$ Ch1 with different amounts of purified gp34<sub>52</sub> and gp36<sub>52</sub>. Indeed a tendency to an effect of gp34<sub>52</sub> on the number and size of the plaques resulting from phage infection could be demonstrated, yet to enable a definite conclusion, a larger approach of titre analysis would be required.

The other part of this thesis contributes to characterization of the inversion process. On one hand certain features of the Int1 target region were worked out by analysis of different clones varying either in the orientation or in the nucleic acid composition of the repeats recognized by Int1. On the other hand the role of the site-specific recombinase Int1 was investigated by deletion of its start codon, yielding a clone failing expression of this protein. Moreover the effect of a possible activator of *int1* expression was examined. In all three cases time course experiments were performed in order to analyze the occurrence of inversion events depending on the growth phase under the respective conditions. However, none of these projects could yield further details about the mechanism of inversion within ORF34 and ORF36.





## Zusammenfassung

Ein Merkmal des haloalkaliphilen Virus  $\phi$ Ch1 ist das Vorhandensein einer genomischen Region welche während des lysogene Zyklus des temperenten Phagens durch die viral codierte Rekombinase Int1 invertiert wird. Da dieses Ereignis einen Austausch der 3' Enden von ORF34 und ORF36 zur Folge hat, ermöglicht es die Bildung verschiedener Genprodukte von ORF34: die uninvertierte Variante (gp34<sub>1</sub>) und jene Variante die den C-terminus von gp36 trägt (gp34<sub>52</sub>). Beide stellen mögliche „Tail-fibre“ Proteine von  $\phi$ Ch1 dar, Strukturelemente die häufig an der Interaktion mit der Wirtszelle zu Beginn einer Infektion beteiligt sind. Aufgrund früherer Studien jedoch wurde eine Bedeutung für die Infektion von *Natrialba magadii*, dem einzigen Wirten von  $\phi$ Ch1, nur bei gp34<sub>52</sub> vermutet.

Um die Funktion von gp34<sub>52</sub> zu bestätigen, war es Ziel dieser Diplomarbeit durch Ersetzen der fraglichen Region durch eine Novobiocinresistenz (Nov<sup>R</sup>) eine ORF34 Deletionsmutante herzustellen. Das Fehlen von gp34 in der lysogenen Kultur *Nab. magadii* L11- $\Delta$ ORF34 wurde mittels Western Blot nachgewiesen. Außerdem konnten bestimmte phänotypische Merkmale der entsprechenden Phagenpartikel aufgezeigt werden. Einerseits konnten durch das Fehlen der „Tail-fibre“ Struktur erklärable morphologische Veränderungen unter dem Elektronenmikroskop beobachtet werden. Andererseits wurde gezeigt, dass  $\phi$ Ch1- $\Delta$ ORF34 in seiner Fähigkeit *Nab. magadii* L13 zu infizieren zumindest stark eingeschränkt ist. Aufgrund dieser Ergebnisse konnte sowohl die Funktion von gp34<sub>52</sub>, als auch seine Bedeutung für die Infektion von *Nab. magadii* nachgewiesen werden.

Zusätzlich zu der Deletion des vermutlichen „Tail-fibre“ Proteins gp34, beschreibt diese Arbeit den Versuch durch Konkurrenz zwischen  $\phi$ Ch1 und verschiedenen Mengen von gp34<sub>52</sub> und gp36<sub>52</sub> eine Reduktion des Phagentiters zu bewirken. Tatsächlich konnte ein tendenzieller Einfluss von gp34<sub>52</sub> auf die Plaquezahl und Größe beobachtet werden, für eine eindeutige Schlussfolgerung jedoch wäre ein größerer Ansatz erforderlich.

Der andere Teil dieser Diplomarbeit dient der Charakterisierung der Inversion. Zum Einen wurden durch Analyse mehrerer Klone, die sich entweder in der Orientierung oder in der Sequenz einzelner Repeats unterscheiden, möglicherweise entscheidende Eigenschaften der Zielregion von Int1 untersucht. Zum Anderen wurde die Bedeutung der Rekombinase Int1 durch Deletion des Startcodons geprüft. Außerdem wurde der Effekt eines möglichen Aktivators der Expression von *int1* untersucht. In allen drei Fällen wurden Zeitreihen durchgeführt um das Auftreten möglicher Inversionsereignisse in Abhängigkeit von der Zeit unter den jeweiligen Bedingungen zu beleuchten. Schlussendlich konnte jedoch keines dieser Projekte weitere Einblicke in den Mechanismus der Inversion zwischen ORF34 und ORF36 liefern.



# Curriculum Vitae

## Personal details:

Name: Petra Till

Date and place of birth: 25<sup>th</sup> of April, 1986 in Vienna, Austria

Nationality: Austria

## Education:

1992 – 1996 Volksschule Perchtoldsdorf, Austria

1996 – 2000 Gymnasium Perchtoldsdorf, Austria

2000 – 2004 BORG Hegelgasse 12, Vienna, Austria (emphasis on arts)  
GCE A-levels 2004 (excellent grades)

2005 – 2011 Study “Molecular Biology” (Diploma), University of Vienna, Austria

2010 – 2010 Study “Biology” (Bachelor), University of Vienna, Austria  
Successful conclusion 2010: Bachelor of Science (BSc)

2010 – 2011 Diploma thesis “Molecular Biology”: Laboratory of Prof. Dr. Angela Witte;  
Department of Microbiology, Immunobiology and Genetics;  
University of Vienna; Austria

## Working experience:

2004 – 2005 Anker Snack & Coffee Gastronomiebestriebs Gmbh Vienna: sales job

2010/2011 University of Vienna: Tutor of student practical trainings in “Übungen in Molekulare Mikrobiologie” and “Übung III A - Molekularbiologische Laborarbeiten”

2010/2011 FH Campus Vienna (University of Applied Sciences): Tutor of student practical trainings in “Molekularbiologische Übungen I”